NASA Contractor Report 158978

BLOWN FLAP NOISE PREDICTION

N. N. Reddy

LOCKHEED-GEORGIA COMPANY
Marietta, GA 30063

CONTRACT NAS1-15068
SEPTEMBER 1978

NASA
National Aeronautics and
Space Administration

Langley Research Center
Hampton, Virginia 23665

1. Report No.	2. Government Accession No.	3. Recipient's Catalog No.
NASA CR-158978		

4. Title and Subtitle	5. Report Date
BLOWN FLAP NOISE PREDICTION	September 1978
	6. Performing Organization Code

7. Author(s)	8. Performing Organization Report No.
N. N. Reddy	LG78ER0237
	10. Work Unit No.

9. Performing Organization Name and Address	11. Contract or Grant No.
Lockheed-Georgia Company Marietta, GA 30063	NAS1-15068
	13. Type of Report and Period Covered

12. Sponsoring Agency Name and Address	13. Type of Report and Period Covered
National Aeronautics and Space Administration Langley Research Center Hampton, Virginia	FINAL - Sept. 77 - Sept. 78
	14. Sponsoring Agency Code

15. Supplementary Notes

Contract Monitor: Dr. W. E. Zorumski, NASA-Langley Research Center

16. Abstract

Theoretical and experimental developments of flow-surface interaction noise with a particular emphasis on blown-flap noise was reviewed. Based on this review, several available blown-flap noise prediction methods were evaluated by comparing the predicted acoustic levels, directivity, and spectra with the recently obtained NASA and Lockheed-Georgia data base. A prediction method was selected and a detailed step-by-step description of this method was provided to develop a computer module to calculate one-third octave band frequency spectra at any given location in the far-field for under-the-wing and upper surface blown configurations as a function of geometric and operational parameters. Additional theoretical and experimental research that are necessary to improve the blown flap noise prediction are outlined.

17. Key Words (Suggested by Author(s))	18. Distribution Statement
Acoustics, Blown Flap Noise, Noise Prediction, High-Lift System Noise, Aircraft Noise	Unlimited

19. Security Classif. (of this report)	20. Security Classif. (of this page)	21. No. of Pages	22. Price*
Unclassified	Unclassified	94	

* For sale by the National Technical Information Service, Springfield, Virginia 22161

CONTENTS

BLOWN FLAP NOISE PREDICTION

N. N. Reddy
Lockheed-Georgia Company

SUMMARY

Theoretical and experimental research on flow-surface interaction noise with a particular emphasis on blown-flap noise prediction was reviewed. The present NASA and other blown-flap noise prediction methods were evaluated by comparing the predicted OASPL, directivity, and spectra with recently obtained test data. Test data obtained by NASA-Lewis Research Center and the Lockheed-Georgia Company were used to evaluate these prediction methods. After evaluating the various available methods for their accuracy and adaptability as a module in the NASA Aircraft Noise Prediction Program, a prediction method was selected and a detailed step-by-step description of this method is provided. From this description one-third octave band spectra at any given location in the far field for under-the-wing and upper surface blown configurations may be calculated. Additional research required to advance the state of the art of blown flap noise and to improve the noise prediction method is identified and discussed. A complete bibliography covering the theoretical and experimental investigations is also presented.

INTRODUCTION

In the past few years a considerable amount of research and development work has been conducted in the pursuit of a feasible integrated powered-lift system for short-haul or short-takeoff and landing (STOL) aircraft. It is anticipated that new near-city-center STOL ports would be in operation in the near future; therefore, the environmental requirements are more stringent for STOL operations than for conventional jet aircraft (CTOL). One of the important environmental problems is the noise requirement. For example, two goals were proposed for STOL aircraft noise criteria: (1) not exceeding 95

EPNdB on a 152.4 m (50 ft.) side line and (2) 90 EPNdB footprint area on the ground is not to exceed one square mile. Whatever the final noise requirements, they will be considerably less than the existing CTOL aircraft noise requirements. In order to evaluate the noise criteria and to provide guidelines for aircraft designers to assess the tradeoff between the noise and performance of STOL aircraft, it is necessary to accurately predict the noise levels.

During early developments of jet-powered STOL aircraft, several concepts of integrated powered-lift systems were evaluated to achieve the required aerodynamic and propulsive performance and to meet the established noise goal. The following concepts of integrated powered-lift systems were considered: (1) augmentor wing, (2) internally blown flap, (3) externally blown flap (upper surface and lower surface blown flaps), and (4) a hybrid system which is a combination of any two concepts. Some of these concepts are shown schematically in figure 1. In order to evaluate the noise impact of these integrated propulsion systems, several preliminary tests were conducted at various NASA research centers and aircraft industries using simulated small-scale static models (refs. 1 and 2). After several exploratory studies of various concepts of powered-lift systems, the externally blown flap (EBF) emerged as one of the leading candidates. In this concept, the jet exhaust is directed towards the wing so that the flow will be attached and turned along the deflected flaps to increase the lift during takeoff and landing operations. This flow deflection may be achieved by having the jet exhaust either under the wing (UTW) or over the wing (OTW). The OTW is also known as upper surface blowing (USB). Figures 1a and 1b illustrate these two configurations. In the case of the UTW configuration (fig. 1a), the jet exhaust is directed against deflected flaps making the flow deflect downward during takeoff and landing operations. The additional lift is obtained through the deflected jet and an increase in the circulation of the flap airfoil. The noise sources associated with this configuration are the interaction of the jet flow with the wing and flap surfaces (flap noise), the modified jet mixing, and the aft radiated engine internal noise. The preliminary test results (ref. 1) indicated that with an advanced quiet engine, the flap noise is the predominant source contributing to the community noise.

The USB configuration (fig. 1b) consists of a jet exhaust located on the upper surface of the wing. The jet flow follows the surface of the wing and large-chord flap by means of the Coanda effect. This generates additional lift due to the deflection of the jet flow and increase in wing/flap circulation. It is known that the thin exhaust jet from high aspect ratio slot nozzles can remain attached to surfaces having large turning angles. Small aspect ratio nozzle jets usually require either large nozzle pitch angles (canted towards the wing) or some mechanical devices to deflect the jet towards the wing surface and form a thin jet sheet on the surface. Examples of mechanical devices to aid the jet flow attachment are retractable deflectors mounted on top of the engine nacelle and side plates on the wing to provide a channel over the wing surface. The primary advantage of the USB configuration over the UTW configuration is the effective shielding from the community of the aft radiated engine internal noise and some of the jet mixing and jet-surface interaction noise that is generated upstream of the trailing edge by the wing and flap surfaces. Therefore, the flow-surface interaction noise generated in the vicinity of the trailing edge (flap noise) is a dominant source for the USB configuration.

Noise Sources

Based on the experimental and analytical studies, it may be hypothesized that the blown-flap related noise can be attributed to five source mechanisms which differ in their geometric location, fundamental aerodynamic noise source mechanism (monopole, dipole, or quadrupole) and/or in their propagation characteristics.

(1) *Flow Mixing Noise.* When the jet flow mixes with the ambient air, the unsteady phenomena that causes the radiated noise is the turbulence generated by the mixing process. The noise intensity, spectra, and directivity depend on the turbulence strength, the space-time scales of the local fluctuations, and the degree of inhomogeneity of the medium in the vicinity of local flow. The flow mixing noise is generated by jet mixing just downstream of the nozzle exit, wall-jet mixing, and trailing edge wake.

(2) *Impingement Noise.* Jet exhaust impingement on the wing flap/surfaces generates fluctuating pressures on the surface. The instabilities in the flow due to the flow impingement generates a quadrupole type of noise as discussed in reference 3. This noise source is very important in the case of the UTW configuration.

(3) *Flow/Edge Interaction Noise.* Experimental and analytical studies indicate that the turbulent flow encountering the wing/flap leading edges and trailing edges either generates additional noise or enhances the noise generated by the turbulent flow. The basic generating mechanism is not clear at the present time. For example, Hayden (ref. 4) postulates that the turbulence encountering the edge either accelerates or decelerates (depending on the situation) thus generating a dipole type of noise. Ffowcs Williams and Hall (ref. 5) analyzed the effect of the edge near the quadrupole source and concluded that the efficiency of quadrupole noise near the edge is much higher than without the edge.

(4) *Wall Jet Boundary Layer.* As the jet flow is deflected by the wing and flap surfaces, a wall jet will be formed. The inner layer will have a high mean shear and can produce a high turbulence level. The noise generated here, associated with the induced fluctuating pressures on the surface, is dipole noise.

(5) *Aeroacoustic Resonances.* If a periodic turbulence is produced in the jet, a feedback loop between the nozzle exit and the impingement point or the flap trailing edge could be established. This would result in an aeroacoustic resonance that can produce discrete frequency tones.

SYMBOLS

A_J	nozzle exit area
A_1, A_2	constants
a	ambient speed of sound
c	total chord length of wing and flaps
c_w, c_i	chord lengths of wing and i^{th} flaps, respectively
c_N	chord length of last (n^{th}) flap
D	hydraulic diameter of the nozzle
f_i	fluctuating force on the surface
f_K	one-third octave band center frequency corresponding to the K^{th} band
G	Green's function
h_w, h_i	distance of the vortex trajectory from the wing surface and i^{th} flap surface, respectively
h_{t_w}	distance between the vortex trajectory and the wing trailing edge
h_{t_i}	distance between the vortex trajectory and the trailing edge of the i^{th} flap
h_{ℓ_i}	distance between the vortex trajectory and the leading edge of the i^{th} flap
h_{ℓ_w}	distance between the vortex trajectory and the wing leading edge
K_w, K_i	amplitude function for fluctuating lift noise of wing and i^{th} flap, respectively
L_I	longitudinal distance of impingement point
L_{TE}	distance between the trailing edge and nozzle exit
M	jet Mach number relative to the ambient speed of sound
M_c	convection Mach number
M_I	impingement Mach number
M_N	jet Mach number relative to the speed of sound in the jet

M_T	Mach number at the trailing edge
N	number of flaps for UTW slotted flaps
P_L^2	one-third octave band acoustic mean-square pressure at fluctuating lift
P_{OAL}^2	overall acoustic mean-square pressure of fluctuating lift
P_{OAQ}^2	overall acoustic mean-square of quadrupole noise
P_{OAT}^2	overall acoustic mean-square pressure of trailing edge noise
P_Q^2	one-third octave band acoustic mean-square pressure of quadrupole noise source
P_{ref}^2	mean-square acoustic reference pressure
P_T^2	one-third octave band acoustic mean square pressure of trailing edge
R	far-field radius distance between the source and observer
S_K	Strouhal number corresponding to the one-third octave band center frequency, f_K
T_{ij}	stress tensor in the turbulence fluid
V_a	velocity of the aircraft
V_I	impingement velocity
V_J	jet exhaust velocity
V_n'	fluctuating displacement of volume
VR_I	ratio of impingement velocity to jet velocity
VR_T	ratio of trailing edge velocity to jet velocity
V_{TE}	flow velocity at the trailing edge
x_i, y_i	coordinates of the i^{th} flap leading edge
x_N, y_N	coordinates of the last (N^{th}) flap leading edge
x_t, y_t	coordinates of the flap trailing edge
x_w, y_w	coordinates of the wing leading edge
w	wall jet width at the trailing edge

α_w, α_i	polar angles relative to the upstream direction along the wing chord and i^{th} flap chord, respectively
δ	wall jet thickness at the trailing edge
δ_f	flap angle ($\delta_w + \delta_N$)
δ_i	i^{th} flap deflection relative to the wing
δ_J	jet flow angle with respect to jet axis
δ_N	flap angle of the last flap with respect to the wing
δ_r	nozzle roof angle (deflector angle or cant angle) with respect to the nozzle axis
δ_w	wing deflection relative to the jet axis
θ	polar angle relative to the upstream direction of jet axis
ρ	ambient density of air
ρ'	fluctuating air density in the far-field
ϕ	azimuthal angle

THEORETICAL BACKGROUND

Lighthill (ref. 6) in his pioneering work in 1952, presented the acoustic analogy of jet noise. In 1955, Curle (ref. 7) extended Lighthill's aerodynamic noise theory to include solid boundaries. In reference 7, it was shown that the effect of rigid surfaces in the turbulent medium is equivalent to a distribution of dipoles representing the force with which a unit area of solid boundary acts upon the fluid. For a stationary solid surface the fluctuating density in the far field is given by:

$$\rho' = \frac{\partial^2}{4\pi a^2 \partial x_i \partial x_j} \int_V \frac{T_{ij}}{R} \left(\bar{y}, t - \frac{R}{a}\right) d\bar{y} - \frac{\partial}{4\pi a^2 \partial x_i} \int_S \frac{f_i}{R} \left(\bar{y}, t - \frac{R}{a}\right) ds(\bar{y}). \qquad (1)$$

The reflection and diffraction effects of solid boundaries are incorporated in the forcing function f_i. It was pointed out in this analysis that for solid boundaries with a linear dimension smaller than the sound wave length,

the second term, representing the dipole source, will dominate. Thus, in many blown flap investigations following this analysis, the dipole source was assumed to be the dominant source.

Phillips (ref. 8) in 1956 extended this concept of dipole source to calculate the noise from Aeolean tones. Sharland (ref. 9) in 1964 analyzed the broadband noise from a small plate in a turbulent flow and extended the theory to predict the noise from the axial flow fans. Doak (ref. 10) in 1960 formulated the solution for the noise from a turbulent flow in the presence of a rigid surface. In this formulation, Green's function was selected to satisfy the boundary condition so that the normal derivative vanishes on the surface. Considering the complimentary part of the solution to the wave equation as zero, Doak has shown that the expression for fluctuating density in the far field is essentially the same as derived by Curle (eq. 1).

Powell (ref. 11) in 1960 considered the noise generated by aerodynamic instabilities of the boundary layer on an infinite plane surface. Using the image principle, he showed that the pressures exerted on a plane boundary are reflections of the quadrupole generators of the flow. Thus, it was argued that the surfaces have a purely passive role in noise generation and radiation. In reference 12, Powell investigated the radiated sound from a finite flat plate moving at zero incidence and conjectured that in addition to the reflected quadrupole noise from the turbulent volume of the boundary layer, the dipole noise, generated from the strips adjacent to the edges of the plate also radiate. According to the dimensional analysis, this edge noise should depend on the sixth power of mean velocity. Since the effective width of the strips along the edges increases with the increase in distance from the leading edge and decreases with the increase in flow velocity, it was argued that the radiated acoustic power depends on the velocity raised to a power between four and five.

Meecham (ref. 13) in 1965, extended Powell's analysis to include the effect of curvature of the rigid surfaces on noise generation. It was shown that the importance of the dipole source relative to the quadrupole depends

on the ratio of boundary layer thickness to the radius of curvature of the surface. In particular, if the radius of curvature is small compared to the boundary layer thickness, the dipole sound source could be important.

Hayden (ref. 14) in 1969 measured the velocity dependence, the directivity, the spectral distribution of the radiated sound of a wall jet on a finite plate. These results indicated that the dominant noise source is the dipole distribution along the trailing edge of the plate. Therefore, Hayden extended Powell's theory of edge noise (ref. 12) to calculate the wall-jet noise.

Ffowcs Williams and Hall (ref. 5) in 1970 developed a theory for the radiated sound field of a quadrupole source located near the trailing edge. From the basic Lighthill equation, an integral solution was formulated in terms of an appropriate Green's function. It was shown that for eddies near the edge, the far-field sound intensities of a quadrupole source can increase considerably as compared to the free quadrupole sources. The velocity exponent of the radiated sound intensity also changes from a typical value of 8 for a free quadrupole to a value of 5 for the quadrupole near the edge.

Chandiramani (ref. 15) in 1974 considered evanescent waves convecting past the trailing edge and their effect on radiated noise. Chase (ref. 16) in 1972, considered Ribner's fluid dilatation theory of aerodynamic sound and used the readily measurable pressure fluctuations as input in Lighthill's acoustic analogy. These two theories essentially consider that the disturbances generated in the flow convecting past the trailing edge must adjust themselves to the sudden change in environment. During the process of adjustment, pressure waves are released giving rise to acoustic radiation.

Goldstein (ref. 17) derived a generalized equation for sound generated by turbulent flow in the presence of solid boundaries. He considered the general integral solution of Lighthill's equation with solid boundaries and derived the fundamental equation governing the generation of sound in the presence of solid boundaries as,

$$\rho'(\bar{x},t) = \frac{1}{a^2}\int_{-T}^{T}\int_{V(\tau)} \frac{\partial^2 G}{\partial y_i \partial y_j} T_{ij}\, d\bar{y}\, d\tau + \frac{1}{a^2}\int_{-T}^{T}\int_{S(\tau)} \frac{\partial G}{\partial y_i} ds(\bar{y})\, d\tau$$

$$+ \frac{1}{a^2}\int_{-T}^{T}\int_{S(\tau)} \rho_o V_n' \frac{DG}{D\tau} ds(\bar{y})\, d\tau \qquad (2)$$

where T_{ij} is the stress tensor

f_i is the applied force

G is the Green's function satisfying the boundary conditions.

The first term represents the generation of sound by volume quadrupole sources, the second term represents the sound generated due to the force exerted on the surface by the fluid, and the last term represents the sound generated due to the volume displacement effects of the surface.

Tam and Reddy (ref. 18) recently argued that for the case of flow on one side of the rigid surface (similar to the blown flap), the velocity gradient just downstream of the trailing edge is very large. This velocity gradient of the sheared flow is associated with an intensified turbulence generation. Since it is known that noise is a result of turbulence generation, a theory is developed for the radiated sound from a two-dimensional shear layer of subsonic velocities typical of a blown flap configuration. It is hypothesized that the sound intensity in any direction and frequency is a function of typical velocity, V; the shear layer thickness, δ; flow Mach number, M; eddy convection velocity V_c; transverse velocity gradient; and the turbulence properties such as scale of anisotropy, longitudinal decay rate of spatial correlation function, and the lateral spatial correlation.

These theoretical developments have been helpful in understanding the various noise source mechanisms of blown flaps. However, the theories are not advanced enough to apply directly in flap noise prediction. Therefore, it is necessary to depend on experimental results in order to develop a reasonably accurate prediction method. In the following section the experimental investigations that are available in the open literature are discussed.

EXPERIMENTAL INVESTIGATIONS

Most of the jet-powered STOL aircraft noise tests conducted prior to 1970 were related to the near-field noise pertinent to the acoustic loading on the wing and flap surfaces. However, some basic flow/surface interaction noise studies applicable to compressor rotors, fans, and helicopter blades were reported in the literature. These results were helpful in providing guidance for the early blown-flap noise studies.

One early experimental study pertinent to blown-flap noise was conducted by Maglieri and Hubbard (ref. 19) in 1958. The primary purpose of these tests was to study the effect on noise characteristics of deflecting the jet flow by wing and flap surfaces. It was found that the directivity and spectra of the radiated sound of the jet were influenced by the presence of the wing and flap. This is illustrated in figure 2, where the spectra are compared for different flap lengths. The following observations were made: (1) The radiated sound of the jet flow was increased for moderate flap lengths. (2) For very long flaps ($\ell/h > 20$), the high frequency jet noise was reduced in the direction opposite to the flow side of the flap due to an effective wing/flap shielding. (3) The frequency of the peak sound pressure levels was decreased as the flap length is increased. Thus, it may be concluded that substantial noise was generated by the interaction of jet flow with the wing and flap surfaces. The directivity and spectral characteristics of the jet with the rigid surface is different from that of the jet alone.

In 1970, Hayden (ref. 4) investigated experimentally the noise characteristics of a wall jet flow on a finite length rigid surface. The experimental configuration consisted of a jet from a rectangular nozzle discharging tangentially on a flat plate forming a wall-jet on a finite length plate. The wall jet was divided into three different flow regions depending on the flow properties: (1) the potential core region, (2) the characteristic decay region, and (3) the radial decay region. It was found from these experiments that the characteristics of the radiated sound field depend on the location of the trailing edge with respect to the jet flow regions. The nondimensional spectra of the radiated sound of a wall-jet are compared in

figure 3 for the trailing edge in the radial decay region. The spectrum shape is broader for the trailing edge in the radial decay region than those of the trailing edge in the potential core and in the characteristic region. An empirical method was also developed in this reference to calculate the radiated noise of a jet flow over a flat plate for all three locations of the trailing edge. In a practical case of blown flaps where the jet is inclined to the wing surface and the flap is curved to deflect the flow, the trailing edge may be assumed to be in the radial decay region of the wall-jet. Therefore, the noise levels are calculated for the trailing edge in the radial decay region and compared with USB noise data in the next section.

Grosche (ref. 20) conducted extensive experimental investigations of the jet flow from slot nozzles over flat plates. The plate length, plate position with respect to the jet centerline, and jet exit velocity were varied. The primary observations of these experimental results were: (1) Additional noise was generated by the jet flow interacting with the surface as indicated in figure 4, (2) the noise generated by the flow surface interaction was increased as the plate length and the distance between the plate and jet reduced, (3) the noise intensity was increased approximately as the jet exit velocity raised to the power 6. Using the acoustic mirror technique, the noise source strength distribution along the longitudinal axis was also determined. The distribution of noise source strength is illustrated in figure 5 by showing the variation with longitudinal distance of the OASPL and the SPL at three octave bands with center frequencies of 4, 8, and 16 KHz. From these experimental observations, it was conjectured that the dominant noise source of the jet flap configuration was the acoustic dipole produced by the turbulent fluctuating pressures distributed along the trailing edge.

The other experimental investigations that are related to basic understanding of the noise generating mechanisms included the mean and turbulent flow measurements, near- and far-field noise measurements, and the correlations between the turbulence structure and the radiated sound field. For example, Reddy and Yu (ref. 21) have measured the spectral and spatial distribution of the radiated sound of a simplified external blown flap configuration with different flap lengths. Foss and Kleis (ref. 22) have

measured the vorticity and the radiated sound field of a jet impinging on a ridig surface and have developed an expression relating the sound to the vorticity. Olsen, Miles, and Dorsch (ref. 3) have measured the correlations of the near-field pressures, fluctuating velocities in the flow, and surface fluctuating pressures with the radiated acoustic pressures to delineate and rank the various noise mechanisms.

In addition to the fundamental studies discussed above, various aircraft companies and NASA research centers have conducted extensive blown-flap noise tests during the last few years. These tests were in response to the established need for a jet-powered short-haul aircraft and were therefore primarily configuration oriented. Simulated models of various sizes were tested in outdoor test facilities, anechoic rooms, wind tunnels, and open-jet facilities. The reports and technical papers containing the results of these studies are summarized in table 1. These data were utilized in the development of quiet integrated propulsion system and powered-lift noise prediction schemes. The following paragraphs contain the discussion of these tests.

UTW Configuration

Tests were conducted to study the effect of various geometric and operational variables on the noise characteristics (e.g. refs. 1, 28, and 29). The spatial and spectral distributions of the noise were measured to establish the general trends and effects of the variables. In most of the tests, unheated compressed air was used for the jet flow. The nozzle shapes tested were simple conical with simulated mixed flow, velocity decayer type which include the multi-tube and multi-lobe and the ejector type. Generally, it was found that the velocity decayer nozzles are the quietest, due to reduced impingement velocity.

The wing and flap systems studied consisted of slotless flaps, two-flap (two slots) configurations and three-flap (three slots) configurations. Slotless flaps were tested primarily to study the effect of slots on noise. The two-flap and three-flap configurations were designed to provide good low-speed

Table 1 - Blown Flap Noise Tests

AUTHOR(S) & REFERENCES	YEAR	CONFIGURATION: NOZZLE	CONFIGURATION: NO. OF FLAPS	CONFIGURATION: FLAP ANGLE	APPROX. MODEL SIZE	OPERATING CONDITIONS: NPR/V_J	OPERATING CONDITIONS: JET TEMP	TEST FACILITIES	REMARKS
Dorsch, R. G., et al. AIAA 71-745	1971	Circular, D = 2"	2	0°, 20° & 60°	1/16	1.1 to 2.2	Ambient	Static Outdoor	Full-scale noise levels were estimated using jet noise scaling laws → UTW configuration.
Goodykoontz, J. et al. NASA TM X-67938	1971	Multi-lobe Nozzle	2	60°	1/2	296 m/s	Ambient	Outdoor	Preliminary tests to study the feasibility of reducing noise by multi-lobed nozzle.
Dorsch, R. G., et al. AIAA 72-129	1972	13" D Circular 8.5" and 23.25" Bypass	2	0°, 20°, 60°	1/2	400 - 100 ft/s.	Ambient	Static Outdoor	UTW Configuration - Scaling laws were verified.
Falarski, et al. NASA TM X-62251	1972	4 Coannular Nozzles JT15D Engines	3 for UTW	0°, 40°, and 55°	--	240 m/s	--	Ames Large-Scale Wind Tunnel	UTW Configuration - Nacelles were not treated. Possibly the fan and core noise were important.
Gibson, F. W., et al. NASA TN D-6710	1972	Circular	0, 2	27°, 55°	1/16	1.1 - 2.2	Ambient	Anechoic Room	Free-field sound was measured and compared with internally blown flap, and augmentor wing configurations.
Goodykoontz, J. et al. NASA TM X-68021	1972	Multi-lobed Nozzle $A_N = 1255\ cm^2$	2	30°, 60°	1/2	1.2 - 1.7 172 - 284 m/s	Ambient	Outdoor	UTW - For larger flap angles, noise was reduced by about 6 dB. For a smaller flap angle - no difference.
Dorsch, R. G., et al. AIAA 72-1203	1972	Circular Slot With Deflector Canted Slot With Side Plate, D-shaped and Multi-lobed	2	0°, 20°, 60°	1/16		Ambient		USB Configuration - Scaling laws were established. Lift and thrust were also measured.
Goodykoontz, J. et al. NASA TM X-2638	1972	Mixer type, $D_e = 6$ cm Circular, eight lobed, $D_{e_2} = 4.1$ cm	2	0°, and 20°, 60°		186, 274, 296, & 334 m/s	Ambient	Outdoor Facility	UTW → Mixer nozzles were simulated with orifice plates. Noise data was obtained for two different-size mixer orifices.
Olsen, W., et al. NASA TN D-6636	1972	Circular with 5.2 cm D	2	0°, 20°, 60°	1/16	1.1 - 1.7	Ambient	Outdoor Facility	UTW Configuration - Nozzle longitudinal and transverse positions were varied. The directivity and spectra were obtained.
Putnam, T. W. & Lasagna, P. L. AIAA 72-664	1972	Daisy Nozzle Conical Nozzle	2	35°, 60°	Full-scale Turbofan Engine and Aircraft Wing	Varied (?)	(?)	Outdoor Test Facility	UTW configuration was tested outdoors using a CF700 turbofan engine.
von Glahn, et al. NASA TM X-68159	1972	Circular, AR5 and AR10	--	35°, 75°	1/16	180 - 280 m/s	Ambient	Outdoor	USB Configuration → Various flow attachment devices were used. Flyover noise data was obtained.
von Glahn, et al. AIAA 72-792 (NASA TM X-68102)	1972	Velocity decay characteristics of a circular nozzle convergent nozzle, 6-tube mixer nozzle, and slot nozzle to be used in blown flap propulsion systems (static and with forward velocity) are presented.							
Falarski, H. D. et al. NASA TM X-62319	1973	Two JT15D-1 Engines With the Corrugative Type Nozzles	--	30°, 75°	1/2 (?)	144 - 254 m/s	--	Wind Tunnel and Outside Static Test Facility	Large-scale USB model with two turbofan engines was tested in wind tunnel for flight effects and static tests outdoor facility.

Table 1 - Cont'd.

AUTHOR(S) & REFERENCES	YEAR	CONFIGURATION: NOZZLE	CONFIGURATION: NO. OF FLAPS	CONFIGURATION: FLAP ANGLE	CONFIGURATION: APPROX. MODEL SIZE	OPERATING CONDITIONS: NPR/V_J	OPERATING CONDITIONS: JET TEMP	TEST FACILITIES	REMARKS
Goodykoontz, J. et al. NASA TM X-2776	1973	Mixer-type Nozzles with A_N = 1255 and 1438 cm^2	2 and 3	20°, 60°	(?)	170 - 290 m/s	Ambient	Outdoor Facility	Two mixer nozzles and two wing models were used in these tests of UTW configuration.
Olsen, W. A. & Friedman, R. NASA TM X-2871	1973	Eight-lobe Mixer Nozzle With Deflector Slot Effect was also evaluated	Deq = 6.1 cm	20°, 60°	1/10	1.25 - 2.0	Ambient	Outdoor Facility	USB Configuration - Effect of multi-lobed nozzle on noise characteristics was studied. These results were compared with that of a conical nozzle.
Reddy, N. N. and Swift, G. ASA Paper - Fall Mtg.	1973	Velocity Decayer Nozzle, A_N = 3.77 $in.^2$	3	35°, 65°	1/16	Varied (?)	Ambient	Anechoic Room	UTW configuration was tested in the anechoic room to measure far-field sound.
Reshotko, M., et al. AIAA 73-631 (NASA TM X-68246)	1973	Convergent Nozzle D = 13" With and Without Deflection	2 Slots Open and Closed	20°, 60°	1/2.5	550 to 1000 ft/s.	Ambient	Outdoor Facility	USB tests using circular nozzle with and without deflector.
Reshotko, M., et al. AIAA 73-1030	1973	D-Nozzle 3.14 $in.^2$ Area	2 Slots Open and Closed	20°, 60°	1/16	600 to 950 ft/s.	Ambient	Outdoor Facility	USB tests were conducted to measure the far-field noise and the static performance.
Samanich, N. E. AIAA 73-1217 NASA TM X-71466	1973	Convergent Coannular Lobed Nozzles 927 $in.^2$	3	40°, 55°	Full-Scale	530 to 950 ft/s.	800° to 1050°F	Outdoor Test Facility	UTW configuration using TF-34 turbo-fan engines - Internal noisw was highly suppressed.
Cole, T. W., et al. NASA CR-114757	1974	AR8 and AR4 A_N = 17.6 $in.^2$ AR4 with Deflector	--	30°, 50°, and 70°	1/5	550 to 950 ft/s.	Ambient	Outdoor Facility	USB and hybrid (combination of USB and IBF). Far-field acoustic and performance data were obtained.
Jones, W. L. et al. SAE 740467	1974	Coannular Mixer and Velocity Decayer	3 for UTW 1 for USB	0°, 40°, 55° for UTW 40° for USB	Full-Scale	400 to 950 ft/s	~800°R	Outdoor Facility	Full-scale UTW and USB tests were conducted using highly suppressed TF-34 engine.
Goodykoontz, J. et al. AIAA 74-192	1974	Multi-lobed Nozzle	2	0°, 20°, 60°	1/2	172 to 296 m/s	Ambient	Outdoors	UTW - Noise reduction was obtained for landing flap settings, but not for takeoff flaps.
Falarski, M. D., et al. AIAA 74-1094 (Also J. Aircraft, vol. 12, No. 4, July 1975 TP600-604)	1974	Coannular for UTW Rectangle with AR5 for USB	3 for UTW 0 for USB	30° - 75°	1/4	650 - 800 ft/s.	--	Ames Large-Scale Wind Tunnel	Noise characteristics were measured using 2 JT15D-1 engines in the large wind tunnel - Both UTW and USB configurations were tested.
Goodykoontz, J., et al. AIAA 75-476	1975	Circular, 2" D and Nozzle	2	20°, 60°	1/16	208, 257 & 290 m/s	Ambient	Outdoor Free-Jet Facilities	UTW Configuration - Flight effects were studied using 13" diameter free jet.
Heidelberg, L. J. et al. SAE 750609	1975	A_N = 1109 $in.^2$, AR4 Slot and Circular with Deflector 35.1" Dia.	--	8°, 40°, 75°	TF34 Engine Full-Scale	600 ft/s 760 ft/s	800°R	Outdoor Facility	USB - Far-field noise and velocity surveys were measured using highly suppressed TF-34 engine.
Pennock, et al. NASA CR-134675	1975	Circular Mixer with Ejector	3	40°, 55°, 33° 65°	1/5 & 1/10	180 - 285 m/s	Ambient	Outdoor Facility and Wind Tunnel	Several configurational variations of UTW were investigated including noise reduction techniques - Full-scale airplane noise levels were estimated.
Preisser, T. S. and Fratello, D. J. AIAA 75-473	1975	2 AR = 6 Rectangular Nozzles (0.96 x 0.16 m) JT15D Engine	--	20°, 60°	Aero Coannular	120 - 280 m/s	(?)	Wind Tunnel & Static	Directivity and spectra of USB were obtained for static case and for low forward velocity case.

Table 1 - Concluded.

AUTHOR(S) & REFERENCES	YEAR	CONFIGURATION: NOZZLE	CONFIGURATION: NO. OF FLAPS	CONFIGURATION: FLAP ANGLE	APPROX. MODEL SIZE	OPERATING CONDITIONS: NPR/V_J	OPERATING CONDITIONS: JET TEMP	TEST FACILITIES	REMARKS
Reddy, N. N. and Brown, W. H. AIAA 75-204	1975	AR8 Rectangle 20.25 cm^2	--	40°	1/16		120 - 295 m/s	Anechoic Chamber	USB model was tested in the anechoic room to understand the noise characteristics.
von Glahn, U., et al. NASA TM X-71807	1975	AR5 with $A_N = 20.4$ cm^2	--	0° Flat Plate	--	203 m/s	Ambient	Outdoor Facility	Nozzle on the flap surface was tested for different nozzle angles to study the effect of attachment and partial attachment on the surface.
von Glahn, U., et al. AIAA 76-499	1976	Conical with D = 5.2 cm	--	20°, 60°	1/16	200 - 259 m/s	Ambient	Outdoor Facility	USB Configuration - The effect of various deflector geometry were studied for propulsive and acoustic characteristics.
von Glahn, U., et al. AIAA 76-521	1976	AR5 $A_N = 20.4$ cm^2	--	20°, 60°	1/16	200 - 266 m/s	Ambient	Outdoor Facility	USB tests were conducted to study the nozzle geometry including roof angle and inside wall cutback - Wing size and flap deflections were also included.
Hayden, R. E. AIAA 76-500	1976	6 cm x 24 cm AR-4 Nozzle With Deflector	--	60°	Aero Coannular Model	1.265 - 207.3 m/s	Ambient	Acoustic Wind Tunnel	USB - Noise reduction tests by trailing edge treatment - static tests.
Olsen, W., et al. AIAA 77-23 NASA TM X-73588	1977	QCSEE and Canted Conical	--	30°, 75°	1/11.5 and 1/28	150, 225 m/s	Ambient	Outdoor and Anechoic Chamber	USB - Spatial and spectral distribution were measured - Flap length, V_J, and nozzle geometry were varied.
Brown, W. H., et al. NASA CR-145143	1977	Several Nozzles	--	0°, 30°, 45° and 60°	1/16 and 1/5	180 - 285 m/s	Ambient	Anechoic Room and Outdoors	USB with several variables. Extensive data base was developed for various static configurations - Flight effects were also studied.

performance. The flap angles were varied in all these tests to cover the range of cruise, takeoff, and landing conditions.

Vertical and longitudinal positions of the nozzle exit, with respect to the wing and flap system, were varied. The nozzle pressure ratios were varied to cover the operating range. Since takeoff and landing modes are critical from the noise point of view, low jet velocities are more important and therefore most of the tests were conducted at low nozzle pressure ratios. In many of these tests the velocity profiles, the flow turning efficiency, and the lift and drag measurements were also made.

Flight effects were investigated by conducting tests in wind tunnels and free-jet facilities. Large-scale models were tested in the NASA-Ames 40' x 80' wind tunnel and in the Lockheed-Georgia low-speed tunnel (refs. 29 and 30). Small-scale models were tested in the NASA-Lewis outdoor free-jet facility (ref. 31) and United Technologies Research Center (UTRC) anechoic free-jet facility (ref. 32). In addition to the acoustic measurements, the aerodynamic characteristics were also measured in these tests. These results were utilized in developing the noise prediction method for the UTW configuration.

Noise reduction techniques for blown-flaps were evaluated by testing the static small scale models with modified flaps (porous flaps, sawtooth trailing edge, etc.) and secondary blowing at the trailing edge. In order to optimize the noise reduction with performance, systematic tests were conducted at Lockheed-Georgia (ref. 30) using a nominal 1/5-scale model with two- and three-flap configurations in the outdoor static test facility. A nominal 1/10-scale model with one- and three-flap configurations was tested in the wind tunnel. These results were used in estimating the flap noise of a full-scale aircraft in flight assuming the models are geometrically similar to the full-scale aircraft.

In addition to these simulated blown-flap model tests, the acoustic data were also obtained with full-scale model static tests (ref. 33). The exhaust jet supply for these tests was from a noise suppressed TF-34 engine with 6:1

bypass ratio. Configurations tested with this engine were a three-flap configuration with a variety of coannular, decayer, and mixer-decayer nozzles and two different flap lengths. These data include all full-scale effects that might be associated with viscous mixing phenomena of the exhaust jet. They also contain the compressibility, turbulence, and refraction effects that might be caused by a hot-core jet containing engine combustion products.

USB Configuration

In 1972, preliminary tests were conducted at NASA-Lewis Research Center to explore the possible use of the USB configuration for STOL operations (ref. 34). These initial exploratory tests were conducted using small-scale models with slotted flaps. It was found that the unslotted flap configuration would have better low-speed performance (takeoff and landing) and low-noise characteristics. Therefore, all subsequent tests were conducted using unslotted flaps.

An extensive test program was conducted to evaluate the effect of various geometric and operational parameters on noise characteristics (see ref. 1). Figure 6 illustrates the community noise levels for USB and UTW configurations. From this figure it is obvious that the USB configuration is quieter than the UTW configuration for a typical STOL aircraft. Since the preliminary tests indicated that the nozzle shape was important, the following nozzle shapes were tested: Rectangular with different aspect ratios, D-shaped, elliptical, circular, and variable geometry for which the side walls can be opened. In some cases the jet flow was deflected towards the wing surface by either using an external deflector vane or canting the nozzle towards the wing. The effect of external deflector on noise characteristics has been extensively investigated at NASA-Lewis Research Center (e.g. see ref. 28). The effect of the flow deflector on one-third octave band spectra is shown in figure 7. It may be seen that the deflector generates substantial noise, but because of the shielding effect, this noise was reduced in the direction below the wing when the wing and flap are introduced. The flap angles were varied to cover the range of cruise, takeoff and landing operations. Larger flap angles (larger

flow turning angles) require thinner jets in order to have an attached flow. Therefore, the flap angle and the nozzle shape are interrelated to some extent. Vertical and longitudinal positions of the nozzle exit with respect to the wing were also varied. The nozzle pressure ratio was varied to cover the range of operations. It was found that the flap radius of curvature, nozzle shape, flap length, and flap angle should be together optimized to provide the maximum low-speed performance and the low noise configuration.

Lockheed conducted an extensive test program on USB configurations during the development of quiet short-haul aircraft (ref. 35). A hybrid system consisting of a jet flap (blowing at the trailing edge) and a jet exhaust on the upper surface of the wing as shown in figure 1c was also tested. The data were analyzed to estimate the full-scale aircraft noise levels. Recently (during 1974-76), Lockheed conducted a systematic test program to study the noise characteristics of USB configurations (ref. 36). The effects of various geometric and operational parameters on the flap noise were investigated using small-scale models under static conditions in the anechoic room. Conical nozzle, rectangular nozzle with different aspect ratios, D-shaped nozzle, elliptical nozzle, and variable geometry nozzles were used in these tests. Flap length, flap angle, and nozzle pressure ratio were also varied. All these parameters were varied systematically to study the individual parametric effects separately. The velocity profiles, flow spreading characteristics, flow turning capabilities, the low-speed performance characteristics, and the radiated sound field were measured in these tests. In addition to these small-scale model tests, some tests were conducted using large-scale geometrically similar models in the outdoor test facility to establish scaling laws.

Bolt Beranek and Newman, Inc. (BBN) has conducted tests to further the understanding of noise source mechanisms and to develop noise reduction techniques (ref. 37). Nozzle and flap modifications were investigated as a way to reduce the noise with minimum performance penalty. It was found from these tests that the use of a porous flap can reduce the noise by about 10 dB with a performance loss of about 2%.

The effects of aircraft forward speed (flight) were investigated at NASA-Lewis (ref. 38) NASA-Ames (ref. 39), BBN (ref. 40), UTRC (ref. 23), and Lockheed-Georgia (ref. 30) by testing scaled models in the free-jet facility and the large low-speed wind tunnel. These experimental data were used in establishing the trends of various parameters on the noise characteristics.

Recently, full-scale model tests were conducted at NASA-Lewis similar to that of the UTW configuration tests using the noise-suppressed TF-34 engine with a circular nozzle, a rectangular nozzle of aspect ratio of 4, and a special mixer nozzle (ref. 41). The circular nozzle was used with an external deflector, and the rectangular nozzle was canted at 20° towards the wing. The mixer nozzle consisted of twelve lobes through which the engine core exhaust was passed to provide a nominally uniform engine exhaust. Each model was tested with two flap lengths. The short flap configuration was tested with an unswept wing for three flap angles (8°, 40°, or 75°). The long flap was tested with a swept wing and a flap angle of 25°.

NASA-Langley has conducted wind tunnel and static tests of a large-scale USB model of an aircraft configuration with turbofan engines in the full-scale wind tunnel. The directivity, the spectral distribution, and the effect of freestream velocity were investigated.

FLAP NOISE PREDICTION METHODS

In recent years several blown-flap noise prediction schemes have been developed by different investigators. In all these methods theoretical considerations of flow-surface interaction noise, experimental observations, and heuristic arguments were utilized in developing either empirical or semi-empirical formulas to predict noise. The different noise prediction schemes use test data from different configurations and facilities to establish empirical constants. Since the blown-flap system is a complex configuration, it is not possible to use theoretical or analytical arguments exclusively to justify any of the available prediction schemes. The best way of evaluating the various blown-flap noise prediction methods is by comparing the predicted

noise (magnitude, directivity, and spectra) with flight test data. Unfortunately flight test data of an aircraft with a blown-flap integrated propulsive system are not available at the present time. However, as soon as the data from the flight tests of the NASA QSRA and the Air Force AMST are available, these predicted results may be compared. An alternative method of evaluating these prediction schemes is to compare with model test data not used in the data base for the development of the prediction method. In this section, various flap noise prediction schemes are discussed and evaluated by comparing with the test data.

ANOP Method

One of the early flap noise prediction programs was developed by Dorsch, Clark, and Reshotko (ref. 42) of NASA-Lewis Research Center. This method was adapted by ANOP as a computer program module to be used in the total aircraft noise prediction. This prediction scheme was primarily based on the analysis of limited test data for static models with simulated cold air flow jets. It was observed from these tests that the radiated noise was varied as velocity raised the power 6 in the forward quadrant (below the wing) and velocity raised to the power 8 in the direction close to the flap angle (deflected flow direction). The peak flyover noise was generally dominated in the first quadrant by the dipole sources. The theoretical considerations based on Curle's analysis of a turbulent flow in the presence of rigid boundaries (ref. 7) and the above-mentioned observation of the directivity and velocity dependence have led to the hypothesis that flap noise is a combination of two basic generating mechanisms, viz. quadrupole and dipole noise sources. The quadrupole noise is generated from the deflected and distorted jet exhaust adjacent to the flaps and downstream of the trailing edge with a directivity peaking at an angle of about 25° with respect to the deflected flap chord line. The dipole noise is generated by the fluctuating forces from the turbulent flow adjacent to the rigid surfaces with a directivity peaking at about 90° with respect to the deflected flap chord line. It was also recognized that other dipole sources will contribute to the radiated sound field. These are a result of (1) the leading edge, (2) the trailing edge, (2) scrubbing, and (4) flow separation. The frequency and directivity

characteristics of each source depends on the geometry and flow condition. However, since the theoretical and experimental studies were not advanced enough to separate the noise contribution from each of the sources, the contributions from all the sources were combined together as a single dipole source with a significant contribution in the directions below the wing. Even though it was recognized that jet mixing (quadrupole) noise is an important source in the direction close to the flap angle, this was not considered as a separate source in the prediction method; instead, the dipole noise was extrapolated to these directions and the magnitude and spectra were adjusted to match with the measured data.

The effect of various geometrical and operational variables of the configuration, and the aircraft forward speed are incorporated as corrections for the reference configuration. The directivity is computed as an incremental value to be added to the value at the reference direction. Since the jet exhaust parameters of the blown flap configuration were readily available during the preliminary design stage, these parameters were used in the noise correlation. The OASPL is computed for the reference configuration in the reference direction as a function of effective jet exhaust velocity and total nozzle exit area. The directivity functions were determined empirically using the measured data. Since this prediction procedure is basically derived as a dipole noise, it is expected that the prediction is less accurate for the cases wherein the quadrupole noise could contribute to the total noise. For example, for the configuration of small flap angles and in the direction close to the flap angle, this method is not very accurate. One-third octave band spectra were determined by using an empirically derived spectral shape based on Strouhal number. The Strouhal number is based on the effective exhaust velocity, V_E, and the equivalent diameter, $D_E = \sqrt{4A_T/\pi}$ and defined as fD_E/V_E. The aircraft motion effects were determined using limited test data from free-jet facilities and wind tunnels. The dynamic amplification and Doppler frequency shifts due to the motion of the source relative to the observer are determined based on Lighthill's theoretical analysis. The effect of the relative airspeed on source strength variation is determined empirically from the test data.

From the noise standpoint, several important differences between UTW and USB installations were recognized. Figure 8 illustrates the major differences in noise source mechanisms due to the installation of an engine with respect to the wing and flap system. It may be recognized from these figures that the jet mixing noise, aft-radiated engine internal noise, and the impingement noise are reflected by the wing and flap surfaces towards the community (below the wing) in the case of the UTW configuration; but for the USB configuration, noise from these sources is reflected away from the community. Generally, multi-slotted flaps are used in the case of the UTW and therefore noise is generated by the interaction of the flow with several leading edges, trailing edges, flap segments and flow through the slots. Since a slotless wing/flap system is used for the USB configuration, these sources are not present. However, wherever the external deflectors are used for USB, additional deflector noise is generated. But, this deflector noise source is generated above the wing and upstream of the trailing edge and therefore is shielded from the community.

Because of these differences between the UTW and USB configurations, the magnitude, directivity, and spectral distribution are different for the two configurations. However, the principle on which the empirical relations are derived is the same. The spectral shapes were given in the graphical form for both configurations. For the UTW configuration, the spectral shape in the flyover plane and wing-tip sideline planes are given. For the planes between the flyover and sideline, interpolation was recommended. In the case of the USB configuration, the polar directivity is the same in any plane between flyover and sideline. It was also suggested that the USB flap noise spectra in the direction below the wing are not very sensitive to the nozzle configuration and the flow attachment devices as a result of the wing-shielding effects. At the wing-tip sidelines, however, the shielding effect is negligible and therefore the flow attachment devices and nozzle shape could have a significant effect on the spectral shape.

This prediction method has been evaluated by Fink in reference 43 by comparing with static test data. Typical comparisons of the spectra and directivity of OASPL are shown in figure 9. From these results, it is clear

that for the UTW configuration this method underpredicts the noise levels in the flyover plane by about 3 to 5 dB, depending on the flap angle. Directivity shape compares well with the measured data. The spectrum appeared to have shifted to higher frequencies by two one-third octave bands (see fig. 9b). In the sideline plane, however, the prediction is in poor agreement for small flap angles (not shown). For the USB configuration, the predicted directivity shape at low velocities in the flyover plane compared well with the test data. But the test data shows that the directivity is a function of jet exhaust velocity unlike the assumption of velocity dependence used in the prediction method. These qualitative observations were found to be true for several configurations (QCSEE nozzle, vane deflected circular nozzle and canted rectangular nozzle with AR = 4). The difference between the prediction and the test data of the USB configuration is probably due to the assumption of the dominant quadrupole noise contribution.

Lockheed-Georgia/FAA Method

Lockheed-Georgia Company has developed a noise prediction method for jet-powered V/STOL aircraft under contract to the FAA in reference 44 and 45. These aircraft utilize an integrated propulsive-lift system. UTW and USB blown flaps are two of the six different jet-propulsive concepts for which noise prediction schemes were developed. The early version of the prediction procedure was published in 1973 (ref. 44). In this version, very limited acoustic data were used in deriving the empirical formulae. The effects of geometric variables such as nozzle vertical and axial positions with respect to wing and flap systems, nozzle pitch angle and number of slots were included. This method was refined and modified in reference 45 to include the latest data base and analytical developments. Since there was a considerable interest in the USB concept of powered-lift system at that time, the data base for this configuration was broadened after publication of the first version of the prediction scheme. Thus, this broad data base and the advancements in the flow/surface interacton noise prediction were included in the second version of the prediction method which was published in 1975. Therefore, by necessity this recent method was strongly directed towards USB configurations.

Since this method is oriented towards predicting the noise of an aircraft with a propulsive-lift system, the various aircraft noise sources contributing to the community noise are included. For example, (1) internally generated engine noise, (2) jet mixing noise, and (3) nonpropulsive noise were included in addition to the lift-augmentation noise. Atmospheric attenuation, effect of aircraft motion, aircraft flight profile, ground reflections, extra ground attenuation, shielding of sound by aircraft components, and noise reduction techniques were also incorporated. Since the scope of the present report is to review blown flap noise prediction methods, the following mechanisms of blown-flap noise are discussed: (1) impingement noise defined as the noise generated by the jet flow impingement on the wing and flap surfaces, (2) wall-jet mixing noise defined as the noise generated by the wall-jet turbulent flow on the wing and flap surfaces (not to be confused with the wall-jet boundary layer noise), (3) trailing edge noise, defined as the noise generated by the turbulent flow leaving the edge, and (4) trailing edge wake noise defined as the noise generated by the jet flow in the trailing edge wake. The impingement noise, wall-jet mixing noise, and trailing-edge wake noise were assumed to vary as velocity raised to the power 8. The trailing edge noise was assumed to be proportional to velocity raised to the power 5. The magnitude, directivity and spectral distribution are derived using the test data.

Jet mixing noise was not considered as a part of blown-flap or lift-augmentation noise. Instead, this noise source was treated separately. The prediction of jet noise is based on the method developed by Stone for ANOP in reference 46. The magnitude of this noise was arbitrarily reduced by 7 dB so that the jet noise component of the aircraft noise will be smaller than the blown-flap noise component as observed in the experiments. This was accomplished by reducing the numerical value of the constant, K, used in reference 46 from 141 to 134. This reduction of jet noise was justified since the undeflected jet mixing volume is smaller than the free isolated jet mixing volume.

This prediction method was evaluated by Fink in reference 32 and 43, by comparing the predicted noise for several models with test data. Typical comparisons are shown in figure 10. For additional comparisons, see reference 32. For large flap angles (approach flaps), this method generally overpredicts

the OASPL in the flyover plane. The spectrum shape is in good agreement with the measured data. For takeoff flaps (small flap angles), this method underpredicts by about 8 dB.

BBN Method

Hayden (ref. 47) developed an empirical relation for the radiated noise of wall jets from a rectangular nozzle over a finite flat plate as a function of wall jet width, thickness, and mean velocity at the trailing edge of the plate. The overall SPL is given by

$$OASPL = 10 \log (\delta w V_t^6) - 20 \log R + 10 \log [\sin^2\theta \cdot \cos^2\phi/2] + K \qquad (3)$$

where
- δ is the wall jet thickness at the trailing edge,
- w is the wall jet width at the trailing edge,
- V_t is the velocity at the trailing edge,
- R is the distance between the measuring point and the trailing edge
- θ, ϕ are the angles in two planes,
- K is a constant depending on whether the trailing edge is in the core region, characteristic decay region, or radial decay region of the jet.

The spectral distribution is given by three graphs derived empirically from the data. The spectral distribution is also assumed to depend on the location of the trailing edge with respect to the jet exhaust. This equation was derived based on the hypothesis that the noise is generated as a dipole by the turbulence convected past the trailing edge. The noise generated in the wall jet upstream of the trailing edge was neglected.

In order to evaluate the applicability of this formula for the flap noise, recently obtained USB experimental results from reference 36, were compared with the prediction. This comparison is shown in figure 11. It is obvious from this figure that this empirical relation overpredicts the noise levels. The noise sources and their generating mechanisms for USB are

probably different from that of a simple wall jet for which the noise prediction method was developed. Therefore, it is apparent that this formula is not adequate for flap noise prediction.

Boeing Method

Boeing Commercial Aircraft Company developed an aircraft noise prediction method in 1973 under contract to NASA-Ames Research Center (ref. 48). Flight profile calculations were included in this prediction procedure so that the ground noise levels may be calculated for an aircraft in flight. This is an empirical procedure developed for turbo-jet, turbo-prop, V/STOL, and helicopter-type aircraft. The UTW blown flap is one of the powered-lift configurations of V/STOL aircraft for which the noise prediction program was presented in this reference. The data base used in the development of this procedure is the preliminary test results of NASA-Lewis Research Center (refs. 1 and 2). The following blown-flap noise mechanisms were assumed: (1) impingement noise, (2) modified jet mixing noise, and (3) shear layer noise at the trailing edge. It was conjectured that when the flaps were deployed (takeoff and landing operations), the impingement noise was more dominant than any other source and when the flaps were retracted (cruise condition) the jet noise dominates. Therefore, during takeoff and landing operations, the impingement noise alone is considered, and during cruise jet mixing noise alone was considered. The jet noise was predicted in a similar way as that for a free jet without any influence of wing and flap surfaces. The OASPL of the impingement noise was assumed to vary as impingement velocity raised to a power between 5 and 6 depending on the direction of propagation. The impingement velocity was calculated as a function of both jet velocity and aircraft velocity for an aircraft in flight. Doppler corrections were also applied to the noise sources as applicable for the dipoles (impingement noise) and quadrupoles (jet mixing noise).

In order to improve the prediction scheme, Filler of Boeing (ref. 49) in 1976 developed a semi-empirical equation to calculate blown flap trailing edge noise based on Chase's theoretical analysis (ref. 16). A generalized model

for surface fluctuating pressures was assumed and subsequently far-field noise data were used to fit the surface pressure spectra. This method was evaluated by calculating the noise spectra for a USB static model tested recently at Lockheed-Georgia Company (ref. 36) and comparing with the Lockheed test data. A typical comparison is shown in figure 12. It is evident from these results that the prediction compares favorably in the low frequency range only. At mid frequency, it overpredicts by about 10 dB. Therefore, it is concluded that this prediction method (ref. 49) must be further improved.

Lockheed-Georgia/Langley Method

Recently (1977) Lockheed-Georgia Company has developed an acoustic data base for USB configurations (ref. 36). In this program, various small-scale and large-scale models were tested in the anechoic room and outdoor test facility to measure the far-field sound. Aircraft forward speed effects were investigated by conducting tests in the free-jet facility. In addition to the acoustic data, flow characteristics were also measured. The spatial and spectral distribution of radiated sound, and the flow characteristics were analyzed to aid in determination of the noise generating mechanisms. It was concluded from these results that the dominant noise is generated in the region just downstream of the trailing edge where the transverse velocity gradients are large. Therefore, a theory was developed in reference 18 for the radiated noise from a two-dimensional shear layer and applied to the USB configuration. The theoretical results were compared with the measured data and the agreement was favorable for a particular configuration. However, at the present time, the theory is not advanced enough to predict the noise for a general configuration and to evaluate the effect of different geometric and operational variables. Therefore, an empirical prediction method was developed in reference 50 based on the recent data base (ref. 36) and analytical developments.

This empirical prediction procedure does not consider different noise source mechanisms of a USB blown flap; instead the flap noise is treated as a single source of an aircraft with a powered-lift system. The test data

indicated that the primary variables controlling the far-field noise were the nozzle exit area, jet exit velocity, and the flow path length. The spectral distribution is a function of flow length (length along the wing/flap surface between the nozzle exit and the trailing edge), jet exit velocity, and flap angle. The magnitude of acoustic pressure is a function of jet exit velocity, nozzle area, nozzle aspect ratio, flow length, and hydraulic diameter. The velocity exponent and the spectral distribution of the radiated noise were found to vary with the direction of propagation. Flight effects are included in the prediction as a correction factor.

The predicted noise was compared with the data of several models that were not a part of a data base considered in the development of the prediction program. Typical comparisons are shown in figures 13 and 14. Predicted values for small-scale model tests are slightly less than the test results as shown in figure 13. However, considering the difference in test setups and configurations, including the nozzle geometry upstream of the exit, the comparison is favorable. Another comparison with the full-scale model static test data of reference 33 is shown in figure 14. The model utilized a highly suppressed TF34 engine with mixed flow and an aspect ratio 4 nozzle exhaust. The prediction method underpredicts the noise levels for this particular configuration. This disagreement between the prediction and the large-scale model data is probably due to the difference in the turbulence structure between the real engine exit and the air jet exit.

Since this prediction program was derived from the data of small-scale static model tests, the following range of parameters were recommended for limitations:

Nozzle shape - Rectangular with aspect ratio between 2 and 8, circular, elliptical, and D-shaped.

Flap deflection - 0 to 60°.

Nozzle exit chordwise location - 20% to 35% chord.

Nozzle vertical position - nozzle exit on the surface.

Jet exit temperature - ambient to 200°F for a mixed flow (typical of high bypass engines with mixed flow).

Jet exhaust velocity - 180 to 285 m/s.

Flow length to hydraulic diameter ratio - 3.2 to 9.3.

Nozzle impingement angle of up to 35° or deflector vanes on the nozzle may be used. However, the nozzle impingement angle is not critical provided the jet flow is attached over a significant spanwise region at the trailing edge. The noise levels for nozzle contours which do not provide a smooth flow distribution at the exit and actual engines where the turbulence characteristics are different from the air jets are not expected to agree well with the prediction.

UTRC Method

Recently Fink of United Technologies Research Center (UTRC) has developed a noise prediction method for blown flaps (ref. 32). The test data obtained at NASA-Lewis Research Center for various configurations were used as a primary data base. The basic philosophy of this method is to compute the contribution to the far-field from various conjectured noise source mechanisms associated with blown flaps. The following acoustically independent (not necessarily aerodynamically independent) noise components are conjectured: (1) compact lift noise (also known as fluctuating lift noise or scrubbing noise) defined as an acoustically compact lift dipole with axis perpendicular to each chord segment of the wing and flaps, (2) trailing edge noise generated by the turbulent flow convecting past the trailing edge, defined as a baffled dipole source with axis perpendicular to the edge, (3) undeflected jet noise generated by the turbulent flow of the jet exhaust in the region where the influence of the wing surface is not felt (in the vicinity of the jet exit), (4) distorted and deflected jet noise generated by the jet flow, with a strong influence of the flap surface (wall jet), and (5) trailing-edge wake

noise generated by flow mixing in the turbulent wake of the flap. These sources and their locations are illustrated in figure 8 for UTW and USB configurations.

In order to understand these sources, some simplified experiments were conducted at UTRC (ref. 43). The flow properties, radiated source characteristics, and various near-field to far-field pressure correlations were measured. These results in conjunction with the data base were used to develop the functional relations between the noise and flow parameters of several acoustically noninteracting noise components. One of the fundamental findings of these cross-correlation experiments was that the region of the flap surface which experiences a large fluctuation of static pressures need not be a location of strong noise generation. Therefore, variation of maximum normalized cross-correlation coefficient with chordwise position of the wing and the concept of large-scale vortex structure convected past the wing and flap surfaces were used to develop a description of the fluctuating lift noise mechanism. It was also found that the relative strength and importance of each source to the far-field will vary from configuration to configuration depending on the type of flow and directivity angle. For each source, even though the functional relation of the noise with the flow and geometric parameters is the same, the constants determining the absolute magnitude were derived from the test data. The flight effects on the flap noise were derived by using the small-scale model test data obtained in the free jet facility.

Using the pertinent noise sources for different configurations, the noise prediction scheme was developed for the following configurations of blown flaps:

(1) UTW slotted flaps with conventional and mixer nozzles.
(2) UTW slotless flaps.
(3) USB slotless flaps.
(4) Engine in front of the wing.

It has been recognized from recent investigations that the configurations which can provide a good low-speed performance acceptable for STOL operations are UTW slotted flaps and USB slotless flaps. Therefore, the comments in this report are limited to these two configurations shown in figure 15.

The noise levels from the compact lift dipole source were predicted by modeling the exhaust jet as a line of discrete vortices at the edge of the jet flow over the surface. The far-field sound was assumed to vary as jet exit velocity raised to the power 6, and the one-third octave band spectra have characteristic slopes of 9 dB per octave and -4 dB per octave at the low- and high-frequency ranges, respectively.

In addition to these physically justified and experimentally verified assumptions, the following major assumption was made: *"Fluctuating lift noise would radiate on both sides of the deflected flaps even though the hypothetical coherent vortices in the exhaust jet are only one side of the flap surfaces."* For the flow on one side of the surface, as in the case of blown flaps, the fluctuating pressures were produced only on the flow side of the surface. Therefore, the noise sources should be located on the flow side of the surface and radiate in the direction perpendicular to the surface and in the hemisphere containing the flow side. It is possible, however, for part of the sound generated by this type of fluctuating pressure to radiate in the "no-flow" direction of the surface by diffracting around the edges of the finite length flaps. However, the assumption of equal radiation in both directions with a directivity of a free dipole with an axis perpendicular to the surface is not fully justified. The experimental agreement shown in reference 43 is probably because of neglecting the shear layer noise from the wake just downstream of the trailing edge which can radiate equally in both directions as shown in reference 18.

In the case of the UTW configuration, the compact lift dipole noise associated with the last flap segment was assumed to be relatively strong. But for the USB configuration, the strongest dipole was from the undeflected part of the wing. Even though the trailing edge noise was associated with all the flaps, it was assumed that only the last flap trailing edge contributed

to the far-field sound. Therefore, the trailing edge noise was independent of number of flaps. The directivity of trailing edge noise was derived arbitrarily to fill the lobes of the predicted fluctuating lift noise.

The undeflected jet, and the deflected and distorted jet were combined together and computed as one source. It was assumed that the noise contribution from this quadrupole source was the same as that of a free jet without the influence of the wing and flap surface. Since it is known that the turbulence characteristics of blown flaps such as intensity, length scale and frequency scale are substantially different from that of a free jet, this assumption is somewhat arbitrary. The directivity of this quadrupole noise component was modified by the reflection and shielding of the wing and flap surfaces.

The noise generated by external flow deflection devices on the USB configuration were calculated in the same way as that for a jet impingement on a wing surface of UTW configuration. But the directivity was modified by the reflection, shielding and edge diffraction of the wing and flap surfaces.

This prediction method was developed basically by matching the test data of noise intensity, spectra, and directivity. In spite of the assumptions discussed above which were not fully justified, the predicted results agreed with the test data. This prediction scheme was evaluated by comparing with various test data not used in the development of the prediction program. In reference 34, the predicted results were compared with recent NASA-Lewis large-scale model data and QCSEE USB and UTW model data. Typical comparisons are shown in figures 16 - 19. It may be seen from these figures that this procedure overpredicts the OASPL for UTW takeoff flap configuration. For UTW approach flap angles and USB configurations, the agreement between the prediction and measured data is good. Figures 20 - 23 shows the comparisons between the prediction and the recently obtained Lockheed USB data (ref. 36). The UTW prediction is compared with the test data of reference 30 in figures 24 - 28. These comparisons indicate that the magnitude, directivity and spectra of flap noise for a simulated test model can be predicted within ±3 dB. As the understanding of flap noise generation and propagation becomes clearer, the

noise characteristics of various source mechanisms may be modified without much difficulty. Therefore, this prediction scheme may be adapted to use as a blown flap noise module in the aircraft noise prediction program.

RECOMMENDED PREDICTION METHOD

The blown flap noise prediction methods available in the literature have been evaluated by comparing the predicted noise levels, directivity, and spectra with existing NASA and Lockheed data bases, as discussed in the previous section. Based on this evaluation, a semi-empirical prediction method developed by Fink, known as the UTRC method (ref. 32) has evolved as the most suitable method for blown flap noise prediction as applied to the UTW and USB configuration. The general description and the detailed calculation procedure are described in this section.

The following source components of flap noise were considered in the development of the prediction scheme. (1) fluctuating lift noise, defined as an acoustically compact lift dipole with an axis oriented perpendicular to the wing and flap chordwise segment, (2) trailing edge noise, defined as the noise generated by the turbulent flow leaving the trailing edge, and (3) quadrupole noise, defined as the noise generated from the mixing process of the jet exhaust with the ambient air. The quadrupole noise source consists of three components, viz, (a) undistorted and undeflected jet exhaust, (b) jet impact on the wing and flap surfaces, and (c) the trailing edge wake shear layer. The undistorted and undeflected jet exhaust noise is treated as noise generated by an isolated jet and is increased by 2 dB in the direction of the flow side of the wing to account for wing/flap reflection. Jet impact noise is generated from the region where the jet is deflected by the flap and is assumed to be stronger than the undeflected jet. Trailing-edge wake shear-layer noise is generated by the mixing process of the wake flow. Since the undistorted and undeflected jet noise is treated as a part of the flap noise, jet mixing noise should not be considered as a separate source in the total aircraft noise prediction.

Coordinate System and Input Variables

The blown flap coordinate system used in the prediction scheme is illustrated in figure 15. For the UTW configuration, the origin is the center of the nozzle exit, positive x is downstream (jet exhaust centerline) and positve y is towards the wing (fig. 15a). For the USB configuration, the origin is the lower tip of the nozzle, positive x is downstream, and positive y is up in the direction away from the wing surface (fig. 15b).

The geometric input parameters that are required in this prediction scheme are: (1) wing leading edge coordinates, (2) wing deflection relative to the nozzle centerline, (3) deflection of flap(s), (4) nozzle exit hydraulic diameter, and (5) far-field radius. In addition to the above parameters, flap leading edge coordinates, number of flap segments (number of slots), and chord length of the last flap segment for the UTW configuration, and in the case of the USB, flap trailing edge coordinates and nozzle roof angle (cant angle or kickdown angle) relative to the nozzle are also essential for computing noise levels. The effects of wing sweep angle and other geometric variables on the radiated sound field are neglected. The general group of geometric and operational variables required in calculation of OASPL and one-third octave band spectra are given in Table 2. This input data may be used in any consistent system of units, such as English (foot, slug, sec. °R) or MKS (meter, kilogram, sec. °K). The units of the input variables are shown in the last two columns of the table.

Noise Calculation Formulas

The prediction formulas use dimensionless variables derived from the basic input parameters to calculate the OASPL and one-third octave band sound pressure levels from various flap-noise components. Using these dimensionless variables, normalized mean-square acoustic pressures are determined in a given direction (polar and azimuthal angle) and radius R for UTW slotted, UTW slotless, and USB configurations. The mean square acoustic pressures is then converted to overall Sound pressure and one-third octave band sound pressure.

TABLE 2

INPUT VARIABLES

VARIABLE	UTW SLOTTED	UTW SLOTLESS	USB	UNITS		
				Symbol	Mks	English
Jet Exhaust Velocity	✓	✓	✓	V_J	m/sec.	ft/sec.
Number of Flaps	✓	✓	✓	N	--	--
Flight Speed	✓	✓	✓	V_a	m/sec.	ft/sec.
Nozzle Hydraulic Diameter	✓	✓	✓	D	m	ft.
Far-Field Radius	✓	✓	✓	R	m	ft.
1/3 Octave Center Frequency	✓	✓	✓	f_k	Hz	Hz
Ambient Speed of Sound	✓	✓	✓	a	m/sec.	ft/sec.
Ambient Air Density	✓	✓	✓	ρ	kg/m^3	$slug/ft^3$
Reference Acoustic Pressure	✓	✓	✓	P_{ref}	N/m^2	lb_f/ft^2
Nozzle Cant Angle or Roof Angle			✓	δ_r	Deg.	Deg.
Wing Deflection Relative to Jet Axis	✓	✓		δ_w	Deg.	Deg.
i^{th} Flap Deflection Relative to Wing	✓			δ_i	Deg.	Deg.
Last Flap Deflection Relative to Wing		✓	✓	δ_N	Deg.	Deg.
Coordinate of Wing Leading Edge	✓	✓	✓	x_w, y_w	m	ft.
Coordinates of i^{th} Flap Leading Edge	✓			x_i, y_i	m	ft.
Coordinate of the Flap Trailing Edge		✓	✓	x_t, y_t	m	ft.
Chord Length of the Last Flap	✓			C_f	m	ft.
Polar Angle	✓	✓	✓	θ	Deg.	Deg.
Azimuthal Angle	✓	✓	✓	ϕ	Deg.	Deg.

First, the general formulas are provided and then the detailed calculation procedure is given.

UTW With Slotted Flap Configuration. Fluctuating lift noise is assumed to be generated by hypothetical coherent vortices in the exhaust jet that radiate sound to both sides of the wing and deflected flaps. The vortex trajectory is taken as a straight line parallel to the nozzle centerline extending downstream from the nozzle lower lip until it gets within half a diameter of the flap surface. For a case where the wing or flap extends below the nozzle centerline, the vortex trajectory becomes parallel to the flap chord and is displaced one-half diameter away from it as shown in figure 29. From this assumption, the overall mean square acoustic pressure in any given direction, α, and distance, R, due to the lift source is calculated using the following expression:

$$p_{OAL}^2 = 10^{-7} \left[\left(\frac{\rho V_I^3}{a}\right)\right]^2 \left(\frac{CD}{R^2}\right) \left(\frac{V_I}{V_J}\right)^2 \left[K_w \sin^2\alpha_w + \sum_{i=1}^{N} K_i \sin^2\alpha_i\right] \cdot \left(1 - \frac{V_a}{V_J}\right)^2 \qquad (4a)$$

where V_I = impingement velocity and is given by

$$V_I/V_J = \{1 + [0.14\ (L_I/D)\ (1 + M_N)^{-\frac{1}{2}}]^4\}^{\frac{1}{4}}$$

L_I = longitudinal distance of impingement point

M_N = jet Mach number relative to the speed of sound in the jet (assumed as M_J)

k_w and k_i = amplitude functions for fluctuating lift noise of wing and i^{th} flap, respectively, and are given by

$$k_w = \frac{c_w}{c} \left(\frac{h_w}{c}\right)^{-2}$$

$$k_i = \frac{c_i}{c} \left(\frac{h_i}{c}\right)^{-2} \qquad (4b)$$

α_w and α_i = polar angles relative to the upstream direction along the wing chord and i^{th} flap chord.

The mean-square acoustic spectral pressure for a Strouhal number, S_k, is given by

$$P_L^2 (S_k) = P_{0AL}^2 \left[0.037\ S_k^4\ (S_k^{8/3} + 0.008)^{-2}\right] \tag{5}$$

where $S_k = \frac{f_k\ V_J}{D}$.

Trailing edge noise is calculated based on the velocity at the trailing edge. The equation for the overall trailing edge mean-square pressure is given by

$$P_{0AT}^2 = 10^{-5} \left(\frac{\rho^2 V_J^5}{a}\right) \cdot \left(\frac{V_{TE}}{V_J}\right)^3 \left(\frac{D}{R}\right)^2 \left[\cos^2\phi + \cos^2 \left(\frac{\theta + \delta_f}{2}\right)\right] \tag{6}$$

where

$$\frac{V_{TE}}{V_J} - \{1 + [0.14\ \left(\frac{V_{TE}}{D}\right)\ (1 + M_N)^{-\frac{1}{2}}]^4\}^{\frac{1}{4}} ,$$

L_{TE} = longitudinal distance of trailing edge.

The trailing edge mean-square acoustic spectral pressure for Strouhal number, S_k, is given by

$$P_T^2(S_k) = P_{0AT}^2\ [0.029\ \ S_k^4\ \ (S_k^{3/2} + 0.5)^{-4}] . \tag{7}$$

Quadrupole noise consists of undeflected jet noise, the increase due to the deflection by the flap segment, and the trailing edge wake noise. Overall mean-square pressure for the undeflected jet is calculated, assuming the jet is isolated, using the following formulas:

For $\theta \leq M_N \cdot 150°$,

$$P_{0AQ}^2 = 1.988 \cdot 10^{-5.9} \cdot \rho^2 a^4 \frac{A_J[M^{7.5}\ \ (1 + 0.01\ M_N^{4.5})^{-1}]}{2R^2[1 + M_c(1 + M_c^5)^{-1/5}\ \cos\theta]^3} \tag{8a}$$

$$(1 + 6\ \sin^2\delta_f)\ \ (1 + \cos^2\phi)$$

For $(M_N \cdot 150°) < \theta < 180°$,

$$P^2_{OAQ} = (1.988) \cdot 10^{-5.9} \cdot (\rho^2 a^4) \frac{A_J[M^{7.5} \quad (1 + 0.01\ M_N{}^{4.5})^{-1}]}{2R^2[1 + M_c(1 + M_c{}^5)^{-1/5}\ \cos\theta]^3} \cdot$$

$$[(1 + 6\ \sin^2\delta_f)\ (1 + \cos^2\phi)]\ 10^{-1.8\left[\frac{M_N\theta}{30} - .5\right]}. \tag{8b}$$

In addition to this quadrupole noise, the trailing edge wake noise is calculated by assuming the wake flow as an isolated jet having a diameter equal to the nozzle diameter and exhaust velocity equal to the trailing edge velocity.

The quadrupole mean-square acoustic pressure spectrum for Strouhal number, S_k, is calculated by using the formula,

$$P^2_Q(S_k) = P^2_{OAQ}\ [0.1\ S_k{}^4\ (S_k{}^{17/12} + 0.11)^{-4}] \tag{9}$$

UTW Slotless Flap Configurations. In addition to the input data provided for the UTW slotted flap configuration, the coordinates of the flap trailing edge should also be specified. Wing-flap geometry is idealized as two straight lines, one for the wing and one for the last flap. For undeflected flap ($\delta_f = 0$), the flap leading edge coordinates (fictitious) are same as the flap trailing edge coordinates; but for undeflected flap ($\delta_f \neq 0$) the flap leading edge coordinates are calculated using the wing leading edge coordinates, flap trailing edge coordinates, and the flap angle as follows:

For deflected flaps ($\delta_f \neq 0$),

$$X_1 = X_t \frac{[Y_w - Y_t\ (X_t - X_w)\ \tan\theta_w]}{\tan\ (\delta_w + \delta_f) - \tan\delta_w}$$

$$Y_1 = Y_w - (X_1 - X_w)\ \tan\delta_w\,. \tag{10}$$

Using these coordinates for the flap leading edge, the fluctuating lift noise, trailing edge noise, and quadrupole noise are calculated in the same way as for the UTW slotted wing configuration using Equations (4) through (9).

USB Configuration. As in the case of the UTW slotless configuration described above, the fictitious coordinates of the flap leading edge are calculated by assuming the wing-flap geometry as two straight lines and using the wing leading edge coordinates, flap trailing edge coordinates, and flap angle. If the aerodynamic turning angle is known, then this angle should be used in place of the flap angle.

Fluctuating lift, trailing edge, and quadrupole noise components are calculated in the same way as for UTW slotted wings. However, the fluctuating lift noise from the flap is taken as 1.5 times that from a hypothetical vortex trajectory. The trailing edge noise magnitude is increased by twice that of UTW. The increase in quadrupole noise due to the nozzle roof angle (cant angle or external vane angle) is calculated in a manner similar to that for an exhaust jet impinging on the flap surface of the UTW configuration. However, this increase is assumed to be shielded from the community by the wing and flap surfaces. The quadrupole noise from the trailing edge wake is calculated in the same way as for the UTW configuration.

Flight Effects. Flight effects are included in the noise calculation procedure by assuming the magnitudes of fluctuating lift noise, trailing edge noise, impingement noise, and trailing edge wake noise vary as $[1 - (V_a/V_J)]^2$ and the undeflected jet noise varies as $[1 - (V_a/V_J)]^6$. One-third octave band spectra are not affected by forward speed for the UTW slotted configuration.

For the USB configuration, however, the Strouhal number is modified by dividing by the factor $[1 - (V_a/V_J)]$. These flight effects include the source strength alteration due to relative motion of the jet flow. These effects are derived with respect to coordinates fixed to the airplane. The effect of aircraft motion (source motion) relative to the ground-fixed observer is not included.

Details of Calculation Procedure

The required geometric and operational variables are calculated from the input data. Using these variables the overall and one-third octave band frequency mean-square acoustic pressure in a given direction and at a given distance are calculated. The detailed calculation procedure is given in this section. The symbols used in this section to describe the geometric, operational and the acoustic parameters are defined in the previous section and in the list of symbols.

Wing and Flap Geometry Calculations. The wing chord length, C_w, is computed as follows:

$$C_w = \sqrt{(X_1 - X_w)^2 + (Y_1 - Y_w)^2}\,. \tag{11}$$

For the UTW slotted wing, X_1 and Y_1 are given as input data. For the UTW slotless wing and USB configurations, X_1 and Y_1 are calculated as follows:

$$\left.\begin{aligned} X_1 &= X_t - \frac{Y_w - Y_t - (X_t - X_w)\,\tan\delta_w}{\tan\,(\delta_w + \delta_N) - \tan\delta_w} \qquad \text{for } \delta_N \neq 0, \\ X_1 &= X_t \qquad\qquad\qquad\qquad\qquad\qquad\qquad\quad \text{for } \delta_N = 0, \\ Y_1 &= Y_w - (X_1 - X_w)\,\tan\delta_w. \end{aligned}\right\} \tag{12}$$

The i^{th} flap chord length, C_i, is given by

$$C_i = \sqrt{(X_{i+1} - X_i)^2 + (Y_{i+1} - Y_i)^2}. \tag{13}$$

The total chord length of the wing and flap, C, is calculated as follows:

$$C = C_w + \sum_{i=1}^{N} C_i \qquad \textit{(for UTW slotted wing/flap)},$$

$$\left.\begin{aligned} *C &= 3\,C_w \quad (\text{for} \quad Y_2 < 0) \\ *C &= C_w \quad\;\; (\text{for} \quad Y_2 > 0) \end{aligned}\right\} \qquad \textit{(for UTW slotless wing/flap)},$$

$$**C = C_1 + C_w \qquad \textit{(for USB configuration)}. \qquad (14)$$

Vortex Trajectory Calculations. The distance between the vortex and leading and trailing edges of wing and flap are calculated as:

$$h_{\ell_w} = \frac{D}{2} + Y_w,$$

$$h_{t_w} = [h_{\ell_w} - C_w \sin\delta_w] \text{ or } \frac{D}{2} \qquad \textit{(whichever is greater)},$$

$$h_{\ell_i} = \left[\frac{D}{2} + Y_i\right] \text{ or } \frac{D}{2} \qquad \textit{(whichever is greater)},$$

$$h_{t_i} = h_{\ell_i} - C_i \sin(\delta_w + \delta_i) \text{ or } \frac{D}{2} \qquad \textit{(whichever is greater)}. \qquad (15)$$

Amplitude Function Calculations. The noise amplitude function of wing and flaps are given by:

**Applies for UTW slotless wing configuration.*
***Applies for USB configuration.*

$$\left.\begin{aligned} k_w &= C\, C_W \left[h_{\ell_w}^{-2} + h_{t_w}^{-2}\right] \\ k_i &= C\, C_i \left[h_{\ell_i}^{-2} + h_{t_i}^{-2}\right] \end{aligned}\right\} \quad \textit{For UTW,}$$

$$\left.\begin{aligned} **k_w &= 2\,\frac{CX_1}{D^2} \\ **k_i &= 1.5\,\frac{CC_1}{D^2} \end{aligned}\right\} \quad \textit{For USB.} \qquad (16)$$

Impingement and Trailing Edge Location Calculations. Distance of impingement point and trailing edge from the nozzle, L_I, L_{TE} are given by :

$$L_I = X_N + \frac{Y_N}{\tan\delta_f} \quad \text{or} \quad X_N + C_N \cos\delta_f \qquad \textit{(whichever is smaller) (for UTW slotted flap),}$$

$$\left.\begin{aligned} *L_I &= X_1 + C_1 \qquad (\text{for } Y_2 > 0 \text{ and } Y_1 > 0) \\ *L_I &= X_1 + \frac{Y_1}{\tan\delta f} \qquad (\text{for } Y_2 < 0) \\ *L_I &= X_w + \frac{Y_w}{\tan\delta f} \qquad (\text{for } Y_2 < 0 \text{ and } Y_1 < 0) \end{aligned}\right\} \quad \textit{(for UTW slotless flap),}$$

$$**L_I = X_1 + C_1 \qquad \textit{(for USB),}$$

$$L_{TE} = X_N + C_N \cos\delta_f\,, \qquad (17)$$

where $\delta_f = \delta_w + \delta_N$. (18)

**Applies for UTW slotless wing configuration.*
***Applies for USB configuration.*

Jet Velocity and Mach number Calculations. Jet Mach number, M_N, and impingement Mach numbers are given by:

$$M_N = \frac{V_J}{a},$$

$$M_I = \frac{V_I}{a}. \tag{19}$$

Impingement velocity, V_I, and trailing edge velocity, V_{TE}, are calculated using the following formulae for the corresponding velocity ratios, VR_I and VR_T.

$$VR_I = \frac{V_I}{V_J} = \left\{1 + \left[\frac{0.14\,\frac{L_I}{D}}{\sqrt{1+M}}\right]^4\right\}^{0.25},$$

$$VR_T = \frac{V_{TE}}{V_J} = \left\{1 + \left[\frac{0.14\,\frac{L_{TE}}{D}}{\sqrt{1+M}}\right]^4\right\}^{0.25}. \tag{20}$$

Jet Angle Calculation. The jet angle with reference to the wing chord and observer is given by:

$$\delta_J = \tan^{-1}\left\{\cos^2\left[\tan^{-1}\frac{\sin\theta\,\sin\phi}{\sqrt{1-\sin^2\phi\sin^2\theta}}\right]\tan\delta_f\right\} \tag{21}$$

Mean-Square Acoustic Pressure Calculations. For each noise source mechanism, the overall mean-square acoustic pressure is calculated. The mean-square one-third octave band acoustic pressure is given as a function of overall pressure and Strouhal number. The Strouhal number, S_k, at the third-octave band center frequency, f_k, is defined as,

$$S_k = \frac{f_k D}{V_J} \qquad \textit{(for UTW slotted flap configuration)},$$

and

$$S_k = \frac{f_k D}{V_J \cdot \left(1 \mp \frac{V_a}{V_J}\right)} \qquad \textit{(for UTW slotless and USB flap configuration)}. \tag{22}$$

Fluctuating Lift Noise. The overall mean-square acoustic pressure is calculated using the following formulae:

$$\frac{p^2_{OAL}}{\rho^2 a^4} = \frac{10^{-7}}{2} \cdot \left(1 - \frac{V_a}{V_J}\right)^2 \cdot \frac{C\,D}{R^2}\, VR_l^2 \cdot M_l^6 \cdot \left\{ K_W \left[\cos\delta_w \sin\theta \cos\phi + \sin\delta_w \cos\theta\right]^2 + \sum_{i=1}^{N} K_i \left[\cos\left(\delta_w + \delta_i\right) \sin\theta \cos\phi + \sin\left(\delta_w + \delta_i\right)\cos\theta\right]^2 \right\} \quad \textit{For UTW slotted} \tag{23a}$$

$$* \quad \frac{p^2_{OAL}}{\rho^2 a^4} = 10^{-7}\left(1 - \frac{V_a}{V_J}\right)^2 \cdot \frac{C\,D}{R^2} \cdot VR_l^2 \cdot M_l^6 \cdot K_W \qquad \text{for } (\theta + \theta_f) < 180^\circ$$

$$* \quad \frac{p^2_{OAL}}{\rho^2 a^4} = 1.998 \cdot 10^{-20} \qquad \text{for } (\theta + \theta_f) > 180^\circ \qquad \textit{For UTW slotless} \tag{23b}$$

$$** \quad \frac{p^2_{OAL}}{\rho^2 a^4} = 10^{-7} \left(1 - \frac{V_a}{V_J}\right)^2 \cdot \frac{C\,D}{R^2} \cdot VR_l^2 \cdot M_l^3 \left[K_W + K_1\right] \qquad \textit{For USB} \tag{23c}$$

**Applies for UTW slotless wing configuration.*
***Applies for USB configuration.*

The mean-square acoustic pressure spectra is given by

$$\left[\frac{p^2\ (S_K)}{P_{0AL}^2}\right]_L = \frac{0.037\ (S_k)^4}{[0.008 + (S_K)^{2.667}]^2} \qquad \textit{for UTW} \qquad (24a)$$

$$^{**}\left[\frac{p^2\ (S_K)}{P_{0AL}^2}\right]_L = \frac{0.029\ (S_K)^4}{(0.05 + S_K^{1.5})^4} \qquad \textit{for USB} \qquad (24b)$$

Trailing Edge Noise. The overall mean-square acoustic pressure is given by:

$$\frac{P_{0AT}^2}{\rho^2 a^4} = 10^{-5}\ (1 - \frac{V_a}{V_J})^2\ \frac{D^2}{R^2}\ \frac{VR_T^3}{VR_I} \cdot \frac{M_I^6}{M} \cdot \cos\left[\tan^{-1}\ \frac{\sin\theta\ \sin\phi}{\sqrt{1 - \sin^2\theta\ \sin^2\phi}}\right] \cdot \cos^2\ (\frac{\theta + \delta_f}{2}) \qquad (25)$$

The acoustic pressure spectra is given by:

$$\left[\frac{p^2\ (S_K)}{P_{0AT}^2}\right]_T = \frac{(S_K)^4}{(0.05 + S_K^{1\ 5})^4} \qquad (26)$$

Quadrupole Noise. The overall quadrupole noise is calculated using the following formulae.

For $(\theta + \delta_f) \cdot M_N \cdot < 2.618$, and for UTW configuration:

**Applies for USB configuration.*

$$\frac{p^2_{OAQ}}{\rho^2 a^4} = \frac{\left(1 - \frac{V_a}{V_J}\right)^2 \cdot (1.998) \cdot 10^{-6} \cdot D^2 (1 + \cos^2\phi)}{R^2} \left[\frac{M_1^{7.5} \left(1 - \frac{V_a}{V_J}\right)^4 + 6 \sin^2\delta_f}{A_1 (1 + 0.01\, M_1^{4.5})}\right.$$

$$\left. \frac{M_T^{7.5} \left[\left(1 - \frac{V_a}{V_J}\right)^4 + 6\, VR_1^{\,8} \sin^2\delta_f\right]}{A_2 (1 + 0.01\, M_T^{4.5})}\right] \cdot \left[1 + \frac{M_c \cos(\theta + \delta_J)}{(1 + M_c^{\,5})^2}\right]^{-3}$$

$$\cdot \left[1 + \frac{\sin^2\delta_J}{\sin^2\delta_f}\right] \qquad (27a)$$

where $A_1 = A_2 = 2$ for UTW slotted flaps;
$A_1 = 8$, $A_2 = 20$ for UTW slotless flaps.

For $(\theta + \delta_f)$ $M_N < 2.618$, and for USB configuration:

** $$\frac{p^2_{OAQ}}{\rho^2 a^4} = \frac{\left(1 - \frac{V_a}{V_J}\right)^2 \cdot (1.998) \cdot 10^{-6}\, D^2\, M_T^{7.5}\, (1 + 6 \sin^2\delta r)}{R^2 (1 + 0.01\, M_T^{4.5})}$$

$$\cdot \left[1 + \frac{M_c \cos(\theta + \delta_J)}{(1 + M_c^{\,5})^{0.2}}\right] \left[1 + \frac{\sin^2\delta_J}{\sin^2\delta_f}\right] \qquad (27b)$$

For $(\theta + \delta_f) \cdot M_N \geq 2.618$; $(\theta + \delta_f) < 3.146$; $(6.2832 - \theta - \delta_f) \cdot M_N > 2.618$; and for UTW configuration:

$$\frac{p^2_{OAQ}}{\rho^2 a^4} = [\text{Equation (27a)}]\left[10^{\{-1.8[1 - |6 - (\theta + \delta_J) \cdot 1.91\, M_J|]\}}\right] \qquad (27c)$$

***Applies for USB configuration.*

For $(\theta + \delta_J)\ M_N > 2.618$; $(\theta + \delta_J) < 3.1416$; and USB configuration:

$$** \quad \frac{P^2_{OAQ}}{\rho^2 a^4} = [\text{Equation (27b)}] \left[10^{\{-1.8\ [1\ -\ |6\ -\ (\theta + \delta_J)\ \cdot 1.91\ M_J|]\}}\right] \tag{27d}$$

For $(\theta + \delta_J)\ \ M_N \geq 2.618$ and $(\theta + \delta_J) > 3.1416$, and $(6.2832 - \theta - \delta_f) \cdot M_N > 2.618$

$$\frac{P^2_{OAQ}}{\rho^2 a^4} = \frac{(1 - \frac{V_a}{V_J})^2 \cdot (1.998)\ 10^{-6}\ D^2(1 + 6\ \sin^2\delta r)}{R^2}$$

$$\left[\frac{M^{7.5}}{1 + 0.01\ M_T^{4.5}} + \frac{M_T^{7.5}}{1 + 0.01\ M_T^{4.5}}\right] \left[1 + \frac{M\ \cos\ (\theta + \delta_J)}{(1 + M_c^5)^{.2}}\right]^{-3}$$

$$\left[1 + \frac{\sin^2\delta_J}{\sin^2\delta_f}\right] \left[10^{\{-1.8\ [1\ -\ |6\ -\ (\theta + \delta_J)\cdot 1.91\ M_N|]\}}\right] \tag{27e}$$

The quadrupole source mean-square pressure corresponding to the Strouhal number of one-third octave band frequency is given by:

$$\left[\frac{P^2_{(SK)}}{P^2_{OAQ}}\right]_Q = \frac{(S_K)^4}{10[.11 + S_K{}^{1.42}]^4} \cdot \tag{28}$$

The overall and one-third octave band mean-square pressures of three components (fluctuating lift, trailing edge and quadrupole noise) are added to obtain the total overall or one-third octave band mean-square acoustic pressures. From these values the sound pressure levels are calculated.

***Applies for USB configuration.*

6. RECOMMENDED RESEARCH

Understanding of the noise generation and propagation mechanisms of blown-flap noise is critical to the improvement of the accuracy of noise prediction. The following experimental and theoretical research is recommended in order to advance the state of the art. As the technology develops the noise prediction from each of the source mechanisms may be either modified or improved.

(1) The turbulence characteristics of the jet flow around the wing and flap surfaces should be evaluated. The turbulence properties such as the integral length scales, the convection velocity, and the velocity gradients should be utilized to evaluate the relative strength of the various noise sources.

(2) Effects of various inhomogeneities in the vicinity of the flow (e.g. the presence of solid surfaces, velocity gradients, etc.) on noise generation and propagation should be investigated. Fundamental investigations of reflection and shielding effects of the wing/flap surfaces with and without jet flow should be investigated. These results must be applied to the flap noise prediction.

(3) Numerical or empirical methods based on test results should be developed to predict the fluid dynamic properties (velocity profiles in the trailing edge wake and flow spreading characteristics). The flap-noise calculations from different noise source mechanisms can be improved with the use of these calculated results.

(4) The fluctuating-lift noise mechanism for one-sided flow similar to the blown flap configuration should be investigated in order to evaluate the source strength and directivity.

(5) Flight effects should be studied experimentally in either a free-jet facility or in a wind tunnel. The data must be analyzed taking account

of the effects of shear layer in the free-jet facility and wall shear interference of the wind tunnel.

(6) When the flyover noise data from USAF Advanced Medium Short Takeoff and Landing Transport (AMST) configurations and NASA Quiet Short-Haul Research Aircraft (QSRA) are available, these data should be compared with the prediction. Additional flyover noise data should be obtained using a powered sail plane with highly suppressed engines.

REFERENCES

1. Dorsch, R. B.; Lasagna, P. L.; Maglieri, D. J.; and Olsen, W. A.: Flap Noise. NASA SP-311, 1972.

2. Falarski, M. D.; Aiken, T. N.; Aoyogi, K.; and Koenig, D. G.: Comparison of the Acoustic Characteristics of Large-Scale Models of Several Propulsive-Lift Concepts. *Journal of Aircraft*, Vol. 12, No. 7, July 1975.

3. Olsen, W. A.; Miles, J. H.; and Dorsch, R. J.: Noise Generated by Impingement of a Jet Upon a Large-Flat Board. NASA TN D-7075, 1972.

4. Hayden, R. E.: Noise from Interacting of Flow With Rigid Surfaces: A Review of Current Status of Prediction Techniques. NASA CR-2126, Oct. 1972.

5. Ffowcs Williams, J.; and Hall, L. H.: Aerodynamic Sound Generation by Turbulent Flow in the Vicinity of a Scattering Half Plane. *Journal of Fluid Mechanics*, Vol. 40, Part 4, March 1970, pp. 657-670.

6. Lighthill, M. J.: On Sound Generated Aerodynamically, I. General Theory. Proceedings of the Royal Society, A211, 1952, pp. 564-587.

7. Curle, N.: The Influence of Solid Boundaries Upon Aerodynamic Sound. Proceedings of the Royal Society, A231, 1955, pp. 505-514.

8. Phillips, O. M.: On the Aerodynamic Surface Sound from a Plane Turbulent Boundary Layer. Proceedings of the Royal Society, A234, 1956, pp. 327-335.

9. Sharland, I. J.: Sources of Noise in Axial Flow Fans. *Journal of Sound and Vibration*, Vol. 1, 1964, pp. 302-322.

10. Doak, P. E.: Acoustic Radiation from a Turbulent Fluid Containing Foreign Bodies. Proceedings of Royal Society, A259, 1960, pp. 129-145.

11. Powell, A.: Aerodynamic Noise and the Plane Boundary. *Journal of Acoustical Society of America*, Vol. 32, No. 8, 1960, pp. 982-990.

12. Powell, A.: On the Aerodynamic Noise of a Rigid Plate Moving at Zero Incidence. *Journal of Acoustical Society of America*, Vol. 31, No. 12, Dec. 1959, pp. 1649-1653.

13. Meecham, W. C.: Surface and Volume Sound from Boundary Layers. *Journal of Acoustical Society of America*, Vol. 37, No. 3, March 1965, pp. 516-522.

14. Hayden, R. E.: Sound Generation by Turbulent Wall Jet Flow Over a Trailing Edge. M.S. Thesis, Purdue University, 1969.

15. Chandiramani, K.: Diffraction of Evanescent Waves with Applications to Aerodynamically Scattered Sound and Radiation from Baffled Plates." *Journal of Acoustical Society of America*, Vol. 55, 1974, pp. 19-29.

16. Chase, D. M.: Sound Radiation by Turbulent Flow off a Rigid Half Plane as Obtained from a Wavevector Spectrum of Hydrodynamic Pressure, *Journal of Acoustical Society of America*, Vol. 52, No. 3, 1972.

17. Goldstein, M.: Unified Approach to Aerodynamic Sound Generation in the Presence of Solid Boundaries. *Journal of Acoustical Society of America*, Vol. 56, No. 2, 1974, pp. 494-509.

18. Tam, C. K. W.; and Reddy, N. N.: Sound Generated in the Vicinity of Trailing Edge of Upper Surface Blown Flap. *Journal of Sound and Vibration*, Vol. 52, No. 2, 1977, pp. 211-232.

19. Maglieri, D. J.; and Hubbard, H. H.: Preliminary Measurements of the Noise Characteristics of Some Jet-Augmented Flap Configurations. NASA-Langley Memorandum, 12-4-58L, Dec. 1958.

20. Grosche, F. R. (D. G. Randall, transl.): On the Generation of Sound Resulting from the Passage of Turbulent Air Jet Over a Flat Plate. Library Trans. No. 1460, Brit. R.A.E.; Oct. 1970.

21. Reddy, N. N.; and Yu, J. C.: Radiated Noise from an Externally Blown Flap. NASA TN D-7908, July 1975.

22. Foss, J. F.; and Kleis, S. J.: Vorticity and Acoustic Measurements in Vertically Impinging Jet Flows. Proceedings of Third Interagency Symposium on Transport Noise, University of Utah, Nov. 12-14, 1975, pp. 425-444.

23. Fink, M. R.: Experimental Evaluation of Theories for Trailing Edge and Incidence Fluctuating Noise. *AIAA Journal*, Vol. 13, No. 11, 1975, pp. 1472-1477.

24. Becker, R. S.; and Maus, J. R.: Acoustic Source Location in the Secondary Mixing Region of a Jet Blown Flap Using a Cross-Correlation Technique. AIAA Paper 77-1364, Oct. 1977.

25. Reddy, N. N.; and Brown, W. H.: Acoustic Characteristics of An Upper Surface Blowing Concept of Powered-Lift System. AIAA Paper 75-204, Jan. 1975.

26. Tam, C. K. W.; and Yu, J. C.: Trailing Edge Noise. AIAA Paper No. 75-489, March 1975.

27. Yu, J. C.; and Tam, C. K. W.: An Experimental Investigation of the Trailing Edge Noise Mechanism. AIAA Paper No. 77-1291, Oct. 1977.

28. Von Glahn, U.; and Groesbeck, D.: "Effect of External Jet Flow Deflection Geometry on OTW Aeroacoustic Characteristics. AIAA Paper 76-499, July 1976 (also NASA TM X-73460).

29. Falarski, M. D.; Aoyagi, K.; and Koenig, D. G.: Acoustic Characteristics of Large-Scale STOL Models at Forward Speed, NASA TMX-62251, 1972.

30. Pennock, A. P.; Swift, G.; and Marbert, J. A.: Static and Wind Tunnel Model Test for Development of Externally Blown Flap Noise Reduction Techniques. NASA CR-134675, Feb. 1975.

31. Goodykoontz, J.; Von Glahn, U.; and Dorsch, R.: Forward Velocity Effects on Under-the-Wing Externally Blown Flap Noise. AIAA Paper 75-476, March 1975.

32. Fink, M. R.: A Method for Calculating Externally Blown Flap Noise. NASA CR-2954, 1978.

33. Heidelberg, L.; Homyak, L.; and Jones, W. L.: Full-Scale Blown Flap Noise. SAE Paper No. 750609, May 1975.

34. Dorsch, R. G.; Reshotko, M.; and Olsen, W. A.: "Flap Noise Measurements for STOL Configurations Using External Upper Surface Blowing, AIAA Paper No. 72-1203, 1972.

35. Cole, T. W.; and Rathbun, E. A.: Small-Scale Model Static Acoustic Investigation of Hybrid High Lift Systems Combining Upper Surface Blowing With the Internal Blown Flap. NASA CR-114757, 1974.

36. Brown, W. H.; Searle, N.; Blakney, D. F.; Pennock, A. P.; and Gibson, J. S.: Noise Characteristics of Upper Surface Blown Configurations – Experimental Program and Results. NASA CR-145143, Oct. 1977.

37. Hayden, R. E.: Reduction of Noise from Airfoils and Propulsive Lift Systems Using Variable Impedance Surfaces. AIAA Paper 76-500, July 1976.

38. Von Glahn, U.; Groesbeck, D.; and Goodykoontz, J.: Velocity Decay and Acoustic Characteristics of Various Nozzle Geometries with Forward Velocity. AIAA Paper 73-629, July 1973.

39. Falarski, M. D.; Aoyagi, K., and Koenig, D. G.: Acoustic Characteristics of a Large-Scale Wing Tunnel Model of an Upper Surface Blown Flap Transport Having Two Engines. NASA TMX-62319, 1973.

40. Hayden, R. E.; Kadman, Y., and Chanaud, R. C.: A Study of the Variable Impedance Surface Concept as a Means of Reducing Noise from Jet Interaction with Developed Lift-Augmenting Flaps. NASA CR-112166, 1972.

41. Olsen, W.; and Burns, R.; and Groesbeck, D.: Flap Noise and Aerodynamic Results for Model QCSEE Over-the-Wing Configuration. AIAA Paper 77-23, 1977.

42. Dorsch, R. G.; Clark, B.; and Reshotko, M.: Interim Prediction Method for Externally Blown Flap Noise. NASA TM X-71768, Aug. 1975.

43. Fink, M. R.; and Olsen, W. A.: Comparison of Prediction and Under-the-Wing EBF Noise Data. AIAA Paper 76-501, July 1976.

44. Guinn, W. A.; Blakney, D. F.; and Gibson, J. S.: V/STOL Prediction and Reduction. FAA RD-73-145, Aug. 1973.

45. Reddy, N. N.; Blakney, D. F.; and Tibbetts, J. G.; and Gibson, J. S.: V/STOL Aircraft Noise Prediction. FA-RD-75-125, June 1975.

46. Stone, J. R.: Interim Prediction Method for Jet Noise. NASA TM X-71618, Dec. 1974.

47. Hayden, R. E.: Noise from Interaction of Flow with Rigid Surfaces: A Review of Current Status of Prediction Techniques. NASA CR-2126, Oct. 1972.

48. Dunn, D. G.; and Peart, N. A.: Aircraft Noise Source and Contour Estimation. NASA CR-114649, July 1973.

49. Filler, L.: Prediction of Far-Field Jet/Trailing Edge Interaction Noise for Engine-Over-the-Wing Installation. AIAA Paper 76-518, July 1976.

50. Reddy, N. N.; Pennock, A. P.; Tibbetts, J. G.; and Tam, C. K. W.: Noise Characteristics of Upper Surface Blown Configurations - Analytical Studies. NASA CR-2812, March 1978.

51. Von Glahn, U.; and Groesbeck, D.: Geometry Effects on STOL Engine Over-the-Wing Acoustics with 5:1 Slot Nozzles. NASA TM X-71820, 1975.

BIBLIOGRAPHY

A complete bibliography related to the generation, the propagation, the prediction, and the suppression of flap noise is given here to aid in further investigations.

Baker, A. J.; and Manhardt, P. D.: Numerical Prediction of Aeroacoustics Jet Flap Flow. AIAA Paper No. 77-1316, October 1977.

Becker, R. S.; and Maus, J. R.: Acoustic Source Location in the Secondary Mixing Region of a Jet Blown Flap Using a Cross-Correlation Technique. AIAA Paper 77-1364, Oct. 1977.

Bhat, W. V.; and Galo, Rosso, D.: Effect of Forward Speed on Jet Wing/Flap Interaction Noise. AIAA Paper 75-475, March 1975.

Blankenship, G. L., and Oetting, R. B.: Jet Impingement Noise Generation and Its Reduction Through Surface Acoustic Treatment. Inter-Noise '76 Proceedings, April 1976.

Bohn, A. J.: Edge Noise Attenuation by Porous Edge Extensions. AIAA Paper 76-80, Jan. 1976.

Brown, W. H.; Searle, N.; Blakney, D. F.; Pennock, A. P.; and Gibson, J. S.: Noise Characteristics of Upper Surface Blown Configurations; Experimental Program and Results. NASA CR-145143.

Chase, D. M.: Sound Radiated by Turbulent Flow Off a Rigid Half Plane as Obtained from a Wave Vector Spectrum of Hydrodynamic Pressure. *Journal of Acoustical Society of America*, Vol. 52, No. 3, Part 2, Sept. 1972, pp. 1011-1023.

Chase, D. M.: Noise Radiated from an Edge in Turbulent Flow. *AIAA Journal*, Vol. 13, No. 8, pp. 1041-1047 (AIAA Paper No. 74-570).

Chestnutt, D.; Copeland, W. L.; and Clark, L. R.: Noise Generation by Plates in the Presence of Jets. NASA LWP-989, Part D, Sept. 1971.

Chestnutt, David; Manglieri, Domenic, J.; and Hayden, Richard E.: Flap Noise Generation and Control. NASA SP-320, Oct. 1972, pp. 413-419.

Chandiramani, K. L.: Diffraction of Evanescent Waves with Applications to Aerodynamically Scattered Sound and Radiation from Unbaffled Plates. *Journal of Acoustical Society of America*, 55 (1974).

Clark, B.; Dorsch, R. G.; and Reshotko, M.: Flap Noise Prediction Method for a Powered Lift System. AIAA Paper No. 73-1028, 1973.

Clark, P. J. F.; and Ribner, H. S.: Direct Correlation of Fluctuating Lift with Radiated Sound for an Airfoil in Turbulent Flow. *Journal of Acoustical Society of America*, Vol. 46, No. 3 (part 2), 1969, pp. 802-805.

Conticelli, V. M.; Di Blasi, A.; and O'Keefe, J. V.: Noise Shielding Effects for Engine-Over-Wing Installations. AIAA Paper 75-474. March 1975.

Curle, N.: The Influence of Solid Boundaries Upon Aerodynamic Sound. Proceedings of Royal Society, A-231 (1955), p. 505.

Doak, P. E.: Acoustic Radiation from a Turbulent Fluid Containing Foreign Bodies. Proceedings of Royal Society A259A (1960), pp. 129-145.

Dorsch, R. G.: Externally Blown Flap Noise Research. NASA TM X-71541, May 1974 (SAE 740-468).

Dorsch, R. G.; Clark, B. J.; and Reshotko, M.: Interim Prediction Method for Externally Blown Flap Noise. NASA TM X-71768, Aug. 1975.

Dorsch, R. G.; Goodykoontz, J. H.; and Sargent, N. B.: Effect of Configuration Variation on Externally Blown Flap Noise. AIAA Paper 74-190, 1974. (NASA TM X-71495).

Dorsch, R. G.; Kreim, W. J.; and Olsen, W. A.: Externally Blown Flap Noise. AIAA Paper No. 72-129, Jan. 1972 (also NASA TM X-67991).

Dunn, D. G.; and Peart, N. A.: Aircraft Noise Source and Contour Estimation, NASA CR-114649, July 1973.

Dorsch, R. G.; Krejsa, E. A.; and Olsen, W. A.: Blown Flap Noise Research. AIAA Paper No. 71-745, June 1971 (NASA TM X-67850).

Dorsch, R. G.; Lasagna, P. L.; Maglieri, D. J.; and Olsen, W. A.: Flap Noise. NASA SP-311, 1972.

Dorsch, R. G.; and Reshotko, M.: EBF Noise Tests with Engine Under and Over the Wing Configuration STOL Technology. NASA SP-320, 1972.

Dorsch, R. G.; Reshotko, M.; and Olsen, W. A.: "Flap Noise Measurements for STOL Configurations Using External Upper Surface Blowing. AIAA Paper No. 72-1203 (also NASA TM X-68167).

Falarski, M. D.; Aiken, T. N.; Aoyogi, K.; and Koenig, D. G.: Comparison of the Acoustic Characteristics of Large-Scale Models of Several Propulsive-Lift Concepts. *Journal of Aircraft*, Vol. 12, No. 7, July 1975, pp. 600-604 (also AIAA Paper 74-1094).

Falarski, M. D.; Aoyagi, K., and Koenig, D. G.: Acoustic Characteristics of Large-Scale STOL Models at Forward Speed. NASA TM X-62251, Oct. 1972, and NASA SP-320, 1972.

Falarski, M. D.: Large-Scale Wind Tunnel Investigation of the Noise Characteristics of a Semispan Wing Equipped with an Externally Blown Jet Flap. NASA TM X-62154, May 1972.

Falarski, M. D: Aspects of Investigating STOL Noise Using Large-Scale Wind Tunnel Models. NASA TM X-62164, June 1972.

Falarski, M. D.; Aoyagi, K.; and Koenig, D. G.: Acoustic Characteristics of a Large-Scale Wind Tunnel Model of an Upper Surface Blown Flap Transport Having Two Engines, NASA TM X-62319, Sept. 1973.

Ffowcs Williams, J.; and Hall, L. H.: Aerodynamic Sound Generation by Turbulent Flow in the Vicinity of a Scattering Half Plane. *Journal of Fluid Mechanics*, Vol. 40, Part 4, March 1970, pp. 657-670.

Ffowcs Williams, T.; and Hawkings, : "Sound Generated by Turbulence and Surfaces in Arbitrary Motion. Philos. Trans. R. Soc. Lond. 264A, pp. 321-342 (1969).

Filler, L.: Prediction of Far-Field Jet/Trailing Edge Interaction Noise for Engine-Over-the-Wing Installations. AIAA Paper 76-518, July 1976.

Fink, M. R.: "Scrubbing Noise of Externally Blown Flaps. AIAA Paper No. 75-469, March 1975.

Fink, M. R.: Prediction of Externally Blown Flap Noise and Turbomachinery Strut Noise. NASA CR-134883, Aug. 1975.

Fink, M. R.: Experimental Evaluation of Theories for Trailing Edge and Incidence Fluctuating Noise. *AIAA Journal*, Vo. 13, No. 11 (Nov. 1975), pp. 1472-1477.

Fink, M. R.: Investigation of Scrubbing and Impingement Noise. NASA CR-134762, Feb. 1975.

Fink, M. R.; and Olsen, W. A.: Comparison of Predictions and Under-the-Wing Noise Data. AIAA Paper 76-501, July 1976.

Fink, M. R.: Additional Studies of Externally Blown Flap Noise. NASA CR-135096, August 1976.

Fink, M. R.: Forward Flight Effects on EBF Noise. AIAA Paper No. 77-1314, October 1977.

Foss, J. F.; and Kleis, S. J.: Vorticity and Acoustic Measurements in Vertically Impinging Jet Flows. Proceedings of 3rd Interagency Symposium on Transportation Noise, pp. 425-444, University of Utah, Nov. 12-14, 1975.

Gibson, F. W.: Noise Measurement Studies of Several Model Jet Augmented Lift Systems. NASA LWP-981, 1971.

Gibson, F. W.: Noise Measurements of Model Jet Augmented Lift Systems. NASA TN D-6710, 1972 (NASA LWP-981, 1971).

Gibson, J. S.: Noise Reduction of EBF Propulsive Lift Systems. SAE Paper 750608, May 1975.

Gibson, J. S.: State-of-the-Art STOL Aircraft Noise. AIAA Paper No. 77-1313, Oct. 1977.

Goldstein, M.: Unified Approach to Aerodynamic Sound Generation in the Presence of Solid Boundaries. *Journal of Acoustical Society of America*, Vol. 56, No. 2, 1974, pp. 497-509.

Goodykoontz, J.; Dorsch, R. G.; and Groesbeck, : Mixer Nozzle - Externally Blown Flap Noise Tests. NASA TM X-68021, 1972.

Goodykoontz, J. H.; Dorsch, R. G.; and Groesbeck, : Noise Tests for a Mixer Nozzle – Externally Blown Flap System. NASA TN D-7236, May 1973.

Goodykoontz, J. H.; Dorsch, R. G.; and Wagner, J. M.: Acoustic Characteristics of Externally Blown Flap Systems with Mixer Nozzles. AIAA Paper No. 74-192, Aerospace Sciences Meeting, 12th, Washington, Jan-Feb. 1974.

Goodykoontz, J.; and Gutierrez, O. A.: Over-the-Wing Model Thrust Reverser Noise Test. AIAA Paper No. 77-1318, Oct. 1977.

Goodykoontz, J.; Olsen, W. A.; and Dorsch, R. G.: Preliminary Tests of the Mixer Nozzle Concept for Reducing Blown Flap Noise. NASA TM X-67938, Oct. 1971.

Goodykoontz, J. H.; Olsen, W. A.; and Dorsch, R. G.: Small-Scale Tests of the Mixer Nozzle Concept for Reducing Blown-Flap Noise. NASA TM X-2638, Nov. 1972.

Goodykoontz, J.; Von Glahn, U.; and Dorsch, R.: Forward Velocity Effects on Under-the-Wing Externally Blown Flap Noise. AIAA Paper 75-476, March 1975.

Goodykoontz, Jack H.; Wagner, Jack M.; and Sargent, Noel B.: Noise Measurements for Various Configurations of a Model of a Mixer Nozzle - Externally Blown Flap System. NASA TM X-2776, April 1973.

Grosch, F. R.: On the Generation of Sound Resulting from the Passage of a Turbulent Air Jet Over a Flat Plate of Finite Dimensions. RAE Library Translation 1460, Oct. 1970.

Gruschka, H. D.; and Schrecker, G. O.: Aeroacoustic Characteristics of Jet Flap Type Exhausts. AIAA Paper No. 72-130, Jan. 1972.

Hayden, R. E.: Noise from Interacting of Flow with Rigid Surfaces: A Review of Current Status of Prediction Techniques. NASA CR-2126, Oct. 1972.

Hayden, R. E.: Fundamental Aspects of Noise Reduction from Powered-Lift Devices. SAE Paper 730376, Air Transportation Meeting, Miami, April 1973.

Hayden, R. E.: Reduction of Noise from Airfoils and Propulsive Lift Systems Using Variable Impedance Surfaces. AIAA Paper 76-500, July 1976.

Hayden, R. W.; et al.: A Preliminary Evaluation of Noise Reduction Potential for USB Flaps. NASA CR-112246, 1972.

Hayden, R. E.; Fox, H. L.; and Chanaud, R. C.: Some Factor Influencing Radiation of Sound from Flow Interaction with Edges of Finite Surfaces. NASA CR-145073, 1976.

Hayden, R. E.; Kadman, Y.; and Chanaud, R. C.: A Study of the Variable Impedance Surface Concept as a Means for Reducing Noise from Jet Interaction with Developed Lift-Augmenting Flaps. NASA CR-112166, July 1972.

Head, R. W.; and Fisher, M. J.: Jet/Surface Interaction Noise Analysis of Far-Field Low Frequency Augmentation of Jet Noise Due to the Presence of Solid Shield. AIAA Paper 76-502, July 1976.

Heidelberg, L. J.; Homyak, L.; and Jones, W. L.: "Full-Scale Upper Surface Blown Flap Noise. SAE Paper 750609, May 1975. NASA TM X-71708.

Hellstrom, G.: Noise Shielding Aircraft Configurations: A Comparison Between Predicted and Experimental Results. Proceedings of the 9th Congress of the ICAS, Vol. 2, pp. 730-740, Aug. 1974.

Hubbard, H. H.; Chestnutt, D.; and Maglieri, D. J.: Noise Control Technology for Jet-Powered STOL Vehicles, ICAS Paper No. 72-50, Aug-Sept. 1972.

Jones, W. L.; and Heidelberg, L. J.: Investigation of Noise from Full-Scale High By-pass Engine and Blown Flap System. SAE Paper 740467, Air Transportation Meeting, Dallas, May 1974 (NASA TM X-71539).

Jones, W. L.; Heidelberg, L. J.; and Goldman, R. G.: Highly Noise Suppressed Bypass 6 Engine for STOL Applications. AIAA Paper No. 73-1031, 1973.

Joshi, M. C.: Acoustic Investigation of Upper Surface Blown Flaps. Ph.D. Thesis, University of Tennessee, March 1977.

Kramer, J. J.; Chestnutt, D.; Lucas, J. G.; and Rice, E. J.: Noise Reduction Aircraft Propulsion. NASA SP-259, 1971, pp. 169-209.

Karchmer, Allen M.; and Friedman, Robert: Noise Tests of an Externally Blown Flap with the Engine in Front of the Wing. NASA TM X-2942, Dec. 1972.

Lasagna, P. L.; and Putnam, T. W.: Externally Blown Flap Impingement Noise. NASA SP-320, 1972.

Maglieri, D. J.; and Hubbard, H. H.: Preliminary Measurement of Noise Characteristics of Some Jet-Augmented-Flap Configurations, NASA Langley Memorandum 12-4-58L, Dec. 1958.

McKenzie, D. J.; and Burns, R. J.: Analysis of Noise Produced by Jet Impingement Near the Trailing Edge of Flat Plate and Curved Plate. NASA TM X-3171, Jan. 1975.

McKenzie, D. J.; and Burns, R. J.: Externally Blown Flap Trailing Edge Noise Reduction by Slot Blowing - A Preliminary Study. AIAA Paper 73-245, Jan. 1973.

McKenzie, D. J.: EBF Noise Suppression and Aerodynamic Penalties. NASA TM-73823, Jan. 1978.

Meecham, W. C.: Surface and Volume Sound from Boundary Layers. *Journal of Acoustical Society of America*, Vol. 37, No. 3, March 1965, pp. 516-522.

Miles, J. H.: Rational Function Representation of Flap Noise Spectra Including Correction for Reflection Effects. *Journal of Aircraft*, Vol. 12, No. 11, Nov. 1975 (AIAA Paper No. 74-193, 1974).

Miles, J. H.: Method of Representation of Acoustic Spectra and Reflection Corrections Applied to Externally Blown Flap Noise. NASA TM X-3179, Feb. 1975.

Newerth, G.: Acoustic Feedback of a Subsonic and Supersonic Free Jet Which Impinges on a Foreign Body. NASA TTF-15719, 1974.

Olsen, W.; Burns, R.; and Groesbeck, D.: Flap Noise and Aerodynamic Results for Model QCSEE Over-the-Wing Configurations. AIAA Paper 77-23, Jan. 1977.

Olsen, W. A.; Dorsch, R. G.; and Miles, J. H.: Noise Produced by a Small-Scale Externally Blown Flap. NASA TN D-6636, 1972.

Olsen, W. A.; Miles, J. H.; and Dorsch, R. G.: Noise Generated by Impingement of a Jet Upon a Large Flat Board. NASA TN D-7075, 1972.

Olsen, William A.; and Friedman, Robert: Noise Tests of a Model Engine Over-the-Wing STOL Configuration Using a Multijet Nozzle with Deflector. NASA TM X-2871, August 1973.

Patterson, G. T.; Joshi, M. C.; and Maus, J. R.: Experimental Investigation of the Aeroacoustic Characteristics of Model Slot Nozzles with Straight Flaps. AIAA Paper 75-471, March 1975.

Pennock, A. P.: Forward Speed Effects on Blown Flap Noise. AIAA Paper 77-1315, Oct. 1977.

Pennock, A. P.; Swift, G.; and Marbert, J. A.: Static and Wind Tunnel Model Tests for Development of Externally Blown Flap Noise Reduction Techniques. NASA CR-134675, Feb. 1975.

Phillips, O. M.: On the Aerodynamic Surface Sound from a Plane Turbulent Boundary Layer. Proc. Roy. Soc. Ser. A, Vol. 234, No. 1198, Feb. 21, 1956, pp. 327-335.

Phillips, O. M.: The Intensity of Aeolian Tones," *J. Fluid Mechanics*, 1, pp. 607-624 (1956).

Pinkel, B.; and Scharton, T. D.: Reduction of Noise Generated by Fluid Flow Over a Plate. *Journal of Acoustical Society of America*, Vol. 53, No. 4, 1973.

Powell, A.: On the Aerodynamic Noise of a Rigid Plate Moving at Zero Incidence. *Journal of Acoustical Society of America*, Vol. 31, No. 12, Dec. 1959, pp. 1649-1653.

Powell, Alan: Aerodynamic Noise and the Plane Boundary. *Journal of Acoustical Society of America*, Vol. 32, No. 8, Aug. 1960, pp. 982-990.

Preisser, J. S.; and Fratello, D. J.: Acoustic Characteristics of a Large Upper Surface Blown Configuration with Turbofan Engines. AIAA Paper 75-473, March 1975.

Preisser, J. S.; and Block, P. W.: An Experimental Study of the Aeroacoustics of a Subsonic Jet Impinging Normal to a Large Rigid Surface. AIAA Paper 76-520, July 1976.

Putnam, T. W.; and Lasagna, P. L.: Externally Blown Flap Impingement Noise. AIAA Paper No. 72-664, 1972.

Reddy, N. N.: Propulsive-Lift Noise of an Upper-Surface-Blown Flap Configuration. AIAA Paper 75-470, March 1975.

Reddy, N. N.; Blakney, D. F.; and Tibbetts, J. G.; and Gibson, J. S.: V/STOL Aircraft Noise Prediction. DOT/FAA Report FA-RD-75-125, June 1975.

Reddy, N. N.; and Brown, W. H.: Acoustic Characteristics of an Upper Surface Blowing Concept of Powered-Lift System. AIAA Paper 75-204, Jan. 1975.

Reddy, N. N.; and Swift, G.: Blown Flap Noise Using Velocity Decayer Nozzle. Paper presented at 86th Meeting of Acoustical Society of America, Nov. 1973.

Reddy, N. N.; and Yu, J. C.: Radiated Noise from an Externally Blown Flap. NASA TN D-7908, July 1975.

Reddy, N. N.; Pennock, A. P.; Tibbetts, J. G.; and Tam, C. K. W.: Noise Characteristics of Upper Surface Blown Configurations - Analytical Studies. NASA CR-2812, March 1978.

Reddy, N. N.; and Gibson, J. S.: Noise Characteristics of Upper Surface Blown Configurations - Summary. NASA CR-2918, 1978.

Reshotko, M.; Goodykoontz, J. H.; and Dorsch, R. G.: Engine-Over-the-Wing Noise Research. AIAA Paper No. 73-631, Fluid and Plasma Dynamics Conference 6th, Palm Springs, July 1973.

Reshotko, M.; and Friedman, R.: Acoustic Investigation of the Engine-Over-the-Wing Concept Using a D-shaped Nozzle. AIAA Paper No. 73-1030, Aeroacoustics Conference, Seattle, Oct. 1973 (NASA TM X-71419).

Reshotko, M.; Olsen, W. A.; and Dorsch, R. G.: Preliminary Noise Tests of the Engine-Over-the-Wing Concept, I- 30° - 60° Flap Position. NASA TM X-68032, 1972.

Reshotko, M.; Olsen, W. A.; and Dorsch, R. G.: Preliminary Noise Tests of the Engine-Over-the-Wing Concept, II. 10° - 20° Flap Position. NASA TM X-68104, 1972.

Samanich, N. E.; Heidelberg, L. J.; and Jones, W. L.: Effect of Exhaust Nozzle Configuration on Aerodynamic and Acoustic Performance of an Externally Blown Flap System with a Quiet 6:1 Bypass Ratio Engine. AIAA Paper No. 73-1217, 1973.

Searle, N.: Acoustic Investigation of a Hybrid Propulsive Lift System. ASME Paper 74-WA/Aero-3, Nov. 1974.

Siddon, T. E.: Surface Dipole Strength by Cross-Correlation Method. *Journal Acoustical Society of America*, Vol. 53, No. 2, Feb. 1973, pp. 619-633.

Scharton, T. D.; Kadman, Y.; and Hayden, R. E.: Investigation of Propulsive Lift Aerodynamic Noise Reduction by Active Control of Blowing Air. AIAA Paper 76-519, July 1976.

Scharton, T.; Pinkel, B.; and Wilby, A.: A Study of Trailing Edge Blowing as a Means of Reducing Noise Generated by the Interaction of Flow with Surface. Bolt Beranek and Newman, Inc., Cambridge, Mass. Report 2593, Sept. 1973.

Schloth, A. P.: Measurement of Mean Flow and Acoustic Power for a Subsonic Jet Impinging Normal to a Large Rigid Surface. NASA TM X-72803, Jan. 1976.

Sharland, I. J.: Sources of Noise in Axial Flow Fans. *Journal of Sound and Vibration*, Vol. 1, pp. 302-322, 1964.

Tam, C. K. W.; and Reddy, N. N.: Sound Generated in the Vicinity of Trailing Edge of Upper Surface Blown Flap. *Journal of Sound and Vibration*, Vol. 52, No. 2, pp. 211-232.

Tam, C. K. W.; and Yu, J. C.: Trailing Edge Noise. AIAA Paper No. 75-489, March 1975.

von Glahn, U.; Groesbeck, D.; and Goodykoontz, J.: Velocity Decay and Acoustic Characteristics of Various Nozzle Geometries with Forward Velocity. AIAA Paper No. 73-629, Fluid and Plasma Dynamics Conference, 6th, Palm Springs, July 1973.

von Glahn, U.; and Groesbeck, D.: Acoustics of Attached and Partially Attached Flow for Simplified OTW Configurations with 5:1 Slot Nozzle. NASA TM X-71807, Nov. 1975.

von Glahn, U.; and Groesbeck, D.: OTW Noise Correlation for Variations in Nozzle/Wing Geometry with 5:1 Slot Nozzles. AIAA Paper 76-521, July 1976.

von Glahn, U.: and Groesbeck, D.: Effect of External Jet Flow Deflection Geometry on OTW Aero-Acoustic Characteristics. AIAA Paper 76-499, July 1976. NASA TM X-73460.

von Glahn, U. H.; Groesbeck, D. E.; and Huff, R. G.: Peak axial-velocity decay with single- and multi-element nozzles. AIAA Paper No. 72-48, Aerospace Sciences Meeting, 10th, San Diego, Jan. 1972.

von Glahn, U.; Reshotko, M.; and Dorsch, R. G.: Acoustic Results Obtained with Upper-Surface-Blowing Lift Augmentation System. NASA TM X-68159, 1972.

von Glahn, U.: Geometry Considerations for Jet Noise Shielding with CTOL Engine-Over-the-Wing Concept. NASA TM X-71562, June 1974.

von Glahn, U.: Influence of Multi-tube Mixer Nozzle Geometry on CTOL-OTW Jet Noise Shielding. NASA TM X-71681, 1975.

von Glahn, U.; Sekas, N.; and Groesbeck, D.: Forward Flight Effects on Mixer Nozzle Design and Noise Considerations for STOL Externally Blown Flap Systems. AIAA Paper No. 72-792, Aircraft Design, Flight Test, and Operations Meeting, 4th, Los Angeles, August 1972.

von Glahn, U.; and Groesbeck, D.: Influence of Mixer Nozzle Velocity Decay Characteristics on CTOL-OTW Jet Noise Shielding. AIAA Paper 75-97, 1975.

Yu, J. C.; and Tam, C. K. W.: An Experimental Investigation of the Trailing Edge Noise Mechanism. AIAA Paper 77-1291, Oct. 1977.

"Page missing from available version"

page 64

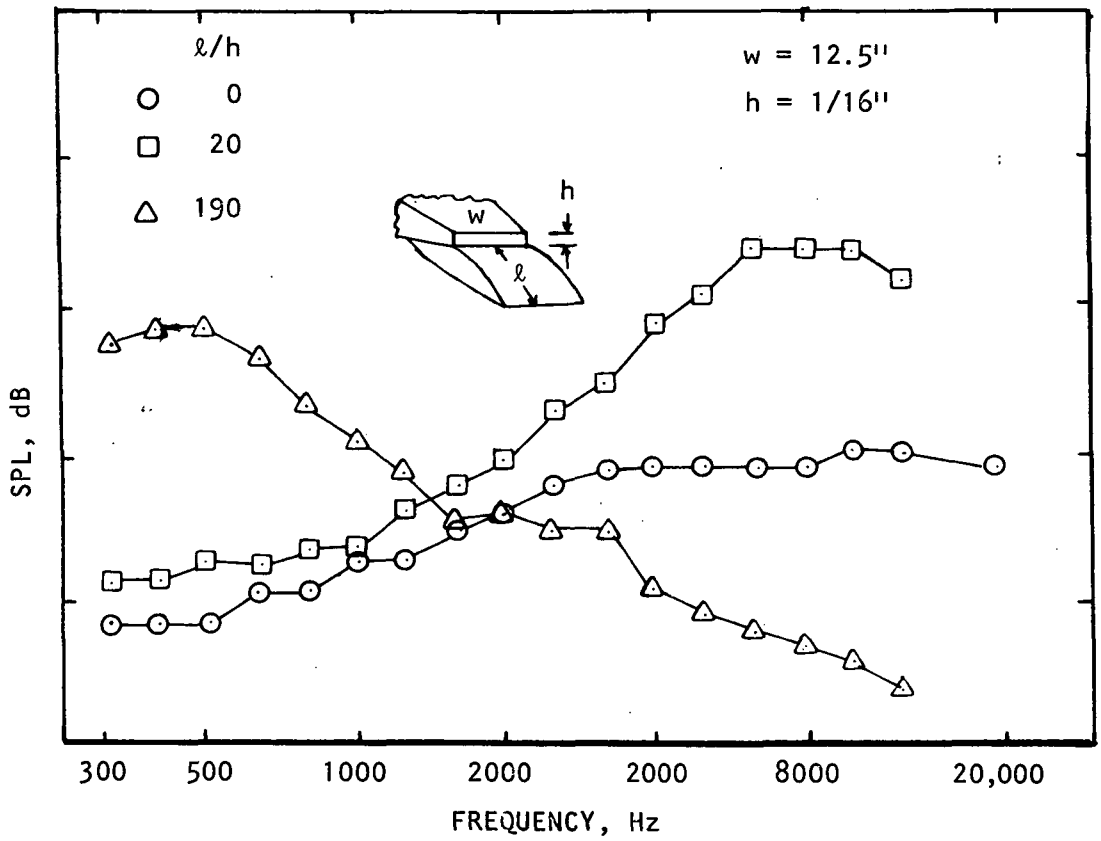

Figure 2 Jet Flap Noise Spectra
($\delta_f = 30°$, $V_J \approx 1050$ ft/sec.)

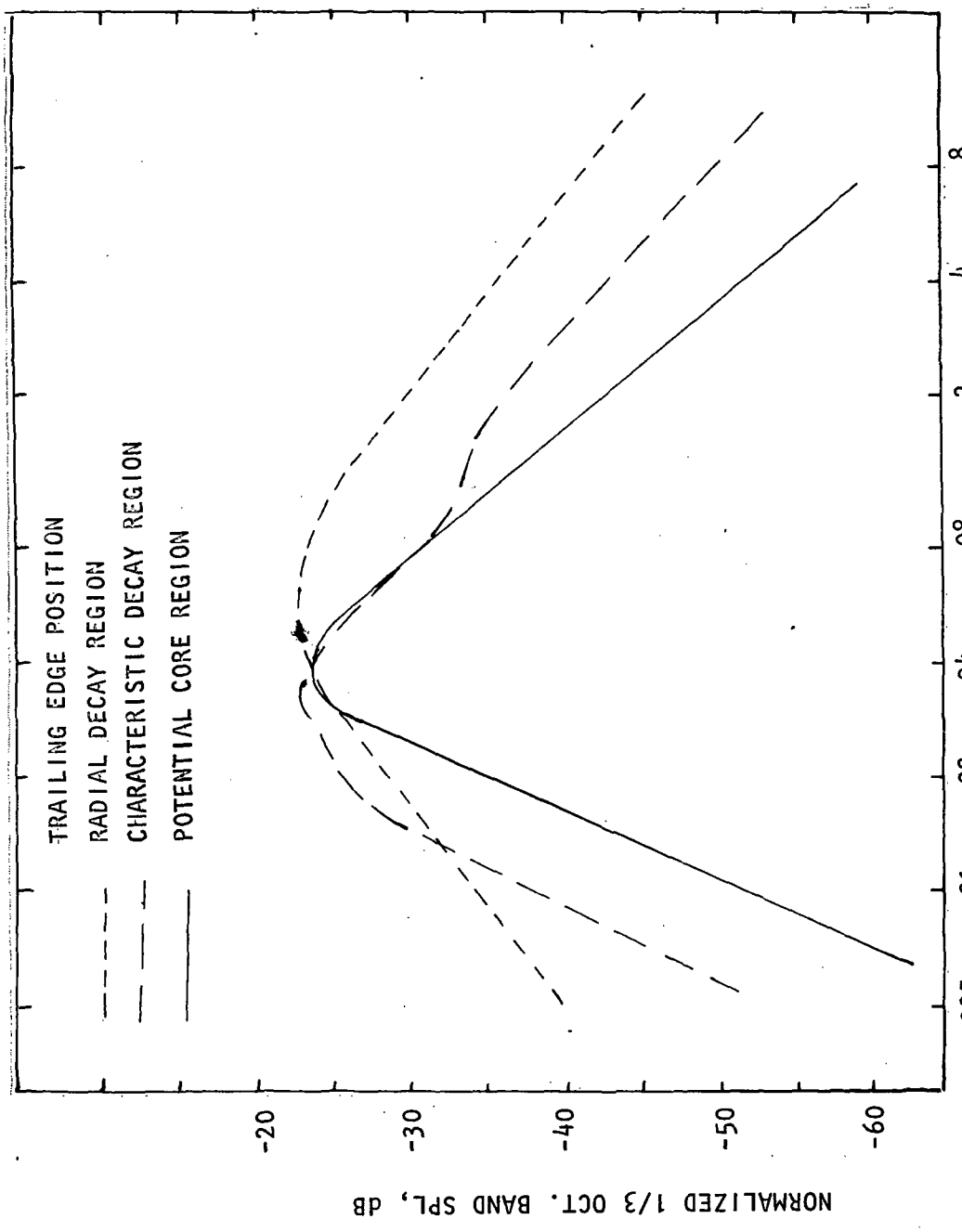

Figure 3 Spectral Distribution of Wall Jet for the Trailing Edge in the Different Regions of Jet Flow

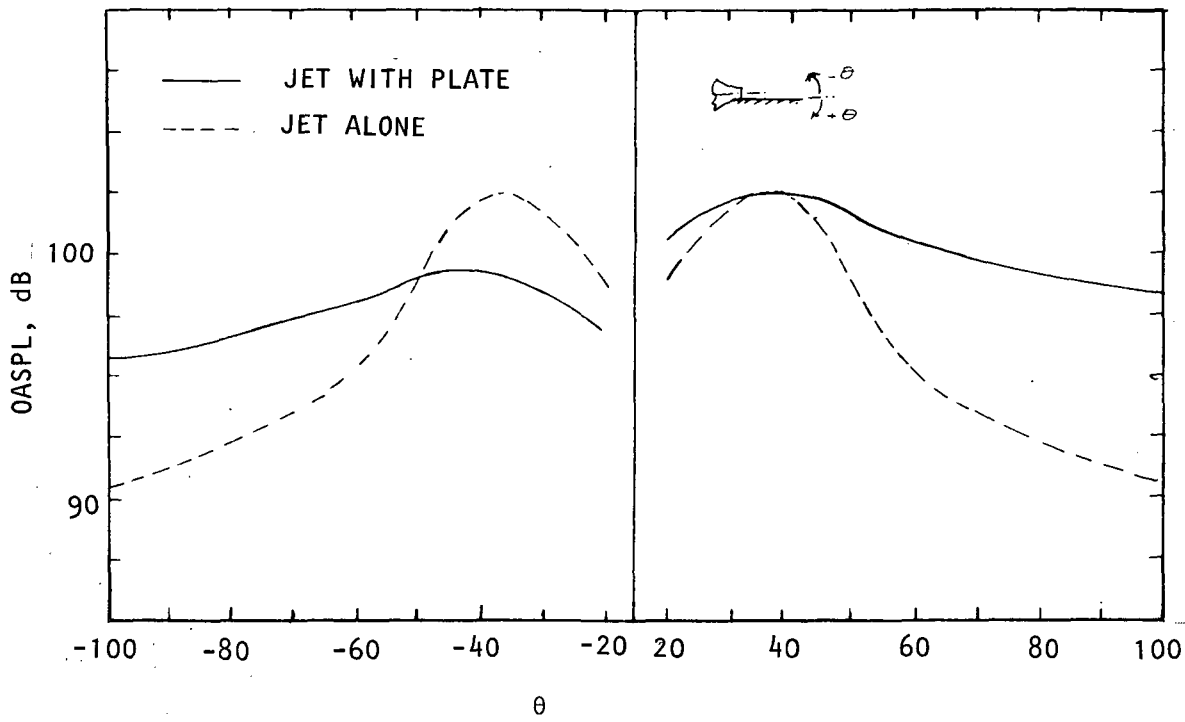

Figure 4 Angular Distribution in the Plane Perpendicular to the Plate Passing Through Jet Axis ($M_J = 0.98$, $\ell/h = 25$)

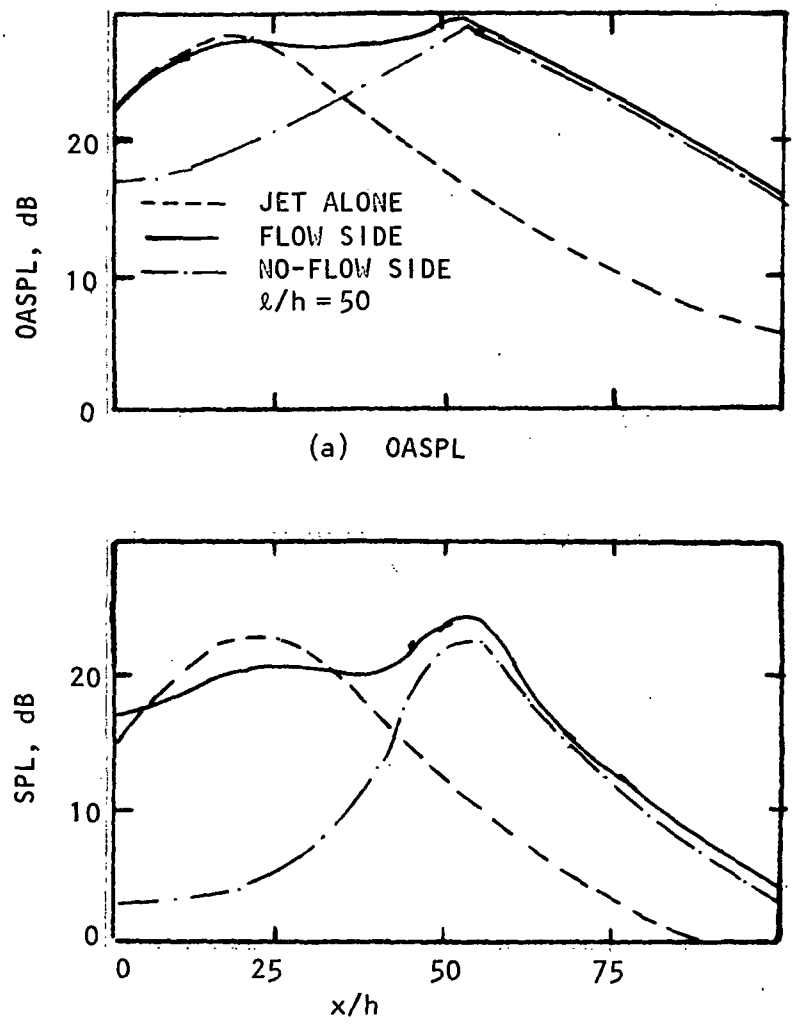

Figure 5 Source Location for Jet Flap Configuration (Acoustic Mirror Measurements)

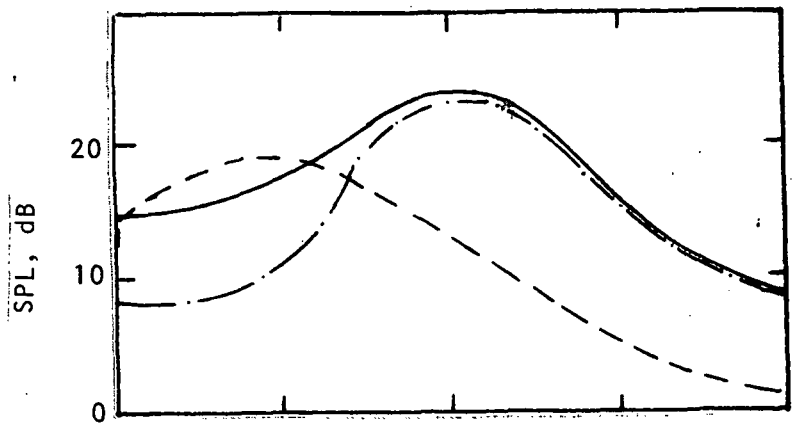

(c) Octave Band Level ($f_c = 8$ KHz)

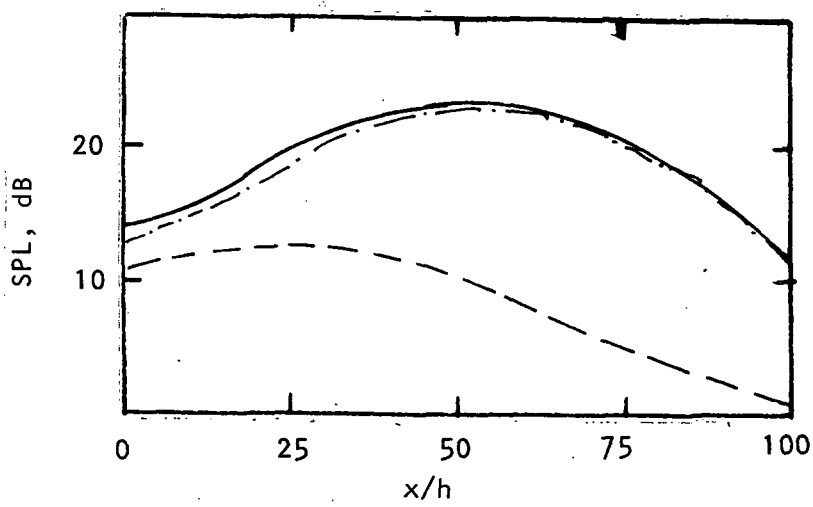

(d) Octave Band Level ($f_c = 4$ KHz)

Figure 5 Concluded.

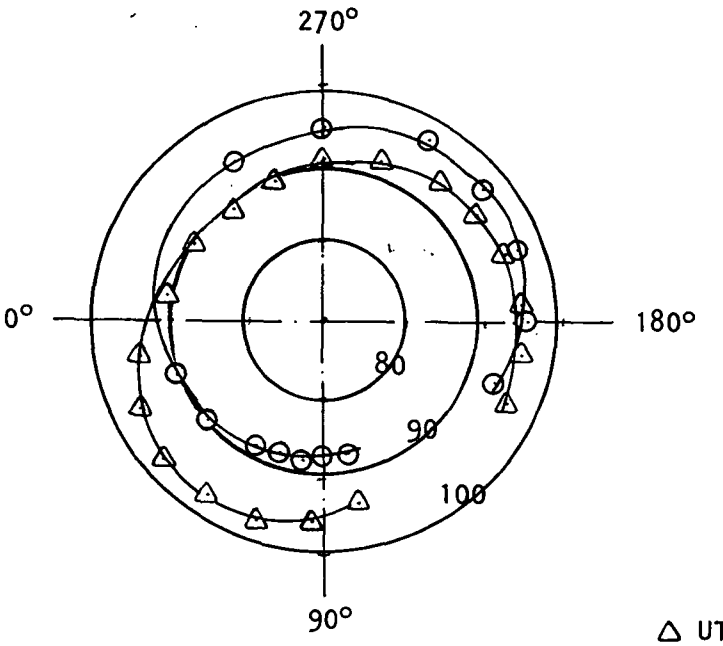

△ UTW CONFIGURATION
○ USB CONFIGURATION

(a) PNL Directivity at 500 ft. Radius in the Flyover Plane

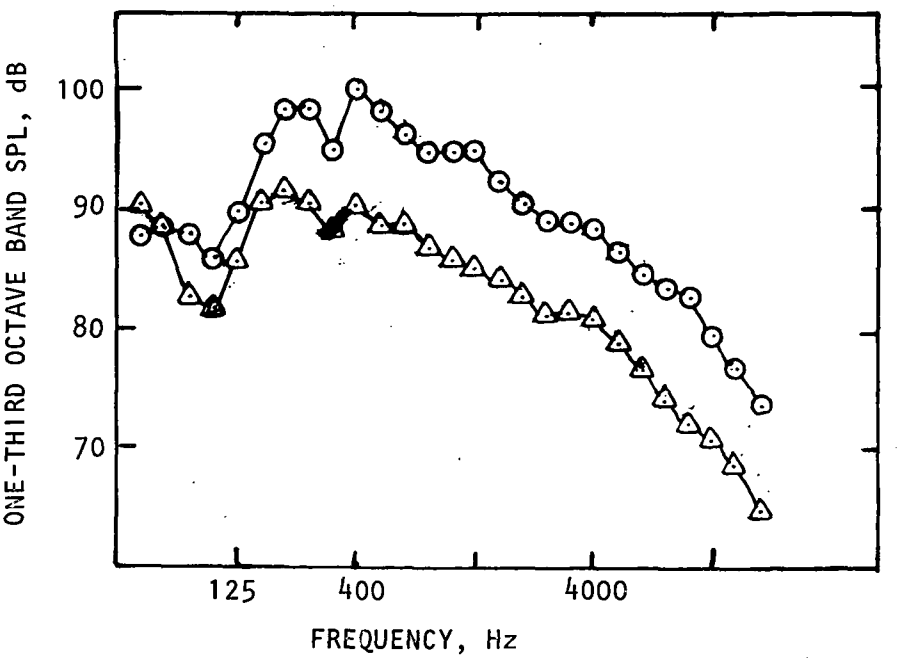

(b) Spectra at 50 ft.

Figure 6 Comparison of Blown Flap Noise Levels.

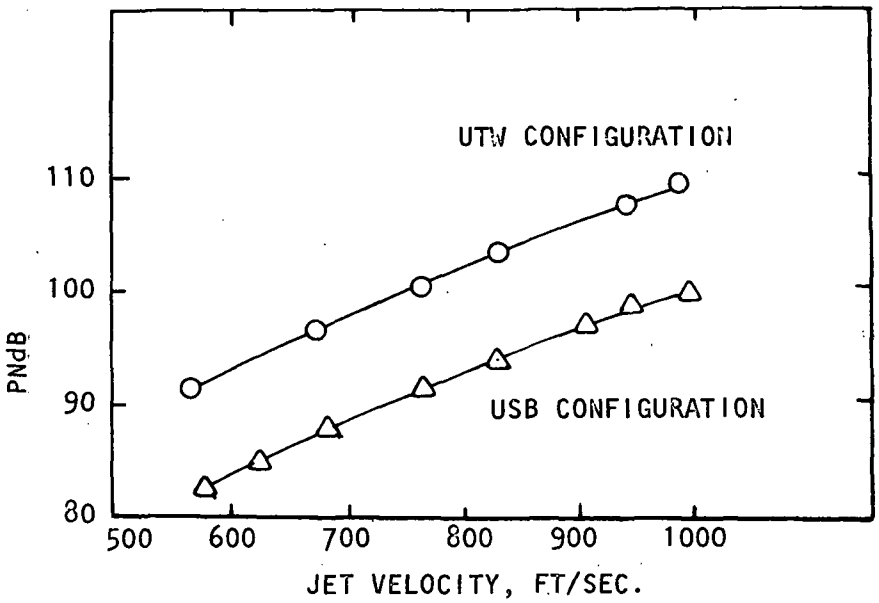

(c) PNL at 500 ft. Sideline

Figure 6 Concluded.

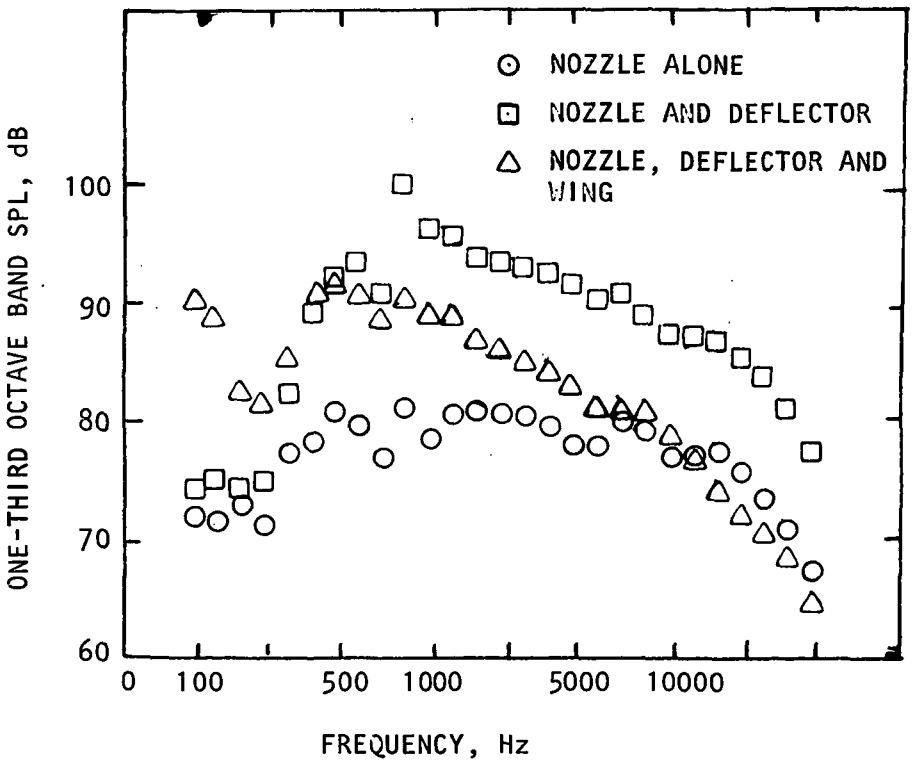

Figure 7 Effect of External Deflector on Spectra

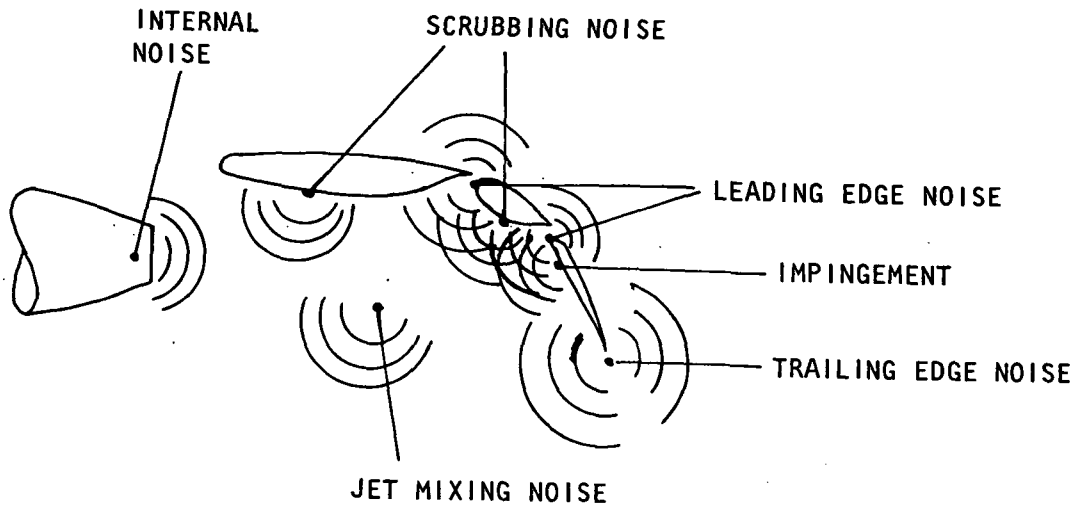

(a) UTW Noise Sources

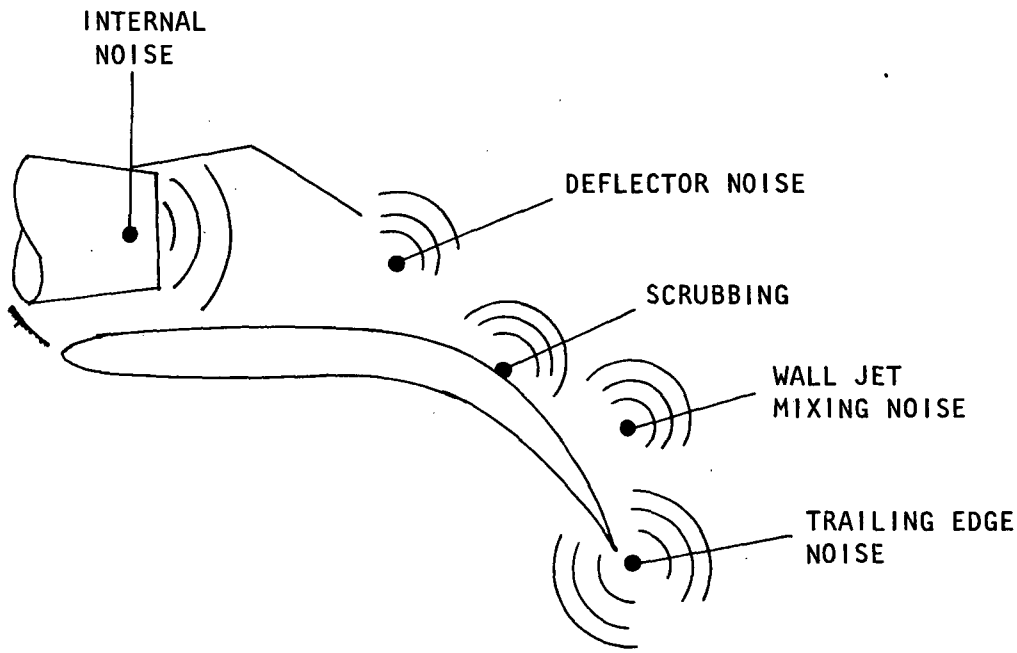

(b) USB Noise Sources

Figure 8 Noise Sources of Blown-Flap Configuration

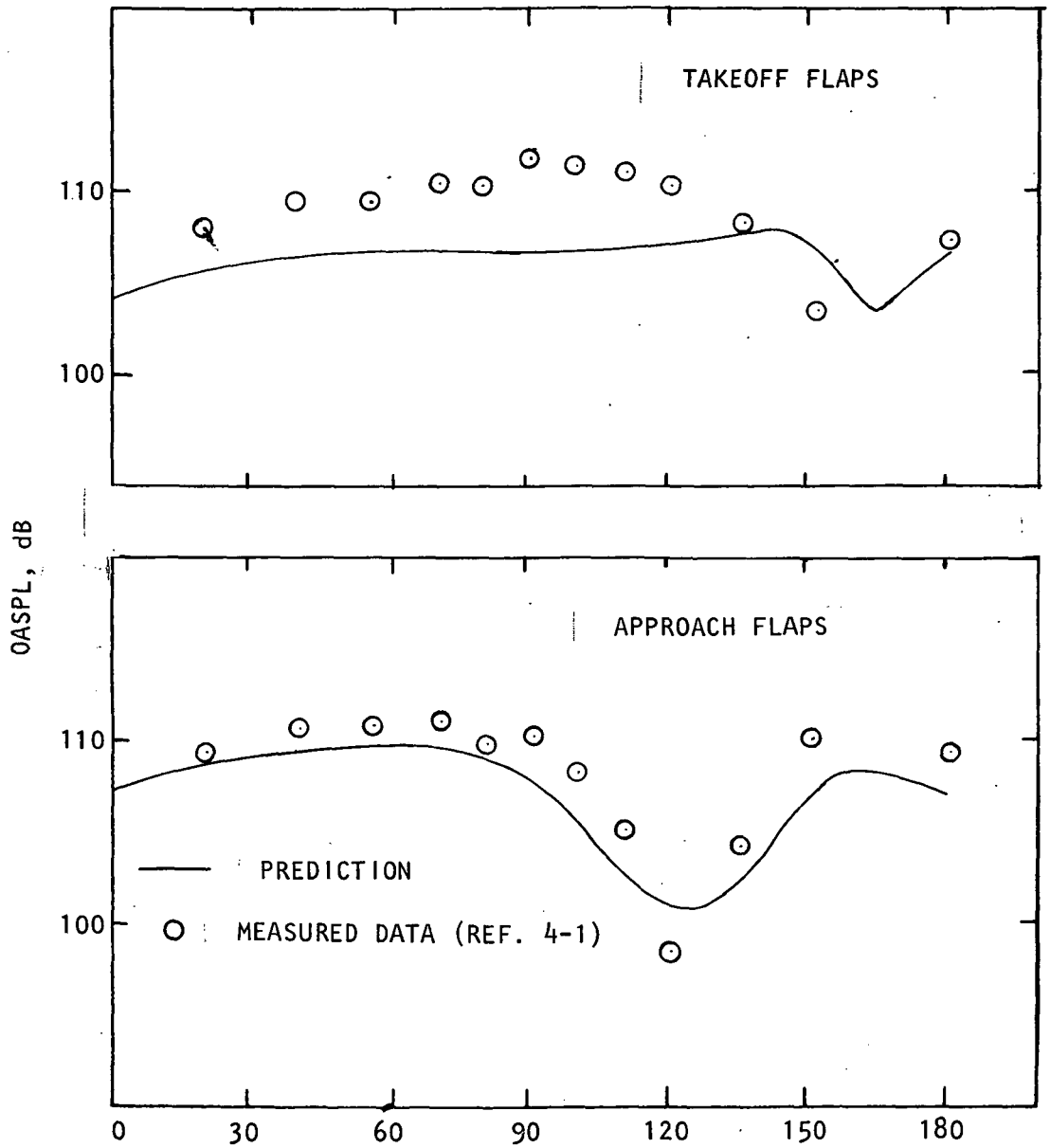

(a) Directivity

Figure 9 Comparison of ANOP Prediction With Test Data (UTW Configuration, Flyover Plane, $V_J = 227$ m/sec.)

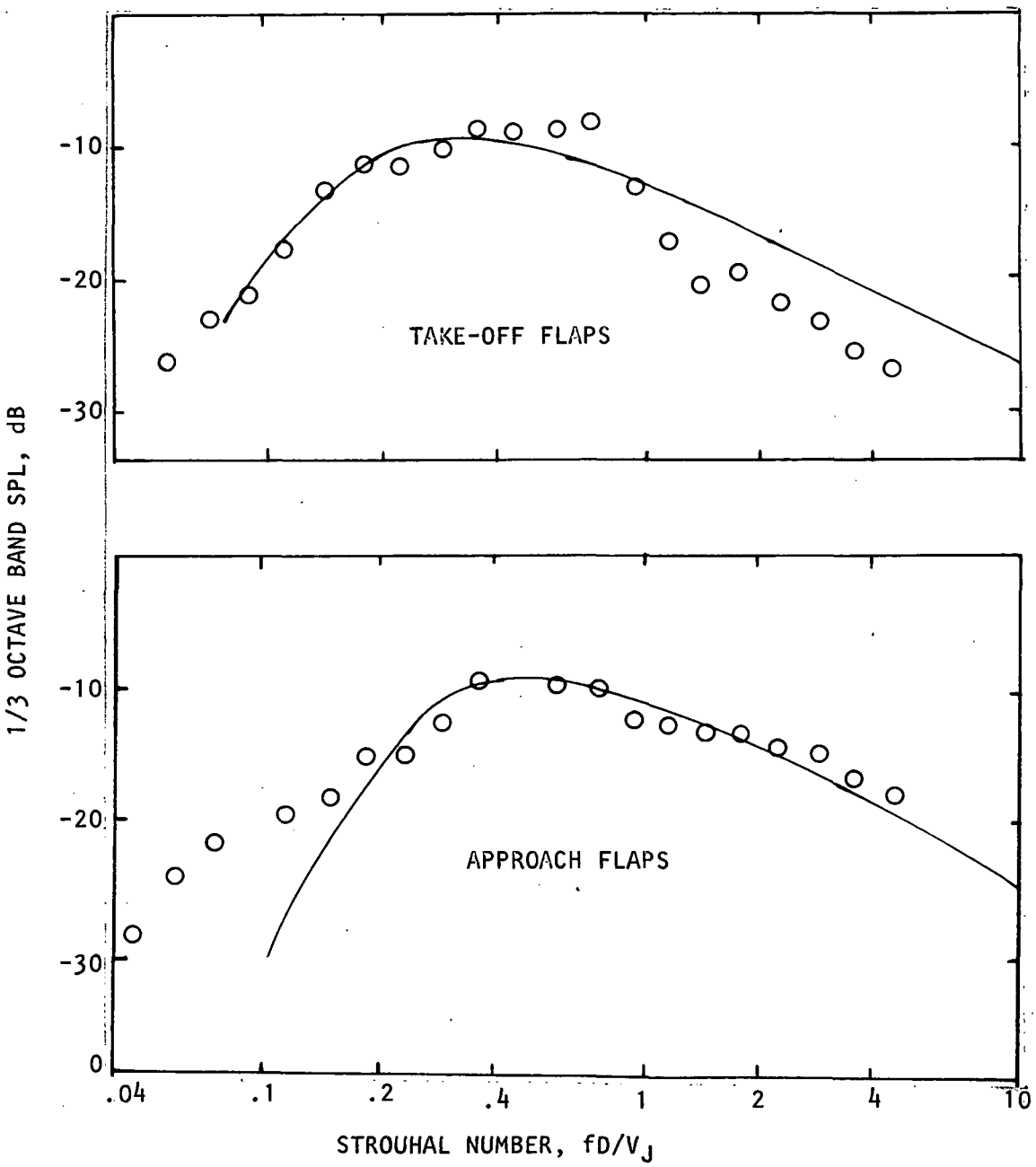

(b) One-Third Octave Band Spectra

Figure 9. - Concluded.

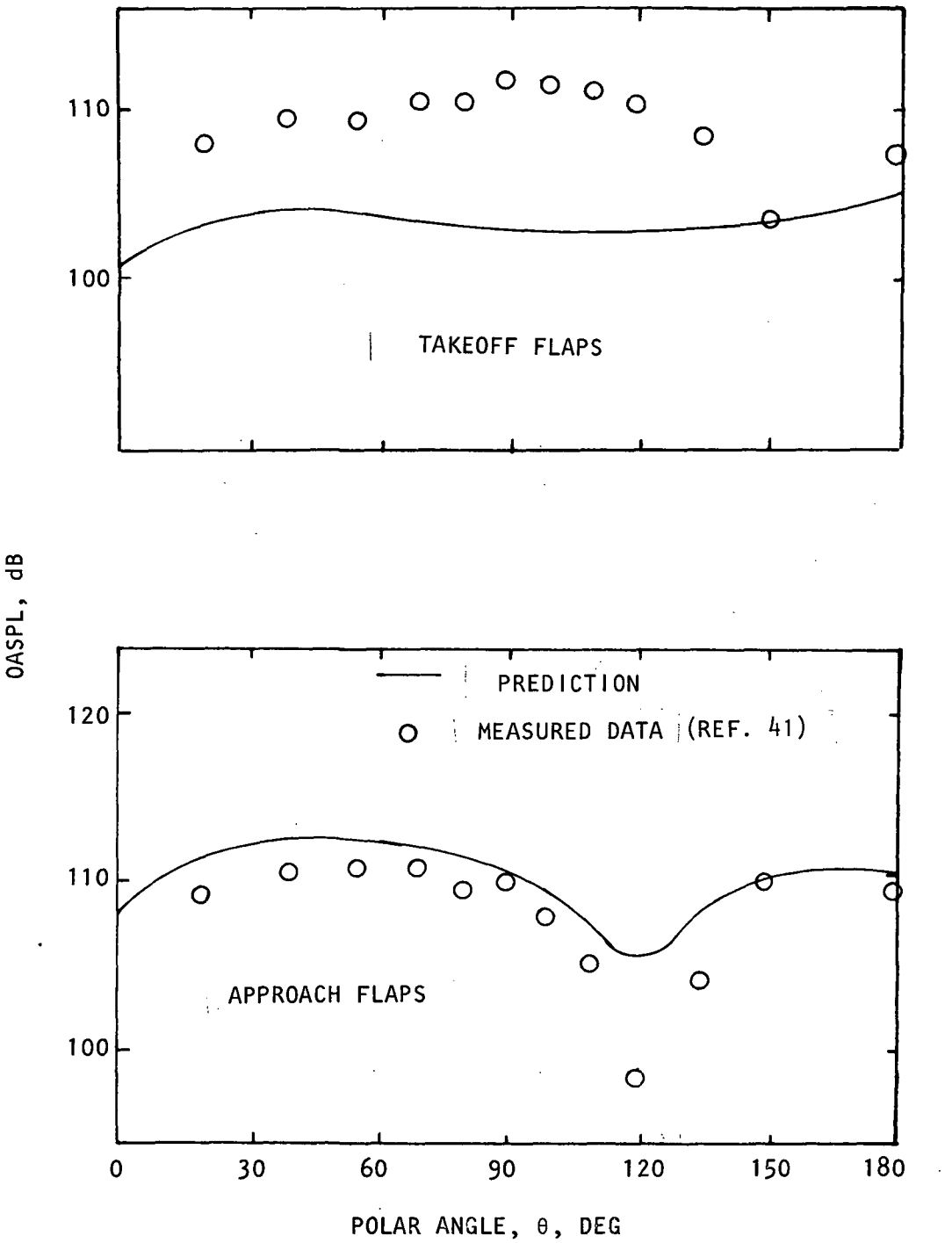

Figure 10 Comparison of Lockheed/FAA Prediction With Test Data (UTW Configurations, Flyover Plane, $V_J = 227$ m/sec.)

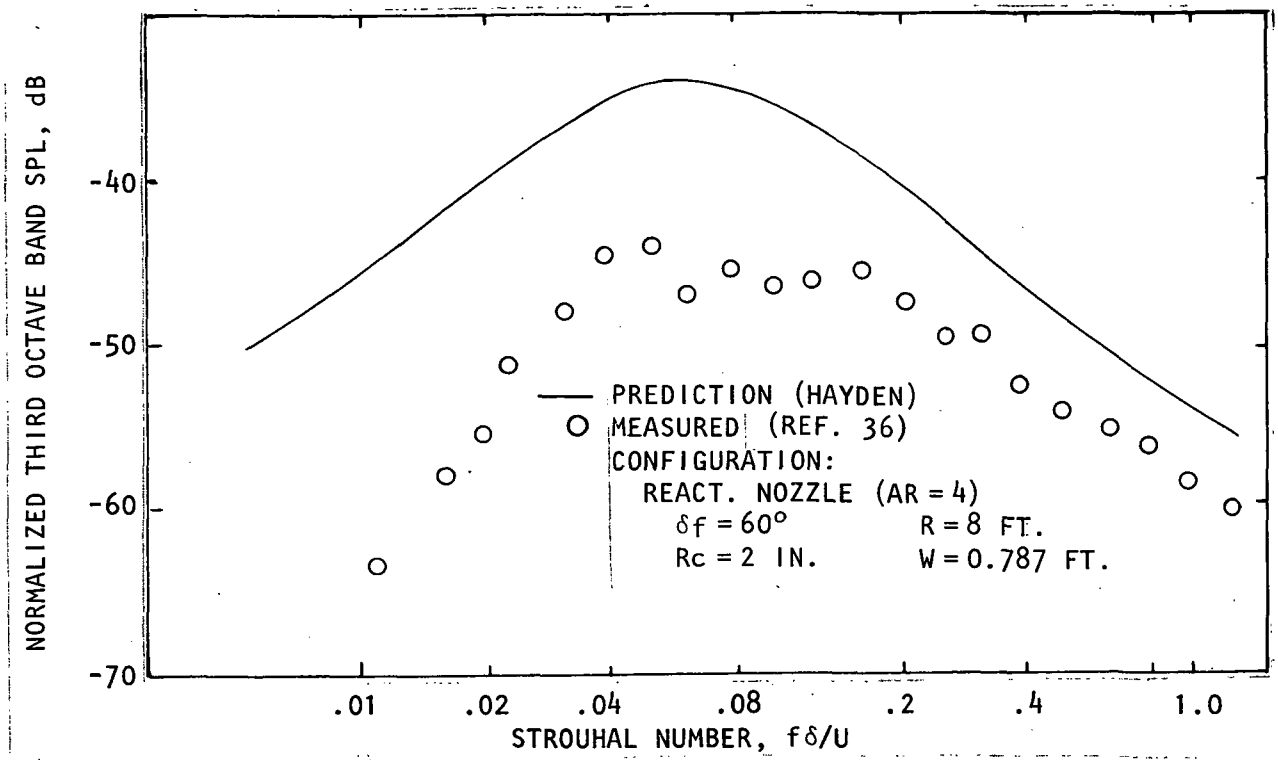

Figure 11 Comparison of BBN Prediction With USB Data.

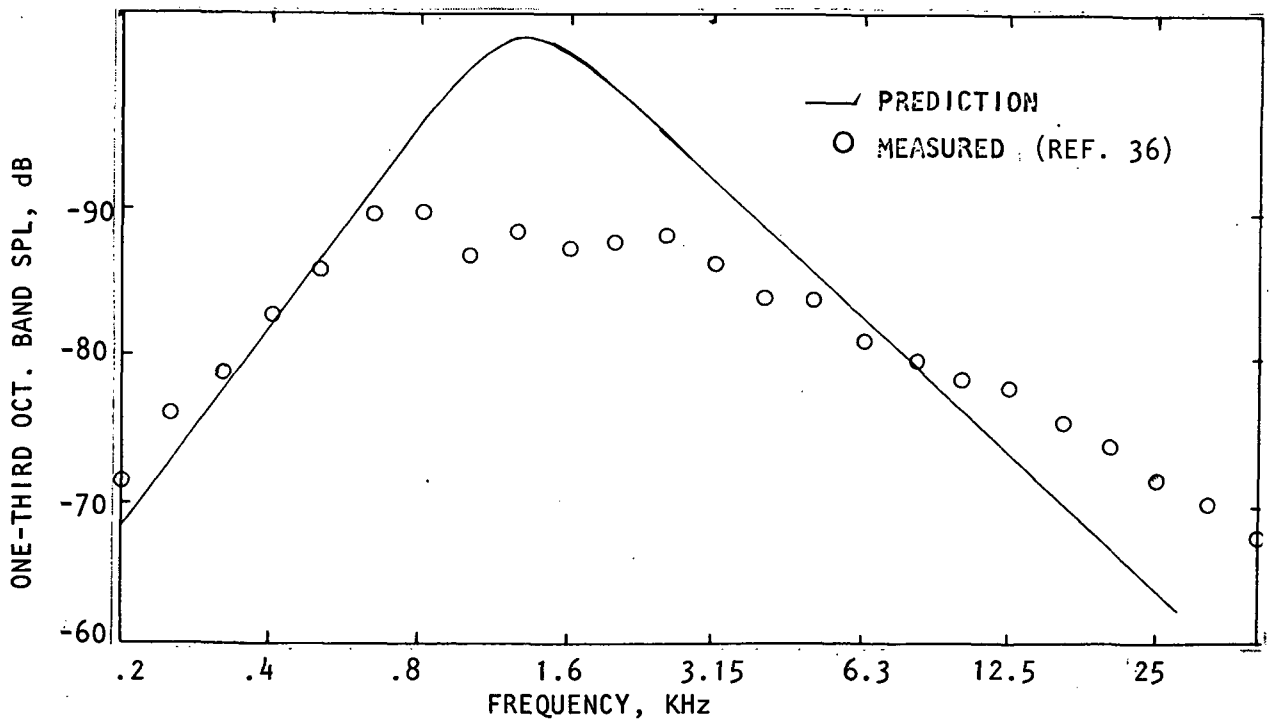

Figure 12 Comparison of Filler's Prediction With Measured Data.

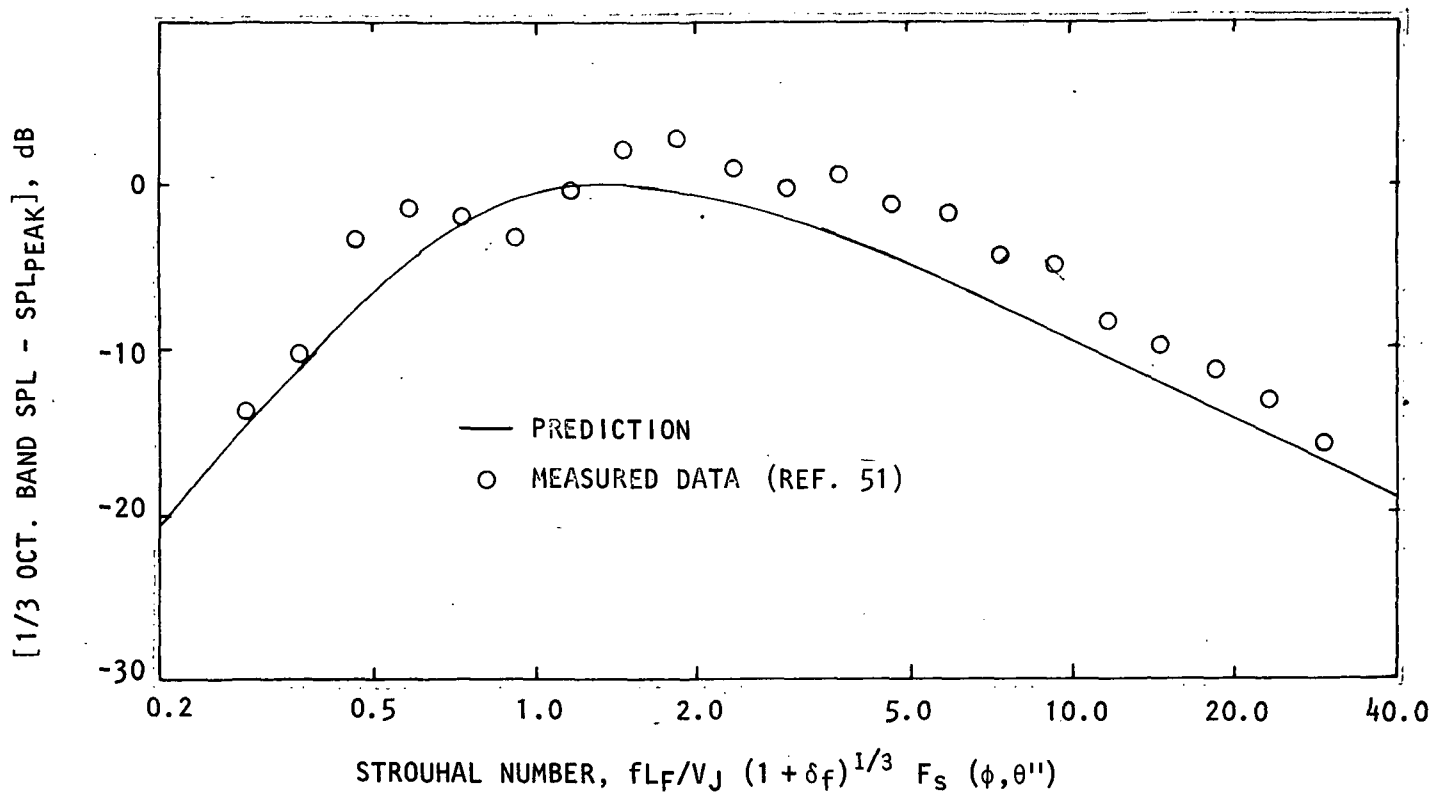

Figure 13 Comparison of Lockheed/NASA Prediction With Full-Scale USB Static Test Data

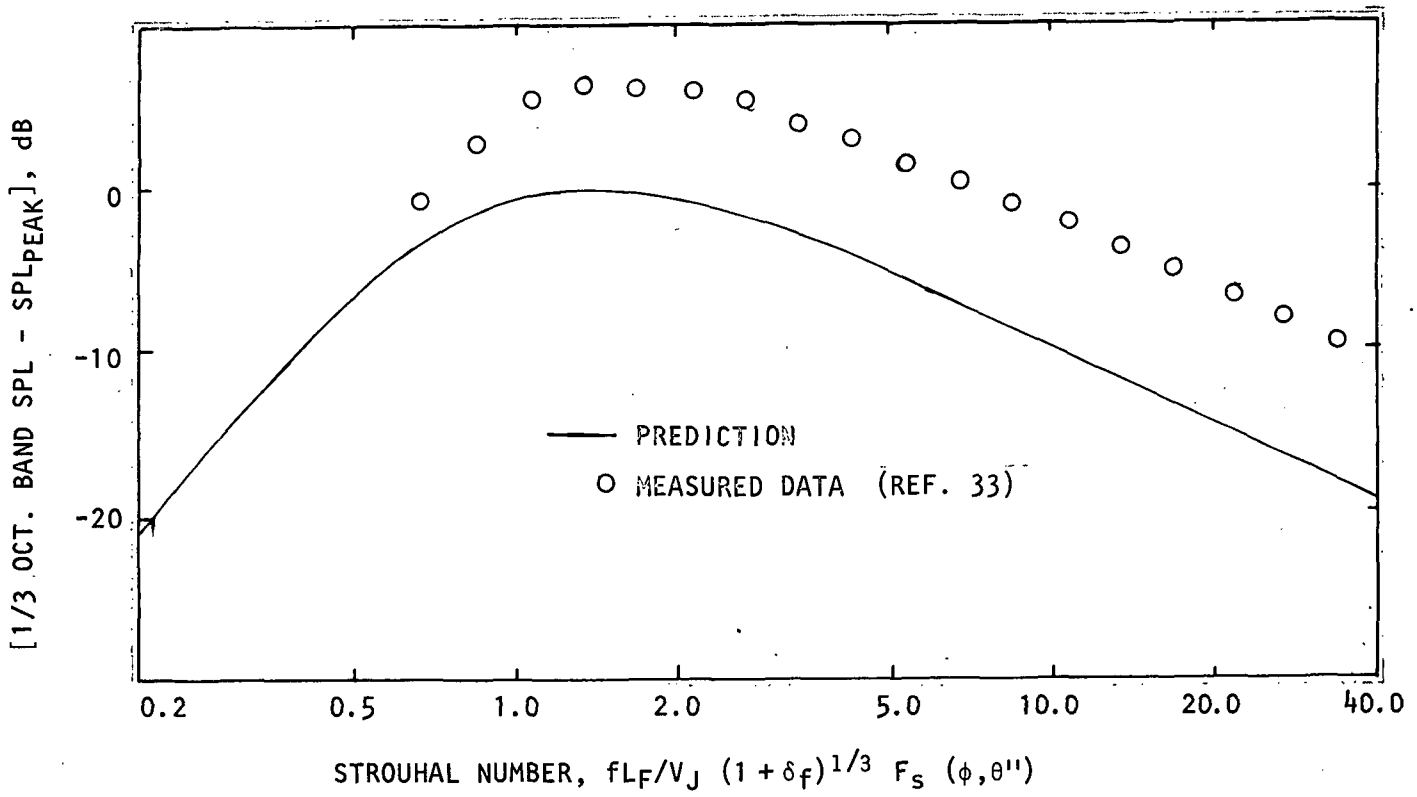

Figure 14 Comparison of Lockheed/NASA Prediction With Small-Scale Model Static Test Data

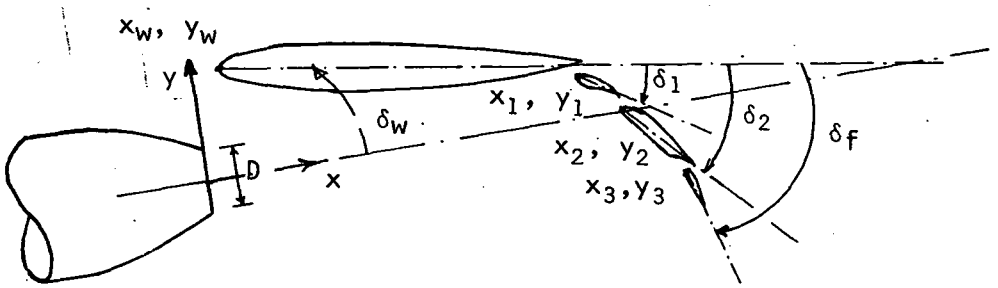

(a) UTW Configuration

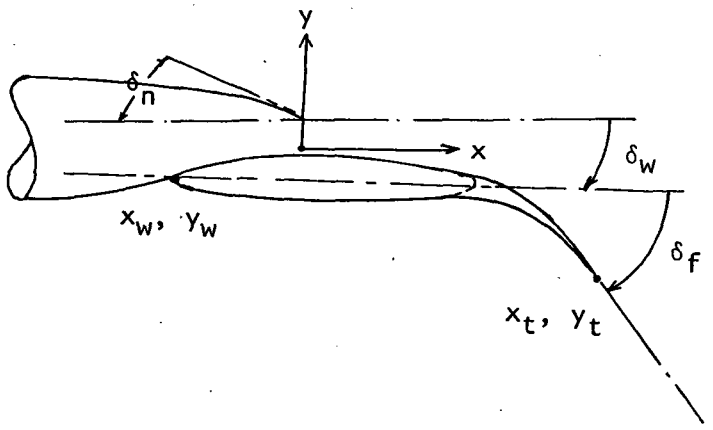

(b) USB Configuration

Figure 15 Coordinate System and Geometry Description

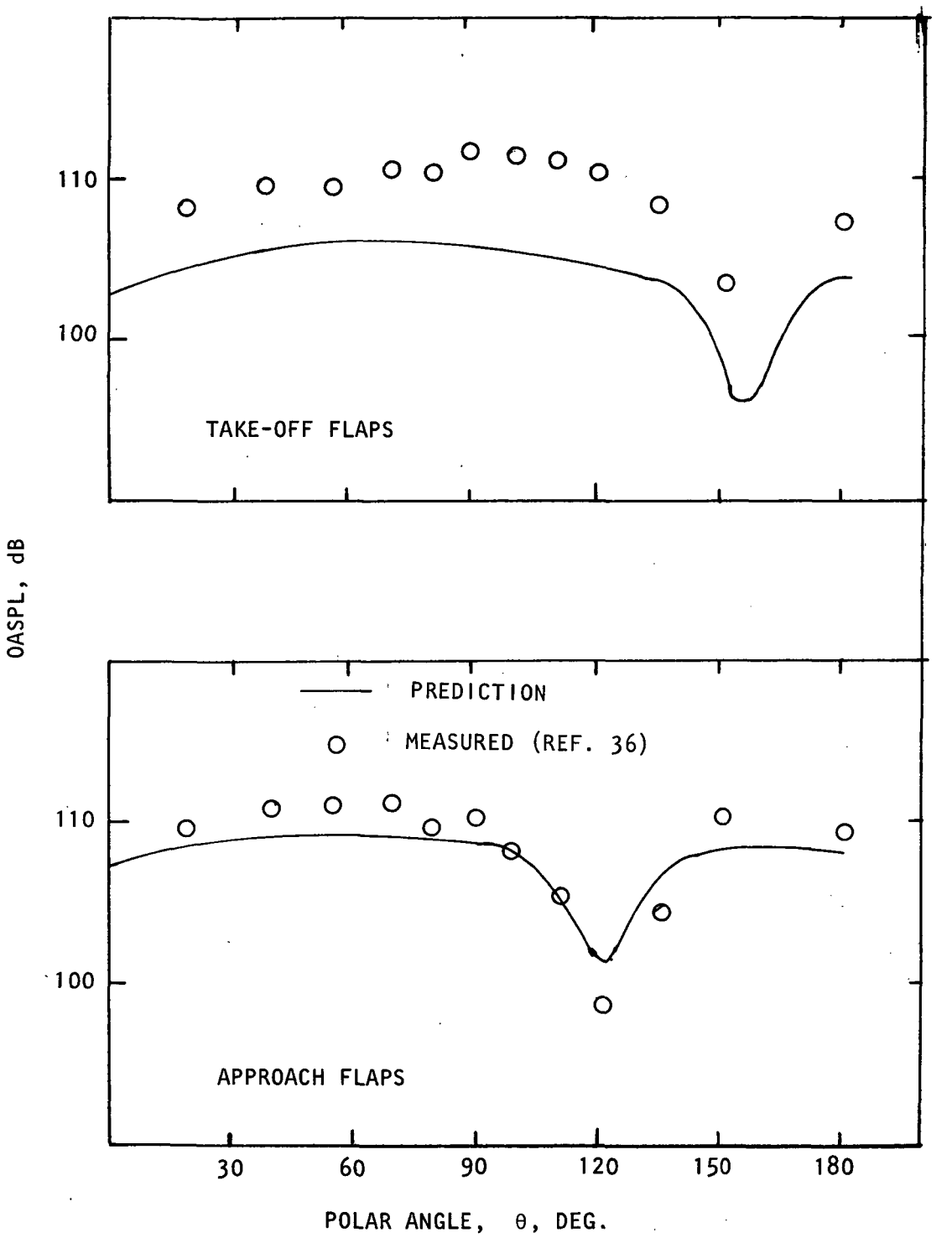

Figure 16 Comparison of UTRC Prediction With Test Data (UTW Configuraton, Flyover Plane, $V_J = 227$ m/sec.)

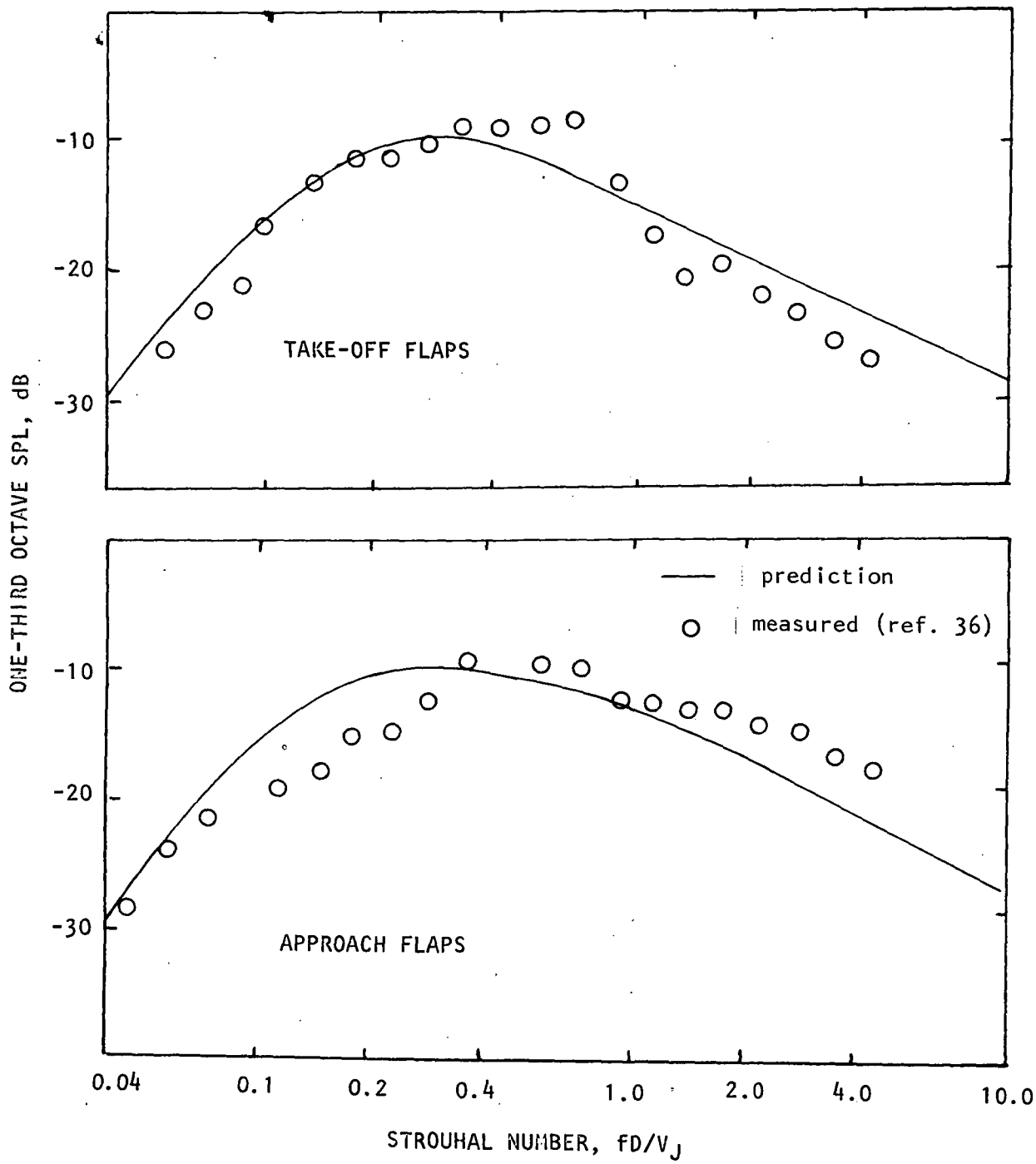

Figure 17 Comparison of UTRC Prediction With Test Data (UTW Configuration; Flyover Plane, $V_J = 227$ m/sec.)

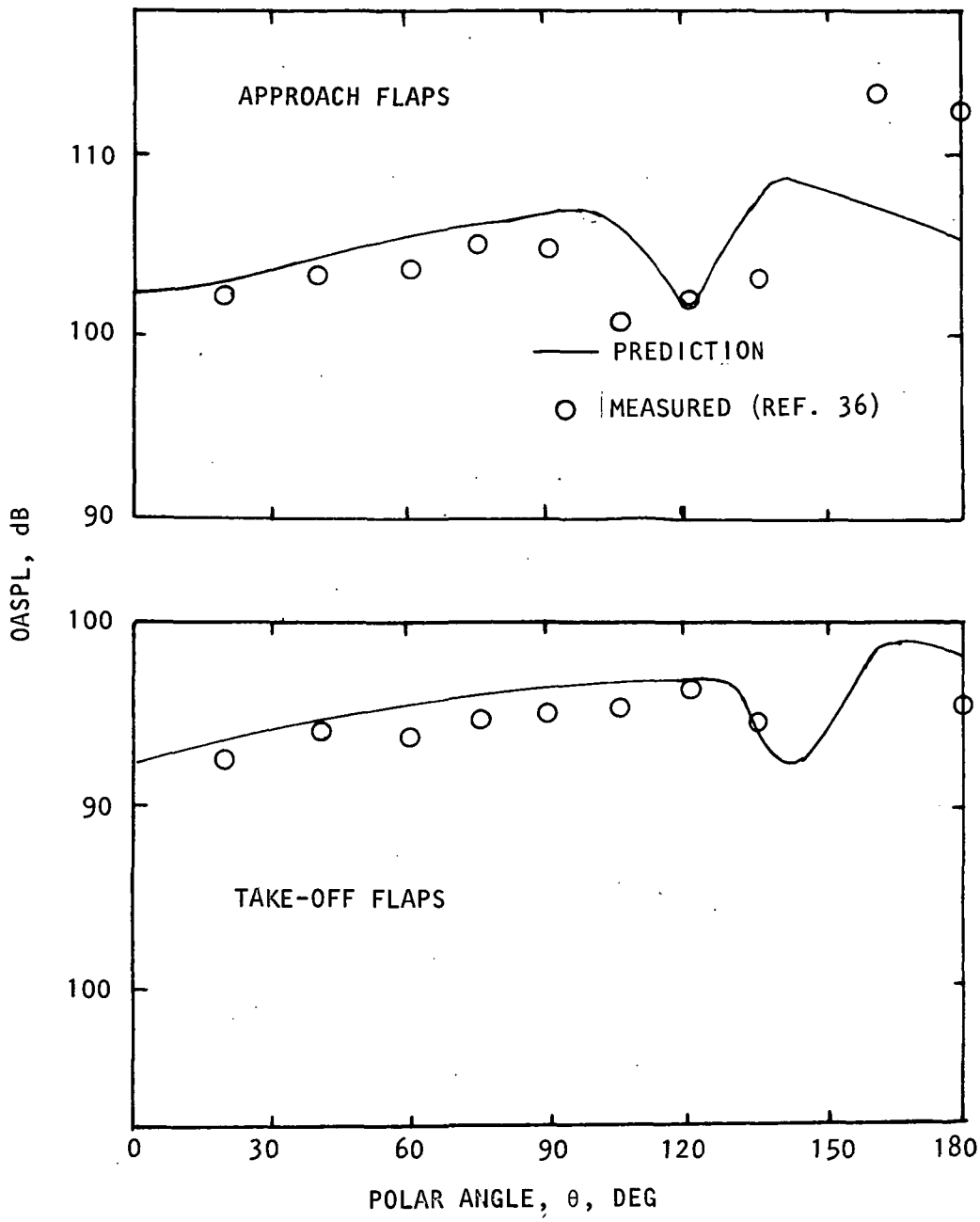

Figure 18 Comparison of UTRC Prediction with QCSEE Model Data (USB Configuration, Flyover Plane, $V_J = 220$ m/sec.)

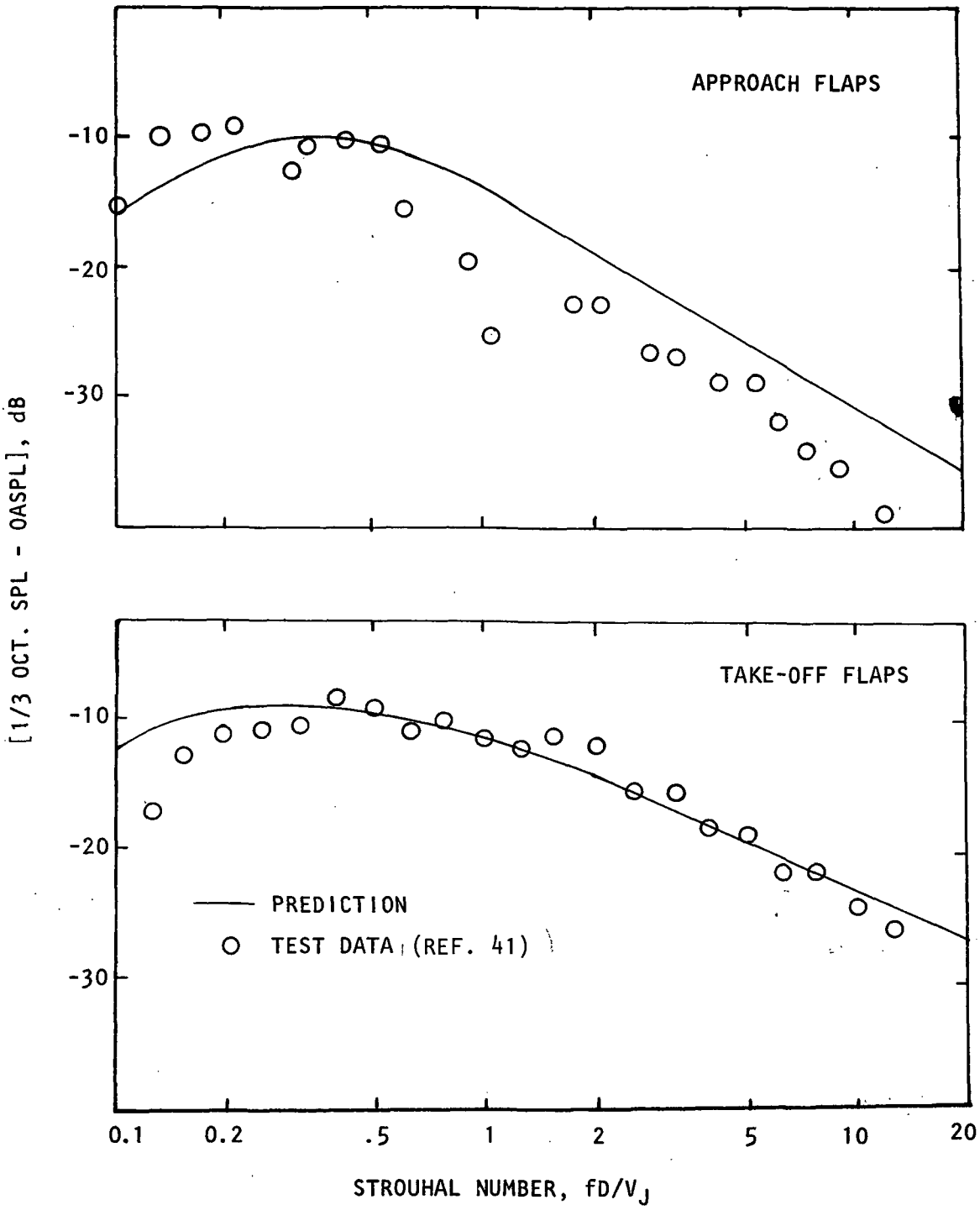

Figure 19 Comparison of UTRC Prediction With QCSEE 1/11.5 Scale USB Model Data

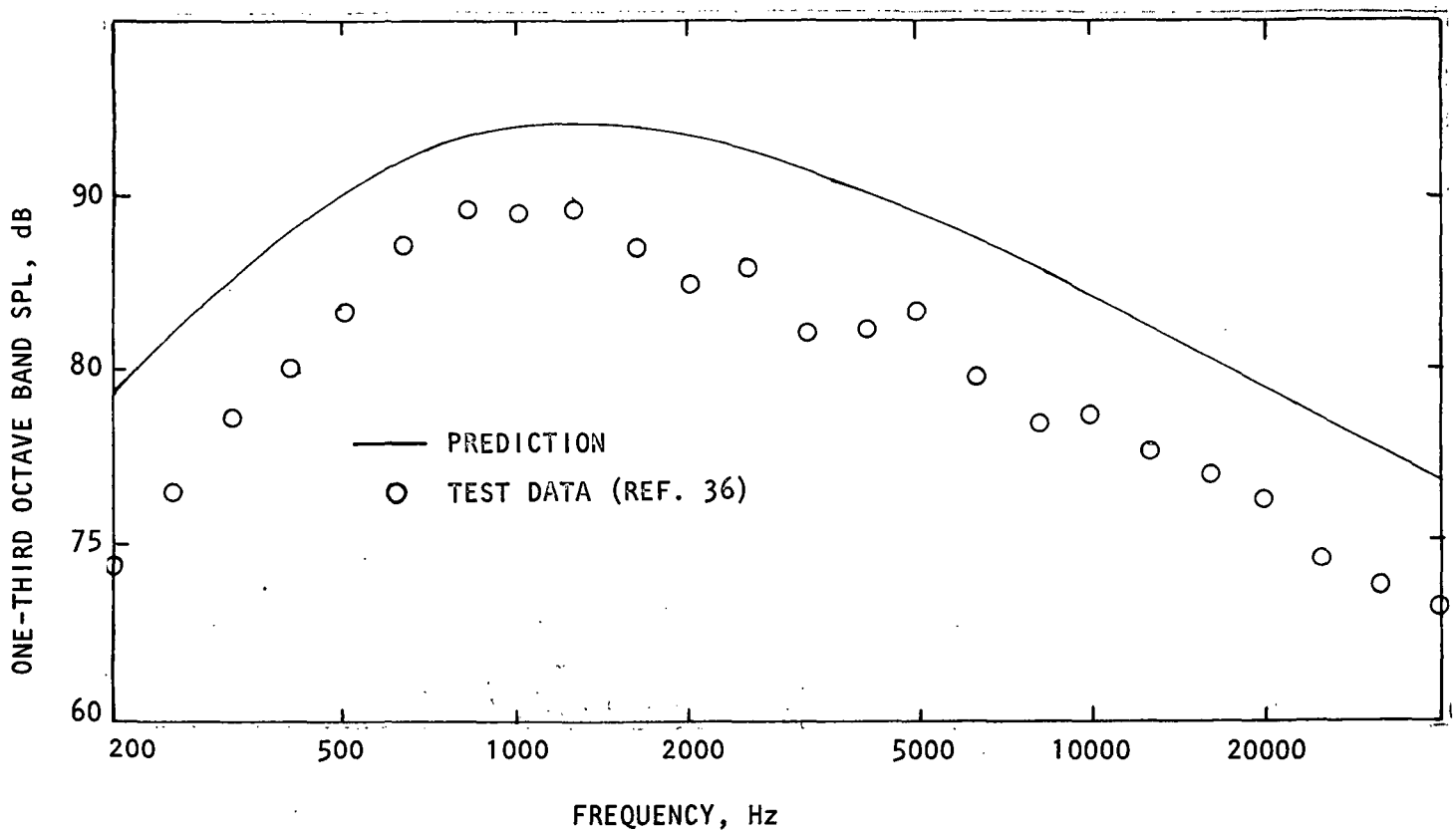

Figure 20 Comparison of UTRC Prediction with Small-Scale USB Test Data (Flyover Plane, $\theta = 60°$)

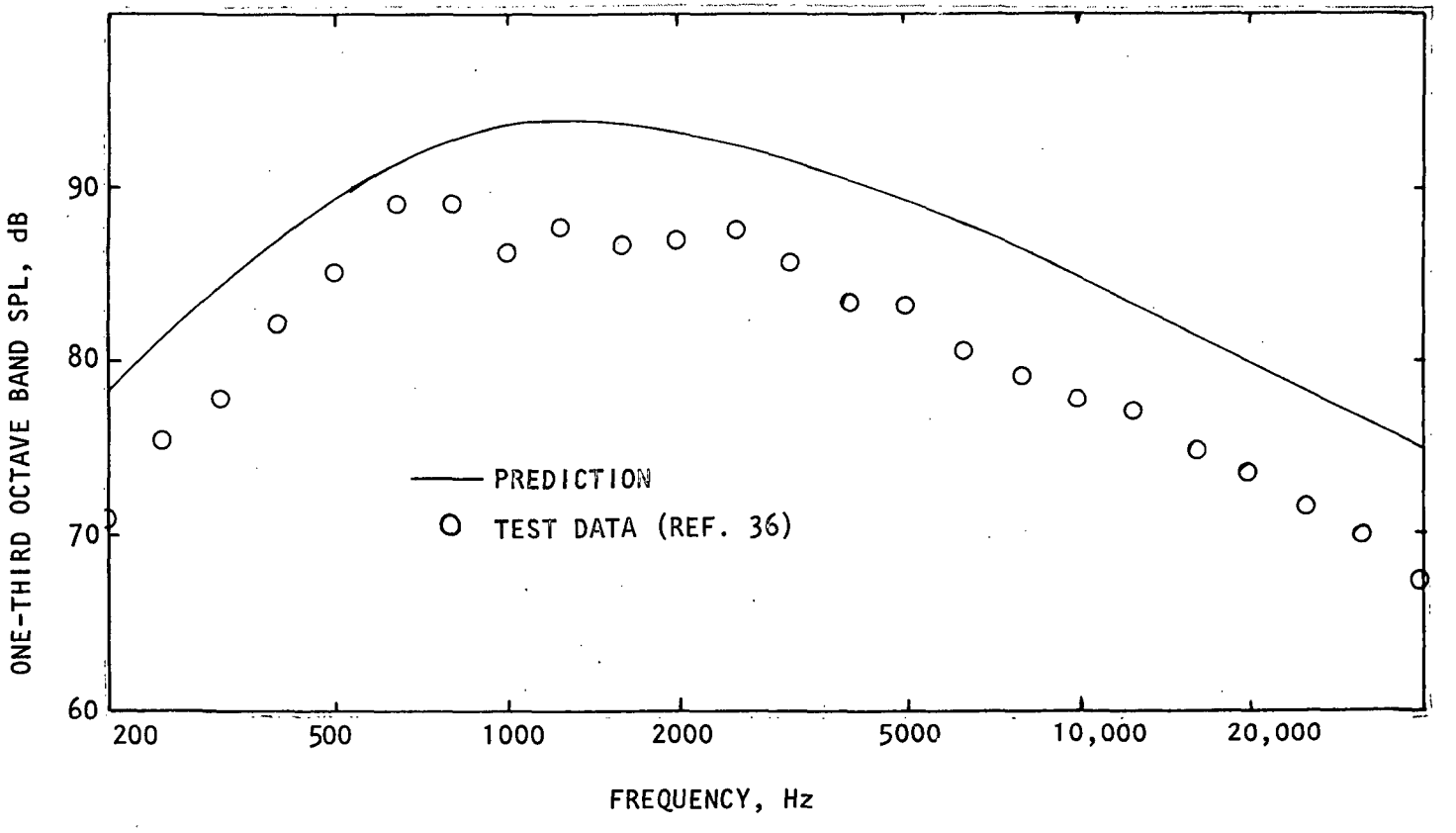

Figure 21 Comparison of UTRC Prediction With Small-Scale Test Data (Flyover Plane, $\theta = 90°$)

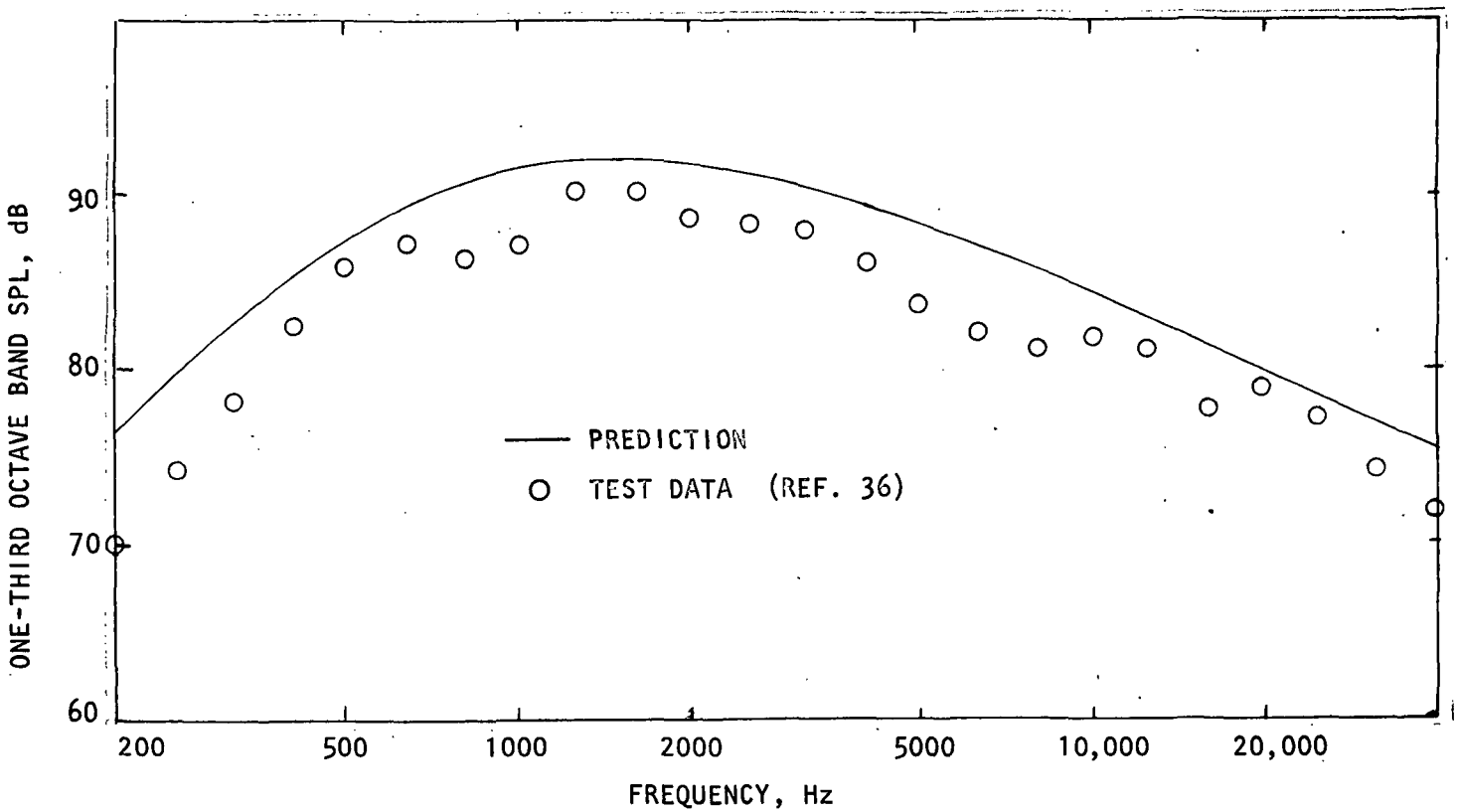

Figure 22 Comparison of UTRC Prediction with Small-Scale Test Data (Flyover Plane, $\theta = 120°$)

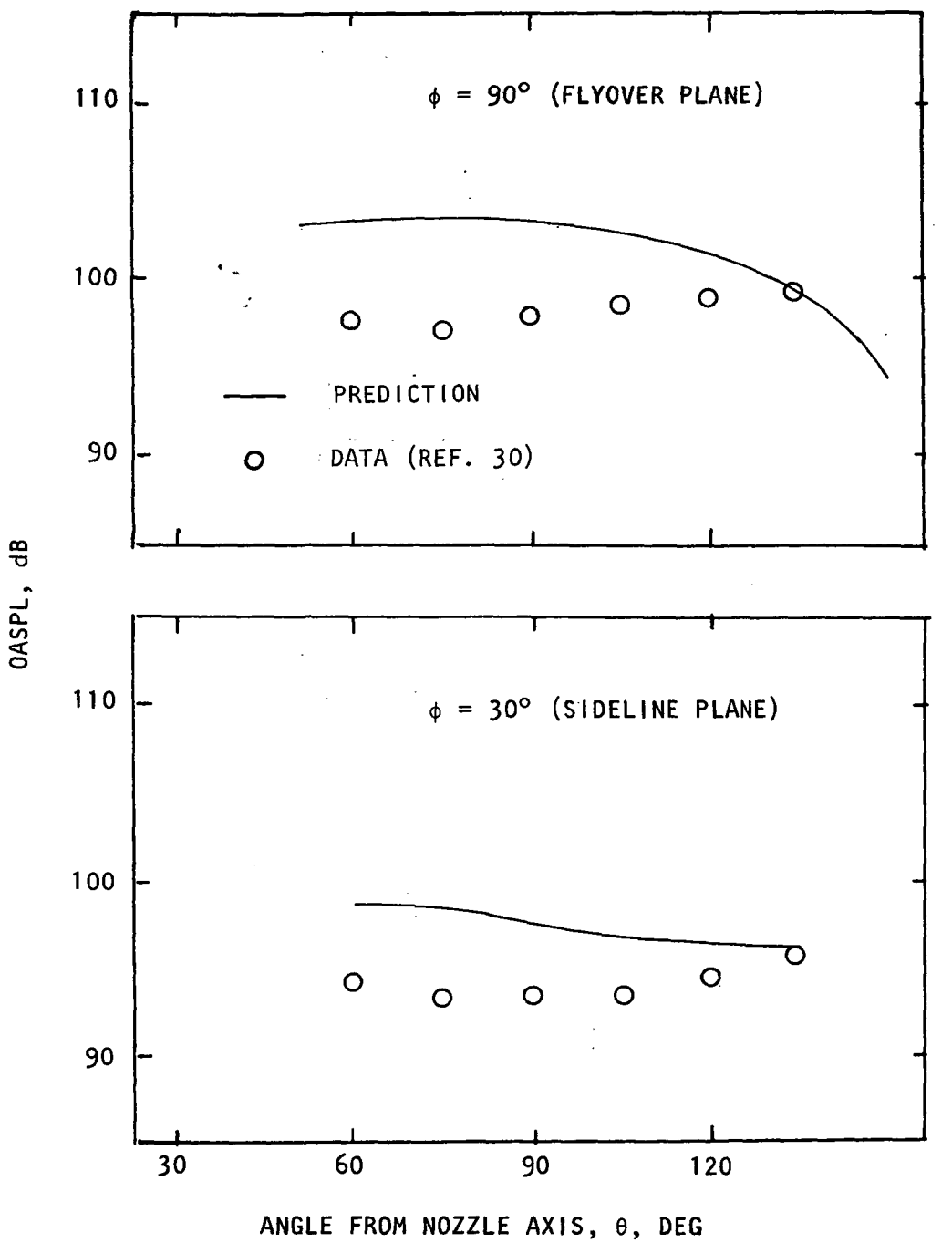

Figure 23 Comparison of UTRC Prediction With Small-Scale Test Data

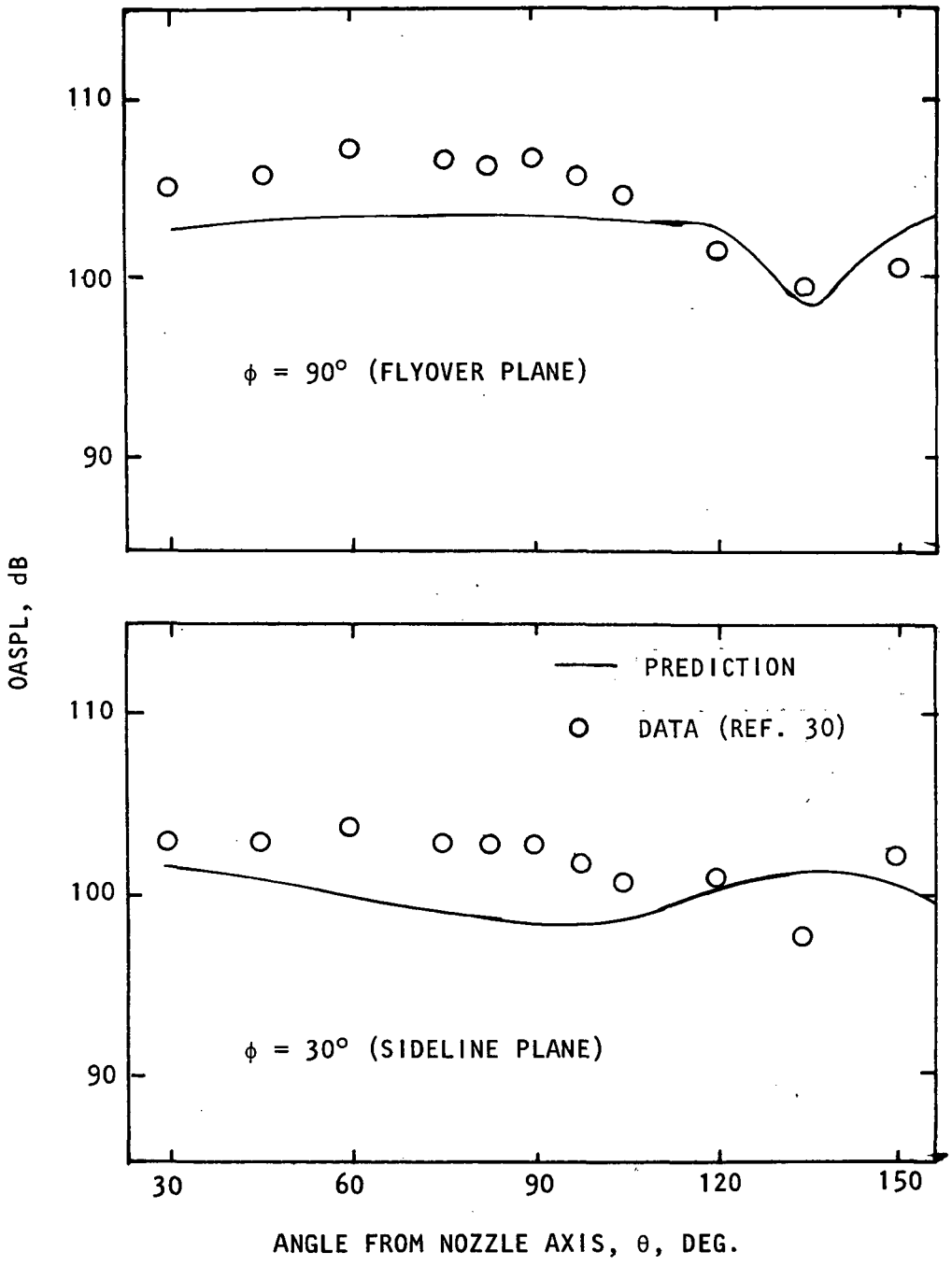

Figure 24 Comparison of UTRC Prediction With Small-Scale Test Data

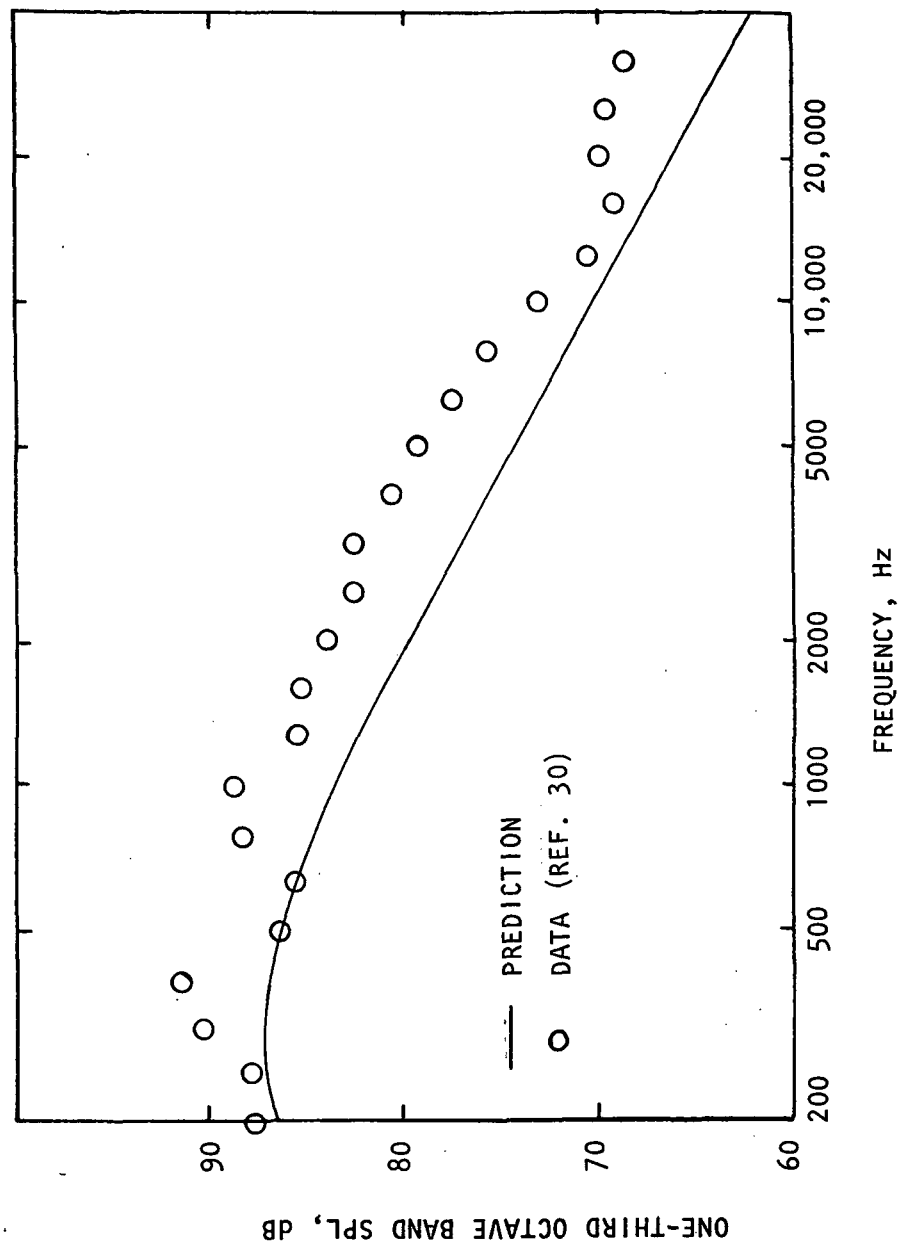

Figure 25 Comparison of UTRC Prediction With Small-Scale UTW Test Data (Flyover Plane, $\theta = 30°$)

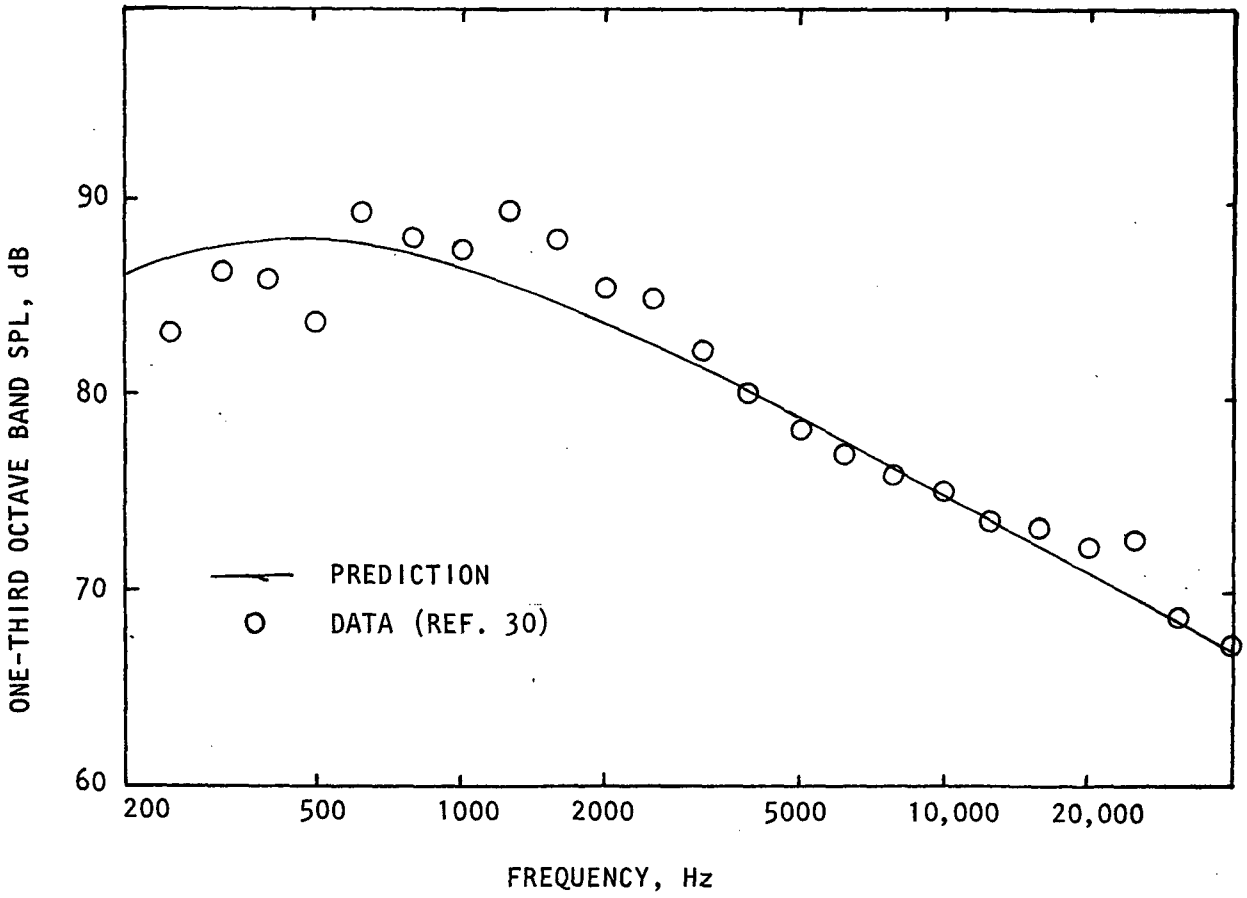

Figure 26 Comparison of UTRC Prediction with Small-Scale UTW Test Data (Flyover Plane, $\theta = 105°$)

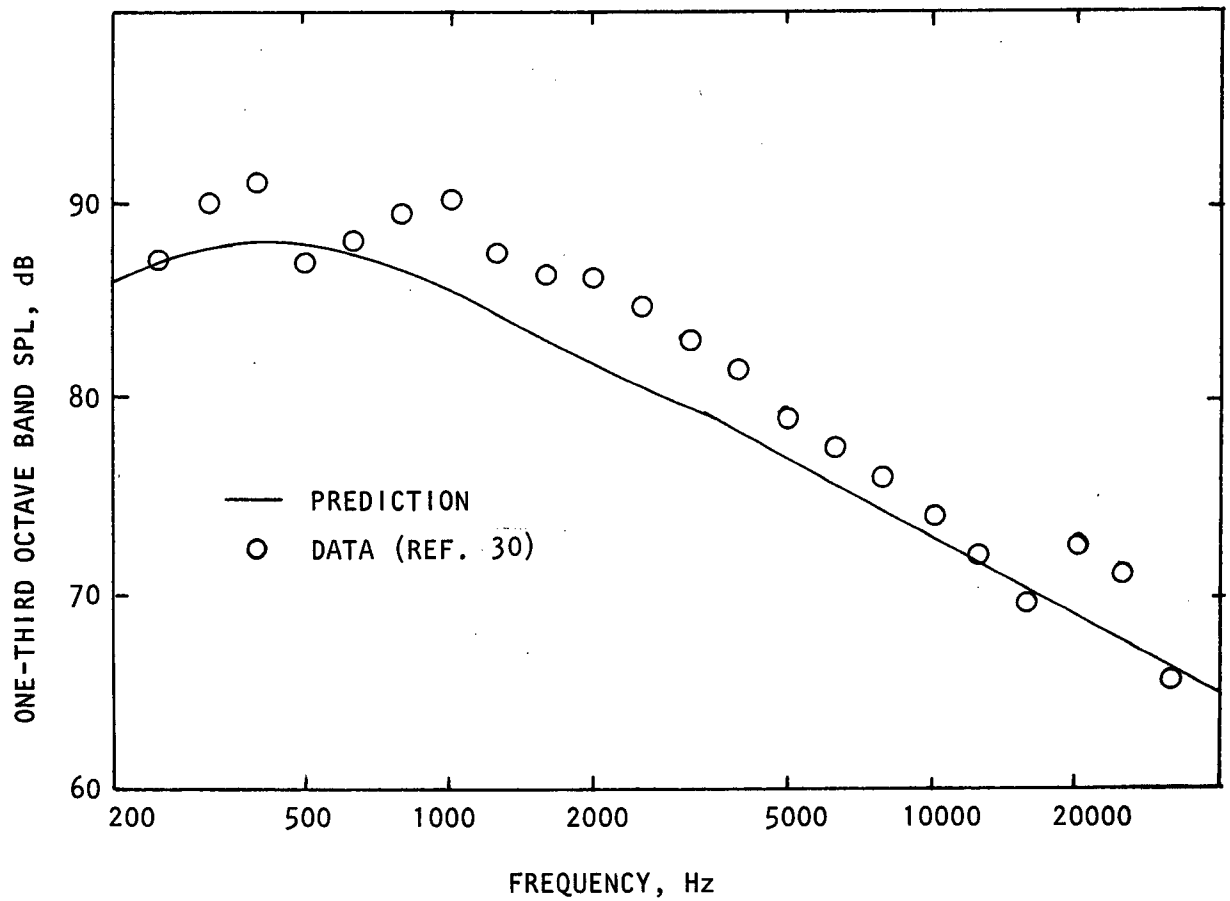

Figure 27 Comparison of UTRC Prediction With Small-Scale UTW Test Data (Flyover Plane, $\theta = 30°$)

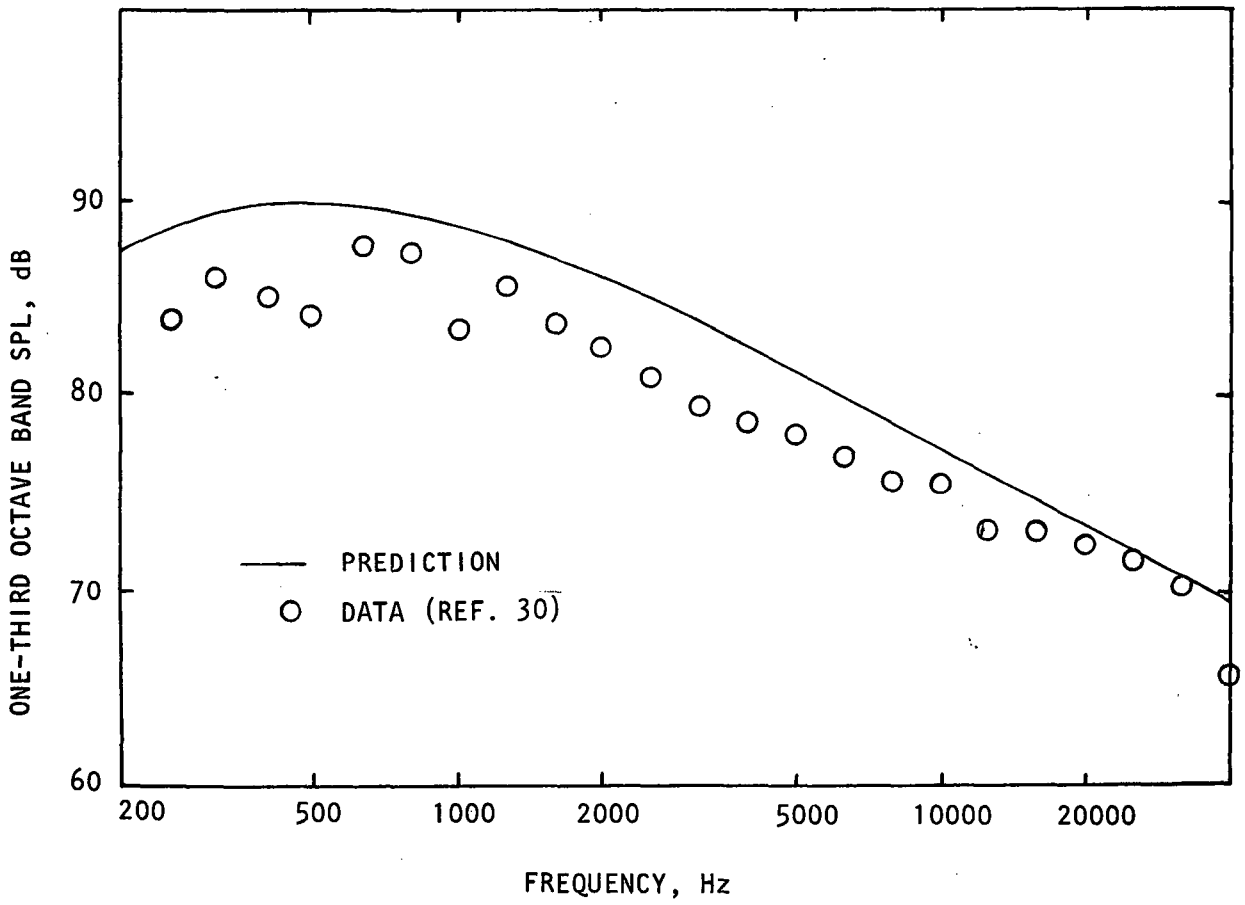

Figure 28 Comparison of UTRC Prediction With Small-Scale UTW Test Data (Flyover Plane, θ = 105°)

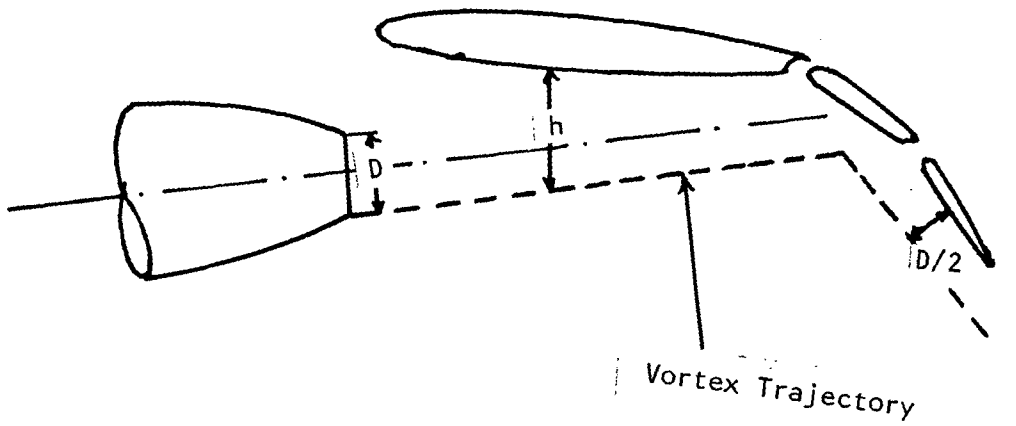

Figure 29. Vortex Trajectory for UTW Configuration